Title

- Defensive polyketides produced by an abundant gastropod are candidate keystone molecules in estuarine ecology.
- Keystone molecules in estuarine ecology.

Authors

Paul Scesa,[1†] Helen Nguyen[2], Paige Weiss[2], Alejandra Rodriguez[2], Matthew Garchow[2], Shannon I. Ohlemacher[3‡], Evangeline Prappas[2], Serena A. Caplins[4], Carole A. Bewley[3], Eric M. Wood[2], Eric W. Schmidt[1], and Patrick J. Krug[2*]

Affiliations

[1] Department of Medicinal Chemistry, University of Utah, Salt Lake City, UT, 84112, USA.
[2]Department of Biological Sciences, California State University, Los Angeles, CA, 90032-8201, USA.
[3]Laboratory of Bioorganic Chemistry, National Institute of Diabetes and Digestive and Kidney Diseases, National Institutes of Health, Bethesda, MD, 20892, USA.
[4]Department of Population Biology, University of California at Davis, Davis, CA, USA

Use superscript numbers (1, 2, 3) to designate author affiliations.

- Each affiliation should be preceded by superscript numbers corresponding to the author list, and each affiliation should end with a period.
- Each affiliation should be a separate paragraph.
- You can include group authors, but please include a list of the actual authors (the group members) in the Supplementary Materials.

*corresponding author; pkrug@calstatela.edu
‡current address:

Teaser

Small molecules that protect sea slugs from predators also attract and repel diverse other species, and may restructure mudflat communities.

Abstract

Secondary metabolites often function as antipredator defenses, but when bioactive at low concentrations, their off-target effects on other organisms may be largely overlooked. Candidate 'keystone molecules' have been proposed to impact community structure and ecosystem functions, generally originating as defenses of primary producers; the broader ecological effects of animal chemistry remain largely unexplored, however. Here, we report the biosynthesis of five novel polyketides (alderenes A-E) in sea slugs that reach exceptional densities (up to 9,000 slugs/m^2) in Northern Hemisphere estuaries. Alderenes render slugs unpalatable to predators, making a potential food resource unavailable and redirecting energy in key nursery habitat. Alderenes also displace infauna from the upper sediment of the mudflat but attract ovipositing snails. Such keystone molecules may thus have unexpected cascading effects on processes

ranging from bioturbation to reproduction of species not obviously connected to the producing organisms, warranting greater attention by ecologists.

INTRODUCTION

For over 50 years, ecological theory has recognized the disproportionate impact of keystone species, low-abundance taxa that control tipping points between alternative states and have many strong links in interaction networks (1-4). Recent advances in chemical ecology led to analogous proposals that 'keystone molecules' may act at low concentrations to impact food webs and community structure, altering expected patterns of energy flow and species distributions (5-10). Such compounds may mediate diverse ecological processes because chemosensory mechanisms are evolutionarily conserved among taxa, and molecules often persist and propagate through food webs. For instance, the same toxin can deter generalists yet attract specialist feeders that accumulate it for their defense; other life stages or species may then detect or deploy that toxin as a pheromone or alarm cue (9). However, most ecological theory has yet to incorporate the pivotal role keystone molecules may play in large-scale processes (7-9).

The best-characterized systems impacted by candidate keystone molecules involve food webs based on marine phytoplankton. Compounds produced during harmful algal blooms (e.g., saxitoxin) become concentrated at higher trophic levels, and can be used by resistant species in defense or as chemosensory cues; by altering foraging behavior of predators, such toxins influence community structure in complex ways and drive large-scale effects associated with red tides (7, 10-11). In pelagic systems, dimethylsulfide (DMS) is produced enzymatically as a breakdown product when phytoplankton are ingested and may directly impact grazing rates and gut physiology of consumers at low trophic levels (12). However, DMS also attracts foraging sea birds at great distances, signaling high-productivity patches where fish and crustacean consumers gather (13-14). DMS signaling promotes energy transfer from marine to terrestrial systems when seabirds excrete wastes on island roosts (7, 15).

Pyrrolizidine alkaloids (PAs) from plants play similarly diverse roles in terrestrial ecosystems, altering the composition of the rhizosphere. PAs suppress hyphal growth in endophytic fungi associated with species lacking PAs, but not mutualistic fungi of PA-producing species (16). These compounds also act as oviposition cues for specialized arctiid moths, which sequester PAs as anti-predator defenses and as mate attractants (9, 17-18). Microbial metabolites may also regulate soil nutrient cycling and plant primary production, but there is a lack of theory synthesizing the impacts of keystone molecules across marine and terrestrial systems (19).

Notably, classic keystone species were recognized through top-down effects, whereas most proposed keystone molecules influence communities via bottom-up effects. However, many primary consumers are chemically rich and rely on secondary metabolites for defense and signaling, including insects (20), gastropods (21) and filter-feeding invertebrates (22). Defensive compounds in abundant consumers may impact food webs by limiting the energy from primary production reaching higher trophic levels. Keystone molecule status may be warranted when a feeding deterrent further links a consumer to other community members in interaction networks through unexpected responses. For instance, many bioactive compounds show both antifeedant and antimicrobial activity, so could deter predators while changing the microbiome of surrounding sediments or surfaces (22). The same secondary metabolite could alter community

structure by differentially attracting or repelling species that would not otherwise interact with the producing organism, and disrupting ecological processes regulated by chemical signaling like spawning or recruitment of neighboring species.

Sea slugs (marine heterobranch gastropods) generally lack a protective shell and employ alternative defenses such as sequestering diet-derived toxins (21) and cnidarian nematocysts (23), or *de novo* biosynthesis of chemical deterrents (24). Ecological impacts of sea slugs have primarily been recognized in disturbed systems: the loss of pteropods due to ocean acidification (25); alteration of infaunal communities by invasive predators (26); or control of invasive macroalgae by herbivores (27). However, bioactive metabolites of sea slugs may play a keystone role in ecosystems by protecting impactful consumers that would otherwise be abundant prey items, while exerting unrecognized effects on the surrounding community (28). Here, we show that sea slugs in one genus are exceptionally abundant grazers in boreal to warm-temperate estuaries throughout the Northern Hemisphere, but a novel chemical defense protects this potential food resource from predation, shunting substantial energy away from higher trophic levels. The compounds are released in slug pedal mucus and potentially in concentrated pulses during mass die-off events. Field experiments indicate slug compounds trigger short-term changes in the infaunal community on mudflats, indicating an unprecedented role for defensive secondary metabolites in altering food webs and community structure at a range of spatial scales.

RESULTS

Boom-and-bust population dynamics of *Alderia*, an abundant estuarine grazer

The yellow-green (heterokont) alga *Vaucheria* is a dominant primary producer in the high intertidal zone of mudflats, forming mossy mats that stabilize sediment. In Northern Hemisphere estuaries, amphibious sea slugs in the genus *Alderia* specialize on *Vaucheria*, surviving in nearly freshwater to fully marine conditions and living out of water for extended periods (29-31). European slugs are *A. modesta* (Lovén, 1844), while a divergent but externally cryptic species, *A.* cf. *modesta*, is widely distributed from San Francisco Bay, USA throughout the North Pacific and western North Atlantic (32-34). A distinctive congener, *A. willowi* Krug, Ellingson, Burton & Valdés, 2007, is found in California, USA (35-36).

Alderia spp. are small but often extraordinarily abundant (Supplementary Table S1). Pooling data across all three species, mean slug density throughout the year increased with latitude (Fig. 1A, and results of a linear regression: $P<0.0001$). Most populations averaged from 100 to 800 slugs/m^2 but the highest latitude population of *A. modesta* had a mean of ~5000 slugs/m^2. Peak density for a year also increased with latitude (Fig. 1B, and results of a linear regression: $P<0.0001$). Most populations peaked at 1000 to 5000 slugs/m^2 but at the highest latitude, maximum density was a remarkable ~9000 slugs/m^2. Even low-latitude populations of *A. willowi* achieved high mean (>150 slugs/m^2) and peak densities (>1000 slugs/m^2).

Population dynamics of both *A.* cf. *modesta* and *A. willowi* were tracked for several years in San Francisco Bay (Fig. 1C-D) (37). The species alternated annually with one major recruitment event each. Annual densities of *A.* cf. *modesta* peaked in Feb-Mar at 650 to 1,150 slugs/m^2 ($N = 3$ yr), when most individuals were juvenile recruits (1-3 mg) (Fig. 1C). Peak densities reached > 5,000 slugs/m^2. However, one month later densities declined by 72% (± 8% SE; $N = 3$ yr). Maximum annual mud temperatures occurred each Apr-May, coinciding with

observed mass die-off events. In Apr 2008, maximum mud temperature during low tides was 41.1°C on a transect where 82.8% (± 9.4% SE; $N = 4$ quadrats) of slugs were discolored and dying in the field; mortality was confirmed by microscopic examination over several hours after collection. In Apr 2009, 36.5% (± 14.9% SE; $N = 4$) of slugs from the same transect were dead in the field on a day when maximum mud temperature was 34.4°C, as were a smaller proportion of slugs from two nearby transects (Fig. 1E). Such temperatures exceed the tolerance of *Alderia* spp. (38). Surviving slugs grew larger but rarer through summer; although the population declined by >99%, *A.* cf. *modesta* was present year-round.

In contrast, *A. willowi* was absent from San Francisco Bay from Mar-Aug, recruiting in late summer (Fig. 1D). Abundance peaked in Oct-Nov; maximum density was 1,393 ± 387 slugs/m^2 in 2008. *Alderia willowi* produces both dispersive larvae and also non-dispersive offspring that recruit locally (36-37); cohorts therefore overlap, and size and density were uncorrelated (Fig. 1D). Although mass die-offs were not directly observed, seasonal mortality was equally marked for *A. willowi*, with abundance falling by 51 ± 5% (± SE; $N = 2$ yr) within 1-2 months of peak density, and >99% by Jan-Feb for each annual cohort.

Novel polyketides and their biosynthesis in *Alderia*

Slugs on the mudflat lack obvious defenses and could be a key food source for invertebrate predators, juvenile fish, and migratory waterfowl or resident shorebirds (33). However, if slugs are chemically defended, primary production from *Vaucheria* may be shunted away from higher trophic levels. As both consumers and potential prey, the role of *Alderia* in estuarine food webs thus remains an open question with implications for resource distribution in sensitive nursery habitat across the Northern Hemisphere (39-41). Their boom-and-bust population dynamics also raise the possibility that defensive chemistry might be released into the environment during episodic mass die-offs with potentially widespread effects on the ecosystem.

Alderia have a pungent odor but were not chemically characterized in prior studies. Two fish and two crab species ate *A.* cf. *modesta* in a laboratory assay, but predators were much larger than slugs, and moreover were given 3 days to potentially exhaust a slug's store of defensive compounds with repeated attacks (42). Phylogenetic evidence suggested *Alderia* might biosynthesize polyketides (PKs), secondary metabolites with a range of biological activities. Superorder Sacoglossa contains superfamilies Plakobranchoidea, comprising chloroplast-retaining, photosynthetic species; and Limapontioidea, comprising largely non-photosynthetic taxa (including *Alderia*) with dorsal appendages termed cerata that may autotomize (43). We recently characterized a novel branch of PK-synthesizing enzymes (AFPKs) in protostome bilaterians (44-45). In highly photosynthetic species in Plakobranchoidea, the enzymes EcPKS1 and EcPKS2 produce unsaturated, medium- and long-chain pyrones using methylmalonyl-CoA as a substrate, otherwise unknown in animal lipid metabolism. The longer unsaturated pyrones may facilitate animal photosynthesis due to their antioxidant or photoprotective properties, usually forming additional cyclic motifs (44). In contrast, cerata-bearing slugs expressed different lineages of AFPKs (46), and all species studied to date contained monocyclic PKs of unknown function. Although sacoglossan polyketides have not been demonstrated to deter ecologically relevant predators (22-23, 47-51), AFPKs are prevalent in shell-less gastropods that otherwise lack strong diet-derived defenses, suggesting a potential role in chemical defense (45-46).

Inspired by their pungent odor and abundance, we chemically characterized both *Alderia* spp. from California. LC/MS analysis of acetone extracts of individual *A*. cf. *modesta* and *A. willowi* revealed peaks with fragmentation patterns and molecular masses consistent with sacoglossan PKs (Fig. 2A, Supplementary Table S2). Individually analyzed *A*. cf. *modesta* (*N*=7) contained at least five PKs in proportions that varied only slightly among individuals (Supplementary Fig. S1). Two of the compounds (**1** and **5**) were also present in *A. willowi*, again in proportions that varied minimally among individual slugs (*N*=7).

Acetone extraction of ~200 whole *A. modesta* specimens, followed by dichloromethane extraction and LCMS, revealed the presence of at least five polyketide metabolites, each with five degrees of unsaturation and varying degrees of methylenation. Reversed phase flash chromatography on C_{18} followed by semi-preparative HPLC on a phenylhexyl column led to the purification of five novel cyercene-class metabolites, alderenes A-E (**1-5)** (Fig 2B). Structures were elucidated by 1D and 2D NMR experiments (HMQC, HMBC and COSY) plus MS/MS. All alderenes exhibited strong UV absorptions with λ_{max} values between 232 and 235 nm, and IR bands around 1712 cm^{-1} typical of α-pyrones. Compared to polypropionate pyrones reported from related molluscs (47-51), these data indicated the *Alderia* metabolites represented a class of dihydro-α-pyrones with a reduced head-group, unprecedented from sacoglossans. Metabolites differed from one another based on various degrees of methylenation, likely reflecting the incorporation of malonyl versus methylmalonyl precursors during polyketide chain extension.

ESI-MS spectra of alderene A (**1**) suggested the molecular formula $C_{14}H_{20}O_3$ with an observed ion at *m/z* 259.1310 $[M + Na]^+$ (calc. *m/z* 259.1305), which was also supported by the overall ^{13}C NMR data (Table 1A). An intense IR band at 1711 cm^{-1} together with a ^{13}C NMR signal at δ_C 163.9 indicated the presence of a conjugated ester with a UV maximum at 232 nm. The γ-pyrone ring of **1** was characterized by ^{13}C NMR resonances of δ_C 167.3 (C-2), 89.7 (C-3), 175.8 (C-4), 34.3 (C-5) and 88.8 (C-6), as well as by four ^1H NMR signals at δ_H 5.11 (H-3), 3.74 (Me-O), 2.80 (H-5), 4.35 (H-6), and 1.04 (Me-5) (Table 1B, Fig. 2B, Supplementary NMR data). Correlations in the 2D COSY spectrum between H-5 and H-6 supported the structure of the dihydro-α-pyrone; this structure was confirmed by correlations in the 2D HMBC, with the position of the enol ether indicated by the cross-peak between the Me-O proton resonance and the C-4 resonance. The presence of the lactone was confirmed by cross-peaks between H-6 and C-2 resonances (Figure 2C, Supplementary NMR data). The ^1H NMR spectrum of **1** also showed two downfield resonances, δ_H 5.91 (H-8) and 5.43 (H-10), that were attributed to the protons of two side chain double bonds, as well as three olefinic methyl resonances, δ_H 1.80 (Me-7), 1.74 (Me-9) and 1.68 (C-11) (Table 1B). The presence of four additional olefinic resonances in the ^{13}C NMR at δ_C 129.2 (C-7), 135.8 (C-8), 132.5 (C-9) and 126.1 (C-10) further supported the presence of this side chain. The connection of the pyrone ring with the unsaturated side chain and the respective position of each methyl group was unambiguously assigned by an array of cross peaks in the HMBC spectrum (Fig. 2C).

The relative configuration of **1** was determined by NMR data analysis, using NOE and *J* coupling relationships as well as chemical shift arguments. A lack of 2D NOESY correlations between H-8 and the Me-7 $^1H_3$ resonances, as well as between H-10 and the Me-9 $^1H_3$ resonances, suggested an *E,E*-geometry of the side chain; this configuration was further supported by the relatively low ^{13}C chemical shifts for Me-7 (δ_C 13.0) and Me-9 (δ_C 16.5) which are typical of *E*-configured polypropionates (46, 48). Comparing molecular models for each

diastereomer in its various conformational states, assisted by density functional theory (DFT) optimization and free energy calculations, facilitated analysis of NOESY data. It was determined that the *E,E*-diene preferred two near *S-cis* conformations twisted out of plane by ±45° in either direction, likely due to significant $A^{1,3}$ strain between Me-7 and Me-9. For the pyrone ring in a *trans*-configuration, two half chair conformations were determined, with H-5 and H-6 adopting a preferred axial orientation. Another conformational state with H-5 and H-6 equatorial likely accounts for the 10 Hz coupling between these protons. This overall structure was confirmed using NOESY correlations (Fig. 2C). NOESY cross peaks between H-5 and Me-7, and between Me-7 and H-10 indicated the planes of the diene chain and pyrone ring were nearly orthogonal, with these protons oriented toward the α-face of the ring. NOESY correlations between Me-5 and H-6 indicated their *cis*-orientation on the ring, and correlations from H-8 to Me-5, H-6 and Me-9 demonstrated these protons were all oriented toward the β-face of the pyrone ring. Overall, these data indicated that **1** possessed the *trans*-pyrone ring with two *E*-double bonds. To determine the absolute configuration, four conformers of this diastereomer were Boltzmann weighted and the electronic circular dichroism spectra (ECD) computed by time dependent DFT. The experimental ECD spectrum was consistent with the predicted spectrum for **1** (Fig. 2D), allowing determination of the 5*S*,6*R*-absolute configuration.

The structures of **2**-**5** were determined primarily by comparison of NMR data to that of **1** (Table 1). Alderenes **1**-**5** all showed similar IR and UV spectra, indicating pyrone and diene functionalities. Different methylation patterns were consistent with the NMR spectroscopic dissimilarities between compounds. Alderenes **2** and **4** possessed an additional olefinic methyl resonance and an increased chemical shift at C-3, indicating methylation at this site. Alderenes **3** and **4** lacked the Me-11 olefinic methyl doublet, showing instead an aliphatic methyl triplet and additional allylic methylene. Furthermore, **3** and **4** showed an olefinic methine triplet at C-10, indicating these metabolites were C-11 homologues of **1**. These proposed structural variations were consistent with HRMS and 2D NMR data (Supplementary Fig. S2, Supplementary NMR data). Alderenes **1-4** showed optical rotations of the same sign, and **1** and **3** showed very similar ECD spectra. As such, **1-4** were determined to be of the same absolute configuration on the basis of these properties, while **5** is likely of the same absolute configuration on biogenetic grounds.

Major alderenes are secreted in the pedal mucus of crawling slugs. LC/MS analysis of *Vaucheria* patches on which slugs had recently crawled detected alderenes **1** and **5,** whereas analysis of egg masses did not detect any PKs (Supplementary Fig. S3). In a standard bioassay for antimicrobial activity, alderene A (**1**) inhibited growth of *S. aureus* at 25 μg/ml but not *E. coli* or *A. baumannii*.

We identified AFPKs in the transcriptome of *A*. cf. *modesta* (AmPKS1 and AmPKS2) that grouped with EcPKS1 and EcPKS2 from *E. chlorotica* in the sacoglossan-specific mo-clade 1 (Fig. 3). AmPKS enzymes belong to a subgroup predicted to biosynthesize short-chain pyrones (46). Thus, the sequenced genes expressed by *A.* cf. *modesta* are consistent with the structures of the alderenes. Factors leading to the unprecedented reduced dihydro-pyrone ring have yet to be elucidated. Expression of AmPKS1 was 3 to 5 times lower than that of the FAS1 and FAS2 genes, normalized to GAPDH, whereas expression of AmPKS2 was comparable to FAS2 but still less than half that of FAS1 (Fig. 3, inset).

Polyketides deter co-occurring predators

We hypothesized that in *Alderia*, PKs primarily function as an adaptation to deter benthic predators likely to encounter small slugs. Antifeedant assays were performed using three size-appropriate, co-occurring mudflat predators: the arrow goby fish *Clevelandia ios*; the polychaete worm *Neanthes arenaceodentata*; and the lined shore crab *Pachygrapsus crassipes*. All worms made repeated predation attempts on live *A.* cf. *modesta*, attacking slugs 2.3 times ± 0.4 SE more often than controls which were consumed after one bite (sign test: $P = 0.002$). However, every worm ($N = 20$) ultimately rejected the slug but consumed a squid control (Table 2, and Fisher's exact test: $P = 7\times10^{-12}$); worms often demonstrated a stress response such as shaking the head, repeatedly everting the proboscis, or rapidly backing away from the slug (supplemental video 1). Similarly, crabs ($N = 9$) rejected all live *A.* cf. *modesta* but ate squid controls (Table 2, and Fisher's exact test: $P = 2\times10^{-5}$). Most crabs passed the slug over their mouthparts, then dropped the slug and walked away. Two crabs attempted to feed on *A.* cf. *modesta* but after the slug released mucus, each crab spent the remainder of the trial holding the slug in one cheliped while using the other to pull mucus strands from its mouth, ultimately dropping the slug (supplemental video 2). Controls were consumed in a significantly shorter time, 25.1 sec ± 3.0 SE (Supplementary Fig. S4A). All slugs survived for 7 d after crab predation attempts. Fish ($N = 10$) attacked live *A.* cf. *modesta* 2.8 times ± 0.3 SE (range: 1-4 attacks) more than the one attempt per control (sign test: $P = 0.002$), but finally rejected all live slugs while consuming squid controls (Table 2, and Fisher's exact test: $P = 5\times10^{-6}$). Fish spent significantly longer mouthing an *A.* cf. *modesta* (29.4 sec ± 4.3 SE) compared to controls (8.1 sec ± 0.6 SE) before finally expelling the slug and its secreted mucus (supplemental video 3).

Responses to live *A. willowi* were comparable. Worms rejected all live slugs ($N = 10$) (Table 2, $P = 5\times10^{-6}$) despite making about twice as many feeding attempts on slugs compared to controls (sign test, $P = 0.002$). Crabs ($N = 9$) ate no live *A. willowi* (Table 2, $P = 2\times10$-5); four attempted to feed for the whole trial but consumed only 1 mm ± 0.2 SE of a slug's body (5 mm mean length). Crabs spent most of the trial removing mucus from their mouth, whereas controls were consumed in only 11.5 sec ± 1.6 SE (Supplementary Fig. S4B). All slugs survived 7 d after attempted crab predation. Fish ($N = 10$) consumed no live *A. willowi* but ate all controls (Table 2, $P = 5\times10^{-6}$), attacking slugs 4.1 times ± 0.4 SE (range = 1-6 attacks) versus one attempt per control (sign test: $P = 0.002$). Fish spent 24.4 sec ± 3.8 SE mouthing *A. willowi* versus 7.1 sec ± 1.0 SE to consume controls.

To determine if active secretion of mucus was an essential component of slug defense, we tested the palatability of dead slugs that had been flash-frozen and then thawed immediately prior to assays. All worms, crabs and fish rejected every dead *A.* cf. *modesta* offered but ate all controls (Table 2); behavioral reactions of predators were comparable to feeding attempts with live slugs. Fish spent 25.7 sec ± 3.2 SE mouthing slug bodies before rejection, versus 7.5 sec ± 0.7 SE to consume controls. All predators similarly rejected every dead *A. willowi* (Table 2), with fish again spending about three times longer mouthing slug bodies before rejection (21.8 sec ± 3.1 SE) versus time to consume controls (6.8 sec ± 0.6 SE). Thus, mucus secretion was not required for slug tissue to repel hungry mudflat consumers.

We next tested whether removing nonpolar secondary metabolites would restore the palatability of slug tissue by offering predators intact slug bodies that had been extracted twice with acetone to remove small organic compounds. All worms, crabs and fish consumed 100% of

extracted *A.* cf. *modesta* and *A. willowi* (Table 2). Worms (Supplementary Fig. S5A, D) and fish (Fig. S5C, F) consumed acetone-extracted slugs of both *Alderia* spp. in the same time as extracted squid controls; crabs took longer to consume extracted *A.* cf. *modesta* (Fig. S6B; independent *t*-test: $t(16) = 3.5$, $P < 3\times10^{-3}$) and extracted *A. willowi* (Fig. S6E; independent *t*-test: $t(16) = 3.5$, $P < 3\times10^{-3}$) than squid controls.

All worms and crabs consumed intact egg masses of *A. willowi* as readily as squid mantle controls (Table 2), displaying no adverse reaction to the egg mases during feeding. Half of tested fish (N=10) rejected *A. willowi* egg masses but ate controls, a significant effect (Table 2, and results of a Fisher's exact test: $P = 0.03$). Fish displayed no adverse reactions to egg masses but some appeared unable to handle intact egg masses with their mouths. In contrast, all fish consumed egg masses cut in half, exposing the gelatinous inner egg strand (Table 2). The results suggested the weak deterrent effect on fish was due to the physical protection offered by the tough outer covering of egg masses and not to a chemical defense, while worms and crabs were more easily able to penetrate the outer coat to feed on the undefended eggs.

To confirm that the deterrent effects of slug tissue were due to alderenes, we tested organic extracts of *Alderia* incorporated into squid pellets. Acetone extracts were concentrated then partitioned between water and ethyl acetate, yielding an organic layer enriched in PKs and nonpolar metabolites (lipids, chlorophyl from dietary algae). The organic layer was concentrated and tested at a per-weight concentration for both *Alderia* spp. Crabs rejected all pellets incorporating *A. modesta* extract but ate all control pellets made with an equal volume of carrier solvent (Table 2, Fisher's exact test: $P = 5\times10^{-6}$). Crabs passed extract-containing pellets over mouthparts using chelae before discarding the pellets (2.7 sec ± 1.0 SE), spending longer to consume control pellets (7.4 sec ± 1.0 SE; Supplementary Fig. S6A, and independent *t*-test: $t(18) = 3.3$, $P < 4\times10^{-3}$). Fish sampled but ultimately rejected all extract-containing pellets while consuming all control pellets (Table 2, and Fisher's exact test: $P = 5\times10^{-6}$). Some fish quickly rejected extract-containing pellets while others made multiple feeding attempts before abandoning the pellet (Supplementary Fig. S6B). Fish made significantly more attempts at treated pellets before rejection (3.0 ± 0.5 SE; range = 1-5), whereas controls were attacked once and consumed (sign test: $P = 0.002$). After tasting extract pellets, some fish reacted by rapidly opening and closing their mouth while fanning gills and everting pharyngeal jaws. Similarly, the organic layer from extract of *A. willowi* deterred all crabs compared to controls (Table 2), and hastened rejection of pellets vs. time to consume controls (Supplementary Fig. S6C, and independent *t*-test: $t(18)= 5.2$, $P < 10^{-4}$). Fish also rejected all pellets containing extract of *A. willowi*, with most quickly abandoning treated pellets while taking longer to consume controls (Supplementary Fig. S6D). Some fish attacked multiple times (2.9 attempts ± 0.5 SE) before rejecting treated pellets, but all made just one attempt prior to swallowing control pellets (sign test: $P = 0.002$).

For bioassay-guided fractionation, we further partitioned the organic layer between hexane, yielding a fraction primarily of fats and sterols, and methanol, yielding a fraction that was ~95% alderenes by NMR spectroscopy (Supplementary Fig. S7). Pellets containing the PK-enriched fraction from *A. willowi* were rejected by fish while controls were all consumed (Fisher's exact test: $P = 5\times10^{-6}$), as were pellets incorporating the hexane fraction enriched in sterols. We therefore compared the feeding response to pure alderenes **1** and **3** versus crude

extract of *A. willowi*, and solvent-only control pellets. Pellets incorporating pure compounds were the smallest that could be made, and did not always induce rejection compared to larger pellets tested previously; however, predators exhibited a range of behaviors indicating aversion or deterrence, comparable to behaviors seen with live or dead slugs.

For crabs, pellets incorporating pure compounds or crude extract did not change overall prey-handling time compared to paired controls, except for the lowest concentration of crude extract (Supplementary Fig. S8; paired sign test, $P<0.005$). However, all concentrations of **1** and **3** (alderenes A and C) significantly reduced cheliped movements from pellet to mouth except the lowest of **1**, as did all concentrations of crude extract tested (Supplementary Fig. S9A, C, E); thus pure alderenes were sufficient to inhibit feeding responses. Both compounds and crude extract also induced prolonged, aversive reactions after feeding, at all concentrations. The duration of post-feeding response was longer for **3** than **1** at both concentrations (Supplementary Fig. S8B, D; $P<0.01$, Mann-Whitney test), but even longer for crude extract. The same behaviors were seen from pellets incorporating pure alderenes and crude extract, but not control pellets: crabs wiped mouthparts with head appendages; bubbled at the mouth; used chelipeds to pull material from the mouth; and rubbed mouthparts against the substrate. All concentrations of **1** and **3** significantly increased the number of times crabs pulled material from their mouths after feeding, an aversive reaction also noted in response to slugs and crude extract but rarely with controls (Supplementary Fig. S9B, D, F; paired Sign test, $P<0.005$). All concentrations of **3** significantly increased the proportion of crabs that rubbed or pressed mouthparts against the substrate after ingesting portions of treated pellets, behavior never seen with controls (Supplementary Fig. S10); a comparable response was seen at all concentrations of crude extract, but alderene A did not elicit this response.

Fish regurgitated significantly more when offered pellets incorporating pure **1** (paired sign test, $P > 0.005$) or extract ($P > 0.01$) at 50% of wet weight, compared to controls (Supplementary Fig. S11B); **3** had a borderline effect ($P = 0.07$). Only crude extract induced regurgitation at a 25% concentration (Supplementary Fig. S11). Neither alderene nor the crude extract reduced prey handling time prior to initial feeding attempts by fish (Supplementary Fig. S12A,C; $P > 0.1$). However, both alderenes increased the time fish spent attempting to consume pellets after the initial bite, including time mouthing, regurgitating and trying to ingest the prey item. These adverse reactions to treatment pellets lasted significantly longer for both compounds at a 25% concentration (Supplementary Fig. S12B; paired sign test, $P < 0.05$), and for **1** at a 50% concentration (Supplementary Fig. S12D; paired sign test, $P < 0.01$). Response to pure compounds was comparable to that for extracts at both concentrations, which similarly extended the time fish spent attempting to consume prey items. Overall, predator responses to purified alderenes were qualitatively and quantitatively comparable to those obtained in trials using live and dead slugs, or to positive controls using organic extracts, confirming PKs comprise the antipredator defense of *Alderia* spp.

Community effects of *Alderia* polyketides

To test the hypothesis that *Alderia* PKs have effects beyond predator-prey interactions, we treated paired patches of the surface of a local mudflat with either the organic layer of *A. willowi* extract or an equal volume of carrier solvent as a control. After one tidal cycle, infaunal community composition changed significantly where extract was deployed (Fig. 4, Table 3A).

Most crustaceans were amphipods (primarily *Monocorophium* spp.) and benthic copepods. Abundance of amphipods declined significantly in extract treatments ($P < 0.01$; Fig. 4A), and copepod abundance was highly significantly reduced in extract-treated patches compared to controls (Fig. 4B; Table 3A). The infaunal worm community was diverse, including five common polychaete genera and abundant nematodes, as well as less numerous oligochaetes and nemerteans (Supplementary Table S3). Sediment exposed to *Alderia* metabolites contained significantly fewer annelids ($P < 0.01$) (Fig. 4C), but nematode density did not change in response to slug extract (Fig. 4D). Infaunal molluscs recovered in cores comprised juvenile bivalves and the heterobranch snail *Acteocina inculta*; mollusc abundance decreased highly significantly in response to *Alderia* extract (Fig. 4E, Table 3A).

In contrast to the reduced infaunal abundance, extract-treated sediment contained significantly more eggs of the California horn snail, *Cerithideopsis californica* (Fig. 4F, Table 3A). The horn snail was the most common invertebrate sampled from the surface of the *Vaucheria* belt at the Salinas de San Pedro saltmarsh, with densities ranging from 6.2 ± 3.5 to 16.7 ± 7.8 snails/m^2 in three surveys from March 2022 to April 2023. Eggs were mostly recovered in treatment cores proximal to vegetated areas where snails were highly abundant. Notably, eggs were sampled even in the winter deployment, whereas horn snails primarily reproduce in summer months.

To assess whether there was an overall effect of PKs on species richness, we calculated two indices of community diversity for all cores and compared mean diversity metrics for extract-treated versus control sediment. There was a borderline significant effect of PK treatment on species richness based on the Shannon-Wiener diversity index (Table 3B), but not based on Simpson's Dominance index, which emphasizes the abundance of common taxa.

DISCUSSION

Abundant but inedible resources and estuarine food webs

Just as keystone species alter population dynamics and community composition at low abundance, molecules of keystone significance are proposed to influence ecosystems with effects disproportionate to their concentrations. Our findings support this hypothesis, showing that alderenes may exert substantial but unrecognized effects on Northern Hemisphere estuaries. We characterized five novel compounds and their biosynthetic enzymes from two grazers, and demonstrated diverse ecological effects of these metabolites on co-occurring predators as well as surface-dwelling and infaunal members of the mudflat community. This work provides a new system for exploring how small molecules structure interaction networks, linking seemingly disconnected species with surprising implications for ecosystem function, food web dynamics and community diversity.

Sea slugs are often discounted as major ecological players, but their impacts are increasingly recognized in disturbed systems including the loss of pelagic pteropods due to ocean acidification (25), alteration of infaunal communities by invasive cephalaspideans (26), and local removal of introduced algal species by sacoglossans (27). The deterrent metabolites of sea slugs may play a keystone role in ecosystems where slugs are impactful consumers and in turn, abundant potential prey items. *Alderia* spp. reach exceptional densities on temperate to boreal mudflats throughout the Northern Hemisphere. Along the U.S. west coast, slugs comprise ~99% of animal biomass in the *Vaucheria* belt of many estuaries (33), with mean densities from 100 to 1,000 slugs/m^2 and peak densities from 1,000 to 3,000 slugs/m^2. Primary production by mats of the xanthophyte alga *Vaucheria* is potentially transferred to higher trophic levels almost

exclusively through these dense herbivore populations. Given mean slug weights, mudflats may regularly have 15 to 30 g of slug tissue per m^2 on the surface available to consumers, and 50 to >125 g/m^2 during peak abundances. Molecules that prevent the consumption of slugs may therefore regulate energy flow within estuarine food webs, redirecting fixed carbon from algal mats to unexpected sinks.

Although the class of metabolites to which the alderenes belong has been known from related molluscs for 30 years, their ecological function has been unexplored until this study. The novel alderenes characterized here are structurally similar to PKs characterized from other species in the ceratiform superfamily Limapontioidea, but with a reduced pyrone ring not previously reported from sacoglossans (22, 44, 47-51). Prior investigations tested slug PKs for toxicity against a freshwater fish, or for inducing tentacle regeneration in hydra, but did not evaluate ecologically relevant bioactivity against co-occurring predators or other community members (21-22). One previous study reported two large fish and two crab species ate *A.* cf. *modesta* (42), but predators were over twenty times a slug's length, were not all mudflat species, and were allowed to make repeated predation attempts for 3 d, which could exhaust a slug's reserve of alderenes. The role of PKs in slug defense has thus been ambiguous.

We found that the alderenes confer an effective chemical defense against small, ecologically relevant invertebrate and fish predators. Live *Alderia* spp. were unpalatable, secreting a mucus that predators found distasteful and that appeared to clog mouthparts and gills; slugs were attacked and often swallowed only to be spit out or dropped, and survived all predation attempts. Dead slug tissue was also rejected by consumers unless organic compounds were removed first. Slug extracts conferred deterrent properties onto food pellets, and pure alderenes were sufficient to cause pellet rejection or aversive behaviors at concentrations as low as 0.025%, demonstrating that PKs are responsible for the antifeedant properties of slugs.

Given their abundance in the high-productivity *Vaucheria* belt, *Alderia* spp. could represent an important food source for a range of invertebrate and vertebrate consumers. Instead, slugs biosynthesize distasteful PKs which shunt substantial energy away from predators that would otherwise consume *Alderia*. This represents a lost potential food resource for juvenile fish and invertebrates in important nursery habitat, as well as for nesting and migrating waterfowl if birds are similarly deterred by slug compounds. The fate of carbon fixed by *Vaucheria* is thus unclear. Dead or dying *Alderia* could be an important subsidy for mudflat scavengers and detritivores if decaying flesh is palatable, but slug tissue was equally repellent in predator assays. Given the high reproductive output of slugs (36), energy flow may be redirected to the nearshore plankton by the tidal export of *Alderia* larvae from mudflats, as slug embryos did not appear to be chemically defended. Given the wide distribution of *Alderia* and the high densities reached by slugs, the alderenes may thus have large-scale impacts on estuarine food webs.

Keystone molecule effects on the ecosystem

Our findings further indicate that alderenes substantially alter the composition of mudflat infauna in the *Vaucheria* belt, causing mobile infauna to leave sediment over one tidal cycle when exposed to ecologically realistic levels of *Alderia* PKs. Treatment of surface sediment rapidly repelled four of five major groups of infauna, significantly reducing amphipod, copepod, annelid and mollusc abundance. Only nematode roundworm abundance did not respond to slug compounds; nematodes exhibit broad tolerance to a range of extreme environments so may not be as susceptible to the repellant effects of alderenes as other taxa.

Even a single application of extract also had a near-significant effect on overall community diversity, indicating slug compounds reduce diversity as well as abundance of mudflat meiofauna and macrofauna dwelling in the upper sediment layers. This strong response suggests that the steady release of alderenes in slug pedal mucus, or in bursts during episodic mass die-offs, may have large but unanticipated effects on the underlying community. The surface layers of mudflats are nutrient-rich but quickly become anoxic; many processes that occur in these sediments are subject to biodiversity-function effects, including bioturbation, nutrient recycling and primary production (52-54). By reducing diversity and abundance of nearby infauna, dense slug populations may in turn affect such ecosystem processes in complex ways that would not be predicted from traditional interaction networks. Microbial processes also profoundly affect the biogeochemistry of mudflats, and may be impacted by alderenes given the antibiotic properties of many PKs and the activity reported here; future work will examine the influence of slug compounds on the microbiome of sediments in the *Vaucheria* belt of estuaries.

In contrast to their deterrent effects on consumers and infauna, alderenes induced oviposition by a common co-occurring gastropod. The California horn snail preferentially spawned in the presence of *Alderia* PKs, depositing egg cases that were rarely sampled in control cores. As horn snails primary graze benthic diatoms, they do not compete with *Alderia* for resources, but may benefit from the local reduction in infauna triggered by repellent slug exudates. Sediment devoid of small invertebrates could represent a protected environment for vulnerable, encapsulated snail embryos during their prolonged period of benthic development, which lasts several weeks (55). Small crustaceans and worms may physically penetrate snail egg masses and allow entry by protists, directly and indirectly causing embryo mortality. Facilitation of snail reproduction by slug compounds could constitute a byproduct mutualism, with a shelled herbivore (*Cerithideopsis*) exploiting the chemical defense of a shell-less herbivore (*Alderia*) to increase the snail's reproductive success and hence fitness (56-57).

A keystone molecule should have ecosystem effects disproportionate to its concentration, but no universal threshold for such a concentration exists. Slugs steadily secrete a suite of alderenes in their mucus secretions, and must release larger pulses during mass die-offs; however the compounds are never expected to be abundant in the environment, outside of slug tissue. Even within slugs, concentrations of alderenes are notably low (0.1%) compared to chemical defenses of many marine invertebrates, which can exceed 10% of dry weight (58). In field trials, if alderenes were dispersed throughout the surface sediments in a core, they would have been present at a concentration of <500 μg/L of mud; however, loss of metabolites to dissolution in seawater, adsorption and oxidation would likely reduce the concentration markedly over the course of a day. We thus propose that alderenes meet the current definition of keystone molecules, exerting strong effects on consumers, infauna, and surface grazers disproportionate to their abundance in the environment.

Broader implications for ecology and evolution

Although few marine heterobranchs reach the exceptional densities of *Alderia*, many invertebrates and algae are both locally abundant and rich in secondary metabolites (22, 58-60). Allelopathy, in which the fitness of competing species is reduced by compounds released from a producing organism, has been well studied in terrestrial plants and some marine organisms (61-62). However, little attention has gone to 'off-target' effects of allomones leaking into the environment on neighboring taxa that do not obviously interact or compete with the producing organism. Marine natural products are often highly bioactive and could alter invertebrate and

microbial communities in adjacent sediments and on nearby surfaces; any suppression in local species could have cascading impacts on biodiversity-function effects. For instance, sponges are the most chemically rich animal group, and could alter their environment via release of compounds into excurrent water flows or shed cells (63-64). Dense stands of chemically defended algae like *Caulerpa* could similarly affect many taxa sensitive to their metabolites. The extent to which chemistry weaves unexpected links in interaction networks thus warrants further study by marine ecologists.

The release of protective compounds also presents opportunities for byproduct mutualisms to evolve, allowing resistant species to benefit from a chemical 'shadow' and exploit the absence of susceptible species near a producing organism. As byproduct mutualisms are thought to be one route to stable mutualisms and cooperative behavior (56-57), such relationships can have evolutionary consequences for species interactions. The potential benefits of 'leaky' defenses for adjacent species thus deserve further exploration, both in the *Alderia-Vaucheria* system and in diverse other marine ecosystems. As abundant but unpalatable organisms also present models for the evolution of Batesian mimics, their chemistry may trigger a range of coevolutionary responses in associated species.

Recent work characterized the AFPKs, a new PK-synthesizing enzyme family that is widespread in bilaterian invertebrates but distinct from the canonical PK synthase enzymes found in animals and other domains of life (44-46). Clade Sacoglossa contains a private lineage of AFPK enzymes not detected in other gastropods, with distinct enzymes in photosynthetic (e.g., *Elysia*) versus non-photosynthetic (e.g., *Alderia*) species (45-46). The AFPK genes identified here are among the first animal genes identified that produce a non-venom chemical defense. Taken together, our findings thus far indicate sacoglossans evolved to produce longer-chain PKs (potential antioxidants and sunscreens) in photosynthetic species from an ancestral defensive role for AFPKs, making shorter-chain antifeedants like the alderenes (46). Comparing the AFPKs identified here, which biosynthesize smaller defensive molecules, to the AFPKs that generate bicyclic pyrones in *Elysia* spp. should inform our understanding of how metabolic pathways evolve novel functions. This work should also contribute to the development of the "keystone genes" concept (65) by linking variants in biosynthetic pathways to functional differences that change the properties of secreted chemicals, which in turn alter community structure and ecosystem function. Sacoglossans are sister to Pneumopulmonata, a hyperdiverse radiation that includes several lineages that evolved amphibious to fully terrestrial lives (43). As several air-breathing lineages (*Siphonaria*, *Onchidium*) also biosynthesize PKs (66-67), AFPK enzymes may have facilitated gastropod transitions to semi-terrestrial habitats and been important pre-adaptations underlying this explosive radiation. The role of this pathway in animal diversification also warrants further evolutionary study.

MATERIALS AND METHODS

Alderia abundance and population dynamics

Mean and peak densities for California populations of *A. willowi* and *A.* cf. *modesta* were estimated where the two species co-occur over a 100 km overlap zone along California's northern coast, from Bodega Harbor (northern range limit of *A. willowi*) to San Francisco Bay (southern limit of *A.* cf. *modesta*) (37). Monthly to quarterly surveys were performed in four estuaries within this overlap zone from Dec 2007 through Mar 2010, with supplemental surveys conducted before and afterwards. Permanent 30 m transect lines were established along the *Vaucheria* belt parallel to tidal channels or the shoreline in Bodega Bay ($N = 2$), Tomales Bay (N

= 2), Bolinas Lagoon (N = 1) and Mill Valley, San Francisco Bay (N = 4). Transect midpoints were recorded using a Garmin eTrex hand-held GPS unit. Temperature data-loggers (Onset Corp; Bourne, MA) were attached to steel rebar anchored into the mudflat next to each transect at the same tidal height. Sensors were buried just under the mud surface to measure ecologically relevant temperatures experienced by *Alderia* at 5 min intervals. Daily maximum temperature of the mud surface was extracted for days when mass die-offs were observed.

Surveys were performed over 1-2 low tides by placing 3-4 quadrats (0.5 m^2) at 10 m intervals along a transect, removing all *Alderia* specimens by hand. A quadrat was surveyed by 1-2 collectors for up to 2 hr until 5 min passed without finding any slugs (full details in ref. 37). Live slugs were typed to species by microscopic examination, or for ambiguous specimens by multiplex PCR using custom primers to amplify species-diagnostic fragments differing in size for the mitochondrial COI gene (P. Krug and R. Ellingson, unpublished data). A haphazardly chosen subset of slugs from each transect (N = 15) were individually blotted dry and weighed to ± 0.1 mg to assess size distributions and recruitment. A non-parametric Spearman's rank correlation was used to test for a relationship between abundance and size for each species in San Francisco Bay over the survey period.

Surveys for *A. willowi* were performed in 2022-2023 at two sites in Los Angeles, California, USA by establishing permanent transects and monitoring at monthly intervals as above. Surveys for ecologically relevant predators were also performed at these sites. Additional density data for *A. modesta* (Europe) and *A.* cf. *modesta* (Oregon, Russia) were taken from (29-33) and corrected for species identity (Table S1). Linear regressions were performed for density, pooled for all *Alderia* spp., versus latitude. As the highest latitude site (Norway) also had the highest reported mean and peak densities, analyses were repeated excluding Norway as a potential outlier (Supplementary Fig. 13), both using raw counts and after natural log-transforming both variables. These sensitivity analyses indicated that removing Norway had little effect on the positive relationship between density and latitude, or on the goodness-of-fit as measured by R^2, and thus Norway was not driving the result.

Isolation and structure elucidation of alderenes

Live *A. willowi* were collected Nov 2020 from San Pedro, CA under a Scientific Collecting Permit (SC 001494) from the CA State Department of Fish and Wildlife. Some slugs (N=7) were individually preserved in EtOH, while two bulk collections (N=50) of a combined 50 mg wet weight were frozen at -20°C prior to shipment on ice to the National Institutes of Health (NIH) in Bethesda, MD. Mass spectrometry of extracts was conducted to establish the relative masses and fragmentation patterns of compounds, and variability among individuals.

Compounds **1** – **5** were isolated as follows: 150 whole *A.* cf. *modesta* (2.3 g wet weight, collected 10/31/2020 from San Pablo Bay, 38°09'07.6"N, 122°26'12.4"W) were extracted five times with acetone under sonication in 5 min intervals. The extract was evaporated under vacuum to produce an aqueous suspension, which was taken up in brine (10 ml) and extracted three times with dichloromethane (10 ml). The organic phase was evaporated under reduced pressure to afford 90 mg of a green oil. This material was loaded onto HP20ss and the resin bed washed with water, then methanol and finally acetone (20 ml each) and the eluent evaporated under reduced pressure. The acetone fraction contained lipids including sterols; the methanol fraction produced a gold-colored oil (29 mg), with polyketides the main compounds noticeable by NMR analysis. The methanol fraction was separated by semi-preparative HPLC performed on a Hitachi Primaide system equipped with a photodiode array detector (1110 pump and 1430

DAD) and a Phenomenex Luna Phenyl-Hexyl 100 Å column (10 x 250 mm, 5 μm), providing compounds **1** (570 μg), **2** (180 μg), **3** (350 μg), **4** (80 μg) and **5** (50 μg).

IR spectra were recorded on a Nicolet iS5 FT-IR spectrometer operating in attenuated total reflectance (ATR) mode (Thermo Scientific). Optical rotations were recorded on a Perkin Elmer Model 343 polarimeter). High-resolution mass spectra (HR-MS) were obtained using a Waters Acquity UPLC linked to a Waters Xevo G2-XS Q-tof. ^{1}H NMR and ^{13}C NMR spectra were recorded on a Varian iNOVA 500 (^{1}H 500 MHz) NMR spectrometer equipped with a 3 mm Nalorac MDBG probe, or a Varian iNOVA 600 (^{1}H 600 MHz) NMR spectrometer equipped with a 5 mm Varian inverse cold probe operated using VNMRJ 4.2. Data were processed and analyzed using MestreNova 9.1.0. Chemical shifts were referenced to the solvent residual proton for ^{1}H NMR (δ 7.25 for $CDCl_3$) and the ^{13}C signal for ^{13}C NMR (δ 77.2 for $CDCl_3$).

Alderene A (1): Clear oil; $[\alpha]_D^{20}$ +43.8 (*c* 0.160, $CHCl_3$); UV (MeOH) λ_{max} (log ε) 232 (4.2); ECD (0.35 mM, MeCN), λ_{max} (Δε) 219 (+19), 260 (-8.3) nm; IR (ATR) ν_{max} 2916, 1711, 1616, 1458, 1360, 1290, 1272, 1223, 1090, 1017; NMR see Table 1; HRESIMS *m/z* 259.1322 (calculated for $C_{14}H_{20}O_3Na^+$, 259.1305).

Alderene B (2): Clear oil; $[\alpha]_D^{20}$ +36.2 (*c* 0.051, $CHCl_3$); UV (MeOH) λ_{max} (log ε) 234 (3.3); ECD (0.11 mM, MeCN), λ_{max} (Δε) 259 (+5.3) nm; IR (ATR) ν_{max} 2923, 1713, 1615, 1459, 1362, 1291, 1271, 1220, 1064, 1015; NMR see Table 1; HRESIMS *m/z* 273.1484 (calculated for $C_{15}H_{22}O_3Na^+$, 273.1462).

Alderene C (3): Clear oil; $[\alpha]_D^{20}$ +31.0 (*c* 0.100, $CHCl_3$); UV (MeOH) λ_{max} (log ε) 231 (4.1); ECD (0.21 mM, MeCN), λ_{max} (Δε) 223 (+24), 263 (-2.4) nm; IR (ATR) ν_{max} 2922, 1713, 1617, 1458, 1361, 1290, 1272, 1223, 1065, 1017; NMR see Table 1; HRESIMS *m/z* 273.1483 (calculated for $C_{15}H_{22}O_3Na^+$, 273.1462).

Alderene D (4): Clear oil; $[\alpha]_D^{20}$ +16.7 (*c* 0.024, $CHCl_3$); UV (MeOH) λ_{max} (log ε) 235 (3.5); ECD (0.06 mM, MeCN), λ_{max} (Δε) 257 (+8.4); IR (ATR) ν_{max} 2922, 2852, 1735, 1685, 1647, 1559, 1458, 1379, 1321, 1092; NMR see Table 1; HRESIMS *m/z* 287.1639 (calculated for $C_{16}H_{24}O_3Na^+$, 287.1639).

Alderene E (5): Clear oil; NMR see table; HRESIMS *m/z* 259.1323 (calculated for $C_{14}H_{20}O_3Na^+$, 259.1305).

Electronic circular dichroism spectral prediction

Alderene **1** was determined to be of the (5*S*,6*R*)-configuration by comparison of predicted and experimental ECD spectra. Briefly, a conformer search was performed manually using a combination of MMFF calculations and comparison to NMR data, primarily NOESY. Four major, non-degenerate conformers were identified including two pyrone conformational states (with *trans* side chain and methyl groups either *pseudo*-equatorial or *pseudo*-axial) and two diene conformational states (*S-cis* configured *E,E*-diene system twisted out of plane plus or minus 45°). These were optimized using density functional theory with a B3LYP functional and a 6-31G(d) basis set in Gaussian v.16 (68). Electronic and thermal energy corrections were calculated at 25°C using frequency calculations. The ECD spectra were calculated using TD-DFT at the previous level of theory along with an acetonitrile CPCM solvent model. Gaussview

v.6 was used to plot and export the ECD spectra, which were then Boltzmann weighted and averaged. A correction factor (+25 nm) was added to account for systematic errors in computed transition energies.

Metabolite quantification

A collection of *A.* cf. *modesta* (20.3 g) was separated into four groups with a mean wet weight of 5.01 g ± 0.48 SD. Each group was extracted in an identical manner by sonicating in acetone (15 ml) three times and pooling extractions for a group, yielding four replicate extracts of ~45 ml each. Samples were diluted to exactly 50 ml in a volumetric flask with acetone. An aliquot (20 µl) of each sample was diluted in methanol (200 µl) in a glass insert and analyzed by LCMS. The peak for compound **1** (R_t 4.01 min) was integrated in each total ion chromatogram and the area compared to a standard curve (prepared by analyzing solutions of purified **1** in 2-fold serial dilution starting at 50 µg/ml). The concentration of **1** in each sample was calculated and determined to be on average 919 ppm (±0.00938 ppm SD), or 0.09% wet weight.

Identification and phylogenetic relationships of biosynthetic AFPKs

Total RNAs were extracted from live *A.* cf. *modesta* (two pools of 10 slugs each) using Trizol extraction (Invitrogen) and DNA was removed using the DNA-*free* DNA Removal Kit (Invitrogen). Illumina sequencing was performed at the Huntsman Cancer Institute High Throughput Genomics Core. The Illumina TruSeq Stranded mRNA Kit was used for library preparation with unique dual indexes (UDI) and the library sequenced using a NovaSeq S4 Reagent Kit to generate 150 bp paired end reads and 2500 M read-pairs total. The raw reads were trimmed using Trimmomatic and trimmed reads *de novo* assembled using SPAdes (69). The transcriptome was searched by tblastn using sacoglossan AFPK protein sequences as queries (44). Phylogenetic analysis was performed using a previously described set of selected PKS, FAS and AFPK protein sequences (44). An initial alignment was made and aligned sequences trimmed to about 1,300 amino acid residues. A second alignment was generated using Geneious (alignment type: global with free end gaps; cost matrix: Blosum 45; gap open penalty: 12; gap extension penalty: 3; refinement iterations: 3) and analyzed by maximum likelihood using the IQ-TREE web tool (Los Alamos National Lab) with the following options: number of sequences 42; Sequence type & substitution model, Amino acids, Blosum62; Rate heterogeneity, None; State frequency, Estimated by ML; Bootstrap branch support, None; Single branch test, None; Tree search, Perturbation strength 0.5, # of unsuccessful iterations to stop = 100; Root tree, None (70). Transcripts were quantified using Salmon (71). Values reported are the average of two biological replicates.

Antifeedant assays: whole slugs and egg masses

Three generalist predators co-occurring with *Alderia* in Californian estuaries were used: the arrow goby *Clevelandia ios*, polychaete worm *Nereis arenaceodentata*, and lined shore crab *Pachygrapsus crassipes*. Fish and crabs were collected by hand using a small net under permit SC 001494. Polychaete worms were purchased from Aquatic Toxicology Support LLC (Bremerton, WA). Slugs were hand-collected in the field and maintained on algae in plastic bins in an incubator at 16°C on a 14:10 light: dark cycle. Live slugs used in experiments were housed for 1 wk after a predation trial to assess delayed mortality in glass dishes in 500 ml of aerated, 24‰ artificial sea water (ASW), with algae changed every 2 d. Predators were housed in individual containers and acclimated for 1 wk before trials. Fish were individually maintained in

tanks with 19 L of ASW following all federal and institutional guidelines for vertebrate work (IACUC protocol number 1013-01). Crabs and worms were housed in individual plastic bins with 100 or 500 ml ASW, respectively, and appropriate substrate. Seawater was changed 3 times/week. Predators were fed squid flesh every 2 d, and worms were also fed dried algae (*Enteromorpha*). Prey items were offered via pipet and each predator was used only once per trial; predators that rejected any prey item were then offered squid to confirm willingness to feed.

In assays with live slugs, fish ($N = 10$), crabs ($N = 9$) and worms ($N = 20$) were used after 2 d of starvation to ensure readiness to feed. In separate trials, each predator was individually offered a live *A.* cf. *modesta* or *A. willowi,* and a control piece of squid of equivalent wet weight and volume to the slug. Predators were offered a slug or control in a randomized order; any that rejected a slug were subsequently offered squid to confirm they were willing to feed. Trials were observed and recorded for 5 min from the time a prey item was introduced, scoring time to fully consume a meal and number of attacks on a prey item. Due to non-normality of the data, time and number of attacks were compared between treatment and controls using non-parametric sign tests, while the proportion of live slugs versus controls consumed was compared using Fisher's exact test (59-60, 72).

Comparable assays were then run testing dead slugs to determine if active mucus secretion was an essential component of slug defense. Slugs were flash-frozen at -80°C overnight, then thawed for 1 hr. Control pieces of squid were frozen/thawed in parallel. Fish and crabs ($N = 10$ each) were offered a frozen/thawed specimen of *A. willowi* or squid in random order as described above. To test whether solvent extraction (removing potential nonpolar feeding deterrents) rendered slug tissue palatable, frozen slugs were incubated in acetone for 24 hr then rehydrated in seawater prior to trials. A control piece of squid of equivalent wet weight and volume to each individual slug was extracted and rehydrated in parallel to ensure feeding cues were not removed by acetone extraction. Fish ($N = 10$), crabs ($N = 9$) and worms ($N = 10$) were offered an acetone-extracted slug (separate trials for each *Alderia* species) and a control in random order. Time spent consuming prey items met assumptions of normality and was compared using independent *t*-tests for trials on extracted slugs.

To test whether slugs incorporate defensive compounds into egg masses, fish and crabs ($N = 10$ each) were offered an egg mass of *A. willowi* and a control piece of squid in random order, and the proportion of each consumed was compared by Fisher's exact test for each predator. A second trial was done cutting egg masses in half to expose the gelatinous string of embryos, to assess whether fish ($N = 10$) would consume embryos more readily without having to bite through the outer casing of the egg mass.

Antifeedant assays: slug extracts and pure alderenes

Bioassay-guided fractionation was employed to identify the compound(s) responsible for deterrent properties of slugs. Collections of *A.* cf. *modesta* and *A. willowi* ($N = 50$ to 100 slugs per species, 100 mg wet weight total per species) were separately extracted three times sequentially with 50 ml of acetone for 24 hr. Combined extracts of each species were concentrated by rotary evaporation and partitioned three times between ethyl acetate and water; the organic layer was concentrated and dried (~11 mg per species). An artificial food for testing extract palatability was made by homogenizing squid mantle in water at a 1:1 ratio by mass and adding sodium alginate to yield a 2% final concentration (59-60). The mass of squid tissue homogenized was equal to the mass of sea slug tissue extracted, to ensure extract was tested in proportion to the natural concentration in slugs; volumes of tissue were also equivalent. We

homogenized 89 mg of squid mantle plus 2 mg of sodium alginate in 0.1 ml water for each *Alderia* sp.; the corresponding organic extract (11 mg) of each species was re-solubilized in 50 µl acetone and added to the homogenate. Ingredients were mixed in a 1 ml syringe and extruded into 0.25 M $CaCl_2$ to solidify into slug-sized (4 mm) treatment pellets. Solvent-only control pellets were made with 100 mg of squid mantle blended in 0.1 ml water with 2 mg of sodium alginate and 50 µl acetone added. After 2 d without food, each predator was offered an extract-treated pellet vs. a control pellet and the proportion of pellets consumed compared using Fisher's exact test; separate trials were run for each *Alderia* sp. × predator combination.

A collection of *A. willowi* made in Nov 2020 from San Pedro, CA (N = 100 slugs; 99 mg wet weight) was frozen at -20°C, extracted in acetone, and partitioned into organic and aqueous layers. The organic layer was further partitioned between a methanol fraction, highly enriched in polyketides (~95% pure by NMR), and a hexane layer containing sterols and fats (Fig. S7). Preliminary feeding assays indicated the deterrent effect of *Alderia* extract was contained in the PK-enriched methanol fraction and not the hexane layer. To confirm that alderenes were responsible for the antipredator activity of extracts, pure compounds **1** and **3** were bioassayed following structure elucidation. A collection of 150 *A.* cf. *modesta* (2.3 g wet weight) in March 2021 yielded a semi-purified extract (29 mg) that was mostly PK by NMR. Purification by HPLC yielded 1.2 mg of pure PKs ranging from 80 to 570 µg per metabolite for bioassays. Alderenes **1** and **3** were tested in crab and fish assays at 0.025%, 0.05% and 0.1% of tissue weight in pellets, or approximately 25%, 50% and 100% of the natural concentration of alderene **1** estimated for *A.* cf. *modesta* by wet weight. A stock solution was prepared by homogenizing 100 mg of squid mantle tissue in 0.1 ml water with 2 mg sodium alginate. The appropriate amount of each compound was taken up in 10 µl of methanol and added to 40 µl of homogenate, then mixed with $CaCl_2$ solution to yield 10 food pellets containing 10 µg (0.025%), 20 µg (0.05%) or 40 µg (0.1%) of each alderene. Consumption was scored compared to both positive and negative controls prepared in parallel during 5 min trials. Negative controls were solvent-only control pellets; positive controls incorporated crude extract prepared freshly and made at 25%, 50% or 100% on a per-weight basis.

Due to limited quantities of pure compounds, pellets were smaller than in previous assays and predators were more likely to ingest at least a portion of treatment pellets. We therefore recorded 5 min feeding trials on video and scored behaviors indicating deterrence. For crabs, such behaviors included time processing pellets during feeding attempts; time spent removing particles or mucus from mouthparts; proportion of individuals that rubbed or pressed mouthparts against substrate; number of cheliped movements into the mouth during feeding attempts; and number of cheliped movements pulling from the mouth post-feeding. For fish, behaviors included the number of times a pellet was regurgitated during feeding attempts; the initial delay before a feeding attempt was made; and total prey-handling time including repeated regurgitation or bites to break pellets into smaller pieces. Fish behaviors could only be tested at 25% and 50% of natural concentrations due to limited quantities of pure alderenes. Response variables recorded as time or number were compared for treatment pellets vs. controls using a nonparametric paired Sign test (both predators); the proportion of crabs pressing mouthparts against the substrate was compared for treated vs. control pellets using Fisher's exact test.

Field assays of community response to alderenes

Manipulative field experiments were performed at the Salinas de San Pedro salt marsh to assess the response of mudflat community species to alderenes. In pilot surveys, dominant

infauna were small crustaceans (amphipods, benthic copepods), diverse worms and molluscs. The only common invertebrate on the mud surface in the *Vaucheria* belt was the California horn snail, *Cerithideopsis californica*, but snails were more abundant among cordgrass higher in the marsh. We assessed the response of the mudflat community in two trials performed in Jun and Dec 2022. *Alderia* had been present year-round in this marsh prior to 2018, but at the time of each 2022 field trial, no *Alderia* were detected in surveys for >2 months during a prolonged population crash. Specimens of *A. willowi* ($N = 75$) were collected from the Golden Shores site (Long Beach, CA), weighed (Jun: 519 mg; Dec: 467 mg), and extracted in acetone twice for 24 hr. Pooled extracts were dried by rotary evaporation, then partitioned three times between ethyl acetate and water; organic layers were dried and weighed (Jun: 3.3 mg; Dec: 3.0 mg).

Slug organic-layer extracts were then applied to the mud surface to simulate the release of PKs in slug pedal mucus or during mass die-off events. Replicate pairs ($N = 5$) of treatment and control patches were marked at 3 m intervals along a permanent transect. Each patch was a circle 5 cm in diameter. Extract was redissolved in 1 ml of methanol and divided into five aliquots. Methanolic extract (200 µl) was applied onto the mud surface of treatment patches, delivering *Alderia* organic-layer PKs corresponding to 15 slugs per aliquot (equal to a moderate density of 300 slugs/m^2). Paired control patches received an equivalent application of 200 µl methanol. Solvent evenly dispersed over the mud surface and was quickly absorbed. After 24 hr (two high tides), each patch was cored to 2.5 cm depth using a pre-marked 5 × 12 cm cellulose acetate butyrate (CAB) plastic liner tubes for infaunal community analysis (73-74). Cores were fixed in 5% neutral buffered formalin for 2 d. Sediment was passed over a 1 mm pre-filter, then infauna were retained on stacked 500 and 300 µm mesh sieves; retained material was transferred to 70% ethanol and stained with Rose Bengal dye (75-76). Macrofauna and meiofauna were separated under a dissecting microscope and identified to the lowest taxonomic group possible following (77). Annelids were identified to the genus level in collaboration with L. Harris and archived in the Los Angeles County Museum of Natural History collection.

Field experiments included a fixed effect, paired treatment versus control cores, as well as a random effect of trial season. The R package lme4 (78) was used to create generalized linear mixed-effect models (GLMM) with the glmer function, to compare mean abundance for each taxonomic group. The Poisson distribution was used for GLMMs as the response variable (abundance) was count data. Analyses were run in R 4.2.3 (79).

To determine if community diversity differed between the treatment and control cores, the Shannon-Wiener Index and Simpson's Dominance Index were calculated for each core. Shannon's index is an information statistic index that assumes all species were represented and randomly sampled in a community. Simpson's index is a dominance index that accounts for both the number of species present and the relative abundance of each species in the community. Mean values were compared between treatment and control cores using the glmer function with a gamma distribution, as the response variables were continuous and non-negative.

REFERENCES

1. R. T. Paine, Food web complexity and species diversity. *Amer. Nat.* **100**, 65-75 (1966).
2. R. T. Paine, A note on trophic complexity and community stability. *Amer. Nat.* **103**, 91-93 (1969).
3. M. Power, D. Tilman, J. Estes, B. A. Menge, W. Bond, L. Mills, G. Daily, J. Castilla, J. Lubchenco, R.T. Paine, Challenges in the quest for keystones: Identifying keystone

species is difficult but essential to understanding how loss of species will affect ecosystems. *BioScience* **46**, 609-620 (1996).
4. F. Jordan, Keystone species and food webs. *Phil. Trans. Roy. Soc. B* **364**, 1733-1741 (2009).
5. G. Pohnert, M. Steinke, R. Tollrian, Chemical cues, defense metabolites and the shaping of pelagic interspecific interactions. *Trends Ecol. Evol*. **22**, 198-204 (2007).
6. M. E. Hay, Marine chemical ecology: chemical signals and cues structure marine populations, communities, and ecosystems. *Annu. Rev. Mar. Sci.* **1**, 193-212 (2009).
7. M. E. Hay, J. Kubanek, 2002. Community and ecosystem level consequences of chemical cues in the plankton. *J. Chem. Ecol*. **28**, 2001-2016.
8. R. P. Ferrer, R. K. Zimmer, Community ecology and the evolution of molecules of keystone significance. *Biol. Bull*. **223**, 167-177 (2012).
9. R. P. Ferrer, R. K. Zimmer, Molecules of keystone significance: Crucial agents in ecology and resource management. *Bioscience* **63**, 428-438 (2013).
10. R. K. Zimmer, R. P. Ferrer, Neuroecology, chemical defense, and the keystone species concept. *Biol. Bull*. **213**, 208-225 (2007).
11. R. Kvitek, C. Bretz, Harmful algal bloom toxins protect bivalve populations from sea otter predation. *Mar. Ecol. Prog. Ser*. **271**, 233-243 (2004).
12. G. V. Wolfe, The chemical defense ecology of marine unicellular plankton: constraints, mechanisms, and impacts. *Biol. Bull*. **198**, 225-244 (2000).
13. M. S. Savoca, G. A. Nevitt, Evidence that dimethyl sulfide facilitates a tritrophic mutualism between marine primary producers and top predators. *Proc. Natl. Acad. Sci. USA* **111**, 4157-4161 (2014).
14. K. L. Van Alstyne, M. Puglisi, DMSP in marine macroalgae and macroinvertebrates: Distribution, function, and ecological impacts. *Aquat. Sci*. **69**, 394-402 (2007).
15. F. Sánchez-Piñero, G. A. Polis, Bottom-up dynamics of allochthonous input: direct and indirect effects of seabirds on islands. *Ecology* **81**, 3117-3132 (2000).
16. W. H. Hol, A. Van Veen, Pyrrolizidine alkaloids from *Senecio jacobaea* affect fungal growth. *J. Chem. Ecol*. **28**, 1763-1772 (2002).
17. J. R. Trigo, Effects of pyrrolizidine alkaloids through different trophic levels. *Phytochem. Rev*. **10**, 83-98 (2011).
18. E. M. Hill, L. A. , Robinson, A. Abdul-Sada, A. J. Vanbergen, A. Hodge, S. E. Hartley, Arbuscular mycorrhizal fungi and plant chemical defense: Effects of colonisation on aboveground and belowground metabolomes *J. Chem. Ecol*. **44**, 198-208 (2018).
19. K. M. Dahlstrom, D. L. McRose, D. K. Newman, Keystone metabolites of crop rhizosphere microbiomes. *Curr. Biol.* **30**, R1131-R1137 (2020).
20. K. Dettner, Toxins, defensive compounds and drugs from insects. Pp. 49-103 in: K. H. Hoffmann (ed), *Insect Molecular Biology and Ecology*, CRC Press, Boca Raton, FL (2014).
21. G. Cimino, M. Ghiselin, Chemical defense and the evolution of opisthobranch gastropods. *Proc. Cal. Acad. Sci*. **60**, 175-422 (2009).
22. J. R. Pawlik, Marine invertebrate chemical defenses. *Chem. Rev*. **93**, 1911-1922 (1993).
23. D. Obermann, B. Ulf., H. Wägele, Incorporated nematocysts in *Aeolidiella stephanieae* (Gastropoda, Opisthobranchia, Aeolidoidea) mature by acidification shown by the pH sensitive fluorescing alkaloid Ageladine A. *Toxicon* **60**, 1108-1116 (2012).

24. P. J. Krug, K. G. Boyd, D. J. Faulkner, Isolation and synthesis of Tanyolides A and B, metabolites of the nudibranch *Sclerodoris tanya*. *Tetrahedron* **51**, 11063-11074 (1995).
25. N. Bednaršek, C. Harvey, I. Kaplan, R. Feely, J. Možina, Pteropods on the edge: Cumulative effects of ocean acidification, warming, and deoxygenation. *Prog. Oceanogr.* **145**, 1-24 (2016).
26. D. B Cadien, J. Ranasinghe, "Invaders in the open sea: establishment of the New Zealand snail *Philine auriformis* in southern California coastal waters" in *Annual report of the Southern California coastal water research project*, S. B. Weisberg, D. Elmore, Eds. (Westminster, 2003), pp. 253–265.
27. C. D. Trowbridge, C. D. Todd, Host-plant change in marine specialist herbivores: ascoglossan sea slugs on introduced macroalgae. *Ecol. Monogr.* **71**, 219-243 (2001).
28. C. E. Kicklighter, M. Kamio, L. Nguyen, M. W. Germann, C. D. Derby, Mycosporine-like amino acids are multifunctional molecules in sea hares and their marine community. *Proc. Nat'l Acad. Sc.i USA*, **108**, 11494-11499. (2011).
29. C. den Hartog, Distribution and ecology of the slugs *Alderia modesta* and *Limapontia depressa* in the Netherlands. *Beaufortia* **7**, 15-36 (1959).
30. U. Seelemann, Rearing experiments on the amphibian slug *Alderia modesta*. *Helgoländer Wissenschaftliche Meeresuntersuchungen* **15**, 128-134 (1967).
31. W. Vader, *Alderia modesta* (Gastropoda, Sacoglossa) in northern Norway. *Fauna Norvegia Ser. A* **2**, 41-46 (1981).
32. A.V . Chernyshev, E. M. Chaban, The first findings of *Alderia modesta* (Lovén, 1844) (Opistobranchia, Ascoglossa) in the Sea of Japan. *Ruthenica* **14**, 131-134 (2005).
33. C. D. Trowbridge, Local and regional abundance patterns of the ascoglossan (=sacoglossan) opisthobranch *Alderia modesta* (Lovén, 1844) in the northeastern Pacific. *Veliger* **36**, 303-310 (1993).
34. R. A. Ellingson, P. J. Krug, Evolution of poecilogony from planktotrophy: Cryptic speciation, phylogeography and larval development in the gastropod genus *Alderia*. *Evolution* **60**, 2293-2310 (2006).
35. P. J. Krug, R. A. Ellingson, R. Burton, A. A. Valdés, A new poecilogonous species of sea slug (Opisthobranchia: Sacoglossa) from California: Comparison with the planktotrophic congener *Alderia modesta* (Lovén, 1844). *J. Moll. Stud.* **73**, 29-38 (2007).
36. P. J. Krug, Poecilogony and larval ecology in the gastropod genus *Alderia*. *Amer. Malacol. Bull.*, **23**, 99-111 (2007).
37. M. N. Garchow, "Population dynamics at the range boundary between sister species of the estuarine sea slug genus *Alderia*: Role of the physical environment versus larval supply," M.S. thesis, California State University, Los Angeles, CA (2010).
38. P. J. Krug, E. Shimer, V.A. Rodriguez, Differential tolerance and seasonal adaptation to temperature and salinity stress at a dynamic range boundary between estuarine gastropods. *Biol. Bull.*, **241**, 105–122 (2021). (https://doi.org/10.1086/715845)
39. K. W. Able, A re-examination of fish estuarine dependence: evidence for connectivity between estuarine and ocean habitats. *Est. Coast. Shelf Sci.* **64**, 5-17 (2005).
40. S. Rosa, J. Granadeiro, C. Vinagre, S. França, H. Cabral, J. M. Palmeirim, Impact of predation on the polychaete *Hediste diversicolor* in estuarine intertidal flats. *Estuar. Coast. Shelf Sci.* **78**, 655-664 (2008).

41. M. Sheaves, R. Baker, I. Nagelkerken, R. M. Connolly, True value of estuarine and coastal nurseries for fish: incorporating complexity and dynamics. *Estuar. Coasts* **38**, 401-414 (2015).
42. C. D. Trowbridge, Defensive responses and palatability of specialist herbivores: Predation on NE Pacific ascoglossan gastropods. *Mar. Ecol. Prog. Ser.* **105**, 61-70 (1994).
43. P. J. Krug, S. A. Caplins, K. Algoso, K. Thomas, Á. A. Valdés, R. Wade, N. L. Wong, D. J. Eernisse, K. M. Kocot, Phylogenomic resolution of the root of Panpulmonata, a hyperdiverse radiation of gastropods: new insight into the evolution of air breathing. *Proc. Roy. Soc. B* **289**, 20211855 (2022).
44. J. Torres, Z. Lin, J. Winter, P. J. Krug, E. W. Schmidt, Animal biosynthesis of complex polyketides in a photosynthetic partnership. *Nature Comm.* **11**, 2882 (2020).
45. Z. Lin, F. Li, P. J. Krug, E. W. Schmidt, The polyketide to fatty acid transition in the evolution of animal lipid metabolism. *Nature Comm.,* in press.
46. F. Li, Z. Lin, P. J. Krug, J. L. Catrow, J. E. Cox, E. W. Schmidt, Animal FAS-like polyketide synthases produce diverse polypropionates. *Proc. Natl Acad. Sci. USA* **120**, e2305575120 (2023). (https://doi.org/10.1073/pnas.2305575120)
47. A. Cutignano, A. Fontana, L. Renzulli, G. Cimino, Placidenes C-F, novel α-pyrone propionates from the Mediterranean sacoglossan *Placida dendritica*. *J. Nat. Prod*. **66**, 1399-1401 (2003).
48. M. Ciavatta, E. Manzo, G. Nuzzo, G. Villani, G. Cimino, J. Cervera, M. Malaquias, M. Gavagnin, Aplysiopsenes: an additional example of marine polyketides with a mixed acetate/propionate pathway. *Tetra. Lett*. **50**, 527-529 (2009).
49. R. R. Vardaro, V. Di Marzo, A. Marin, G. Cimino, α-and γ-Pyrone-polypropionates from the Mediterranean ascoglossan mollusc *Ercolania funerea*. *Tetrahedron* **48**, 9561-9566 (1992).
50. R. R. Vardaro, V. Di Marzo, A. Crispino, G. Cimino, Cyercenes, novel polypropionate pyrones from the autotomizing Mediterranean mollusc *Cyerce cristallina*. *Tetrahedron* **47**, 5569-5576 (1991).
51. V. Di Marzo, A. Marin, R. R. Vardaro, L. De Petrocellis, G. Villani, G. Cimino, Histological and biochemical bases of defense mechanisms in four species of Polybranchioidea ascoglossan molluscs. *Mar. Biol.* **117**, 367-380 (1993).
52. A. M., Karlson, F. J. Nascimento, J. Näslund, R. Elmgren, Higher diversity of deposit-feeding macrofauna enhances phytodetritus processing. *Ecology* **91**, 1414-1423 (2010).
53. E. N. Ieno, M. Solan, P. Batty, G. J. Pierce, How biodiversity affects ecosystem functioning: roles of infaunal species richness, identity and density in the marine benthos. *Mar. Ecol. Prog. Ser*. **311**, 263-271 (2006).
54. R. Pinto, V. N. de Jonge, J. C. Marques, Linking biodiversity indicators, ecosystem functioning, provision of services and human well-being in estuarine systems: application of a conceptual framework. *Ecol. Indicators* **36**, 644-655 (2014).
55. M. S. Race, Field ecology and natural history of *Cerithidea californica* (Gastropoda: Prosobranchia) in San Francisco Bay. *Veliger* **24**, 18-27 (1981).
56. J. L. Sachs, U. G. Mueller, T. P. Wilcox, J. J. Bull, The evolution of cooperation. *Quart. Rev. Biol*. **79**, 135-160 (2004).
57. G. Chomicki, E. T. Kiers, S. S. Renner, The evolution of mutualistic dependence. *Annu. Rev. Ecol. Evol. Syst.* **51**, 409-432 (2020).

58. C. J. Freeman, D. F. Gleason, Chemical defenses, nutritional quality, and structural components in three sponge species: *Ircinia felix*, *I. campana*, and *Aplysina fulva*. *Mar. Biol.* **157**, 1083-1093 (2010).
59. J. R. Pawlik, Antipredatory defensive roles of natural products from marine invertebrates. Pp. 677-710 in: E. Fattorusso, W. H. Gerwick, O. Taglialatela-Scafati (eds), *Handbook of Marine Natural Products*, Springer, New York (2012). doi: 10.1007/978-90-481-3834-0_12
60. M. E. Hay, J. J. Stachowicz, E. Cruz-Rivera, S. Bullard, M. S. Deal, N. Lindquist, Bioassays with marine and freshwater macroorganisms. Pp. 39-141 in: K. F. Haynes, J. G. Millar (eds), *Methods in chemical ecology*, vol. 2, Chapman & Hall, New York (1998).
61. M. J. Reigosa, N. Pedrol, L. González (eds) *Allelopathy: A physiological process with ecological implications*. Springer, Dordrecht, Holanda (2006). doi:10.1007/1-4020-4280-9
62. F. V. Ribeiro, B. A. da Gama, R. C. Pereira, Structuring effects of chemicals from the sea fan *Phyllogorgia dilatata* on benthic communities. *PeerJ* **5**, e3186 (2017).
63. M. Maldonado, Sponge waste that fuels marine oligotrophic food webs: a re-assessment of its origin and nature. *Mar. Ecol*. **37,** 477-491 (2016).
64. J. E. Thompson, K. D. Barrow, D. J. Faulkner, Localization of two brominated metabolites, aerothionin and homoaerothionin, in spherulous cells of the marine sponge *Aplysina fistularis* (= *Verongia thiona*). *Acta Zool.* **64**, 199-210 (1983).
65. M. A. Barbour, D. J. Kliebenstein, and J. Bascompte, A keystone gene underlies the persistence of an experimental food web. *Science* **376**, 70-73 (2022).
66. D. C. Manker, D. J. Faulkner, T. J. Stout, J. Clardy, The baconipyrones. Novel polypropionates from the pulmonate *Siphonaria baconi*. *J. Org. Chem*. **54**, 5371-5374 (1989).
67. D. R. Beukes, M. T. Davies-Coleman, Novel polypropionates from the South African marine mollusc *Siphonaria capensis*. *Tetrahedron* **55**, 4051-4056 (1999).
68. M. E. Frisch, G. W. Trucks, H. B. Schlegel, G. E. Scuseria, M. A. Robb, J. R. Cheeseman, G. Scalmani, V. P. Barone, G. A. Petersson, H. J. Nakatsuji, X. Li, et al., Gaussian 16, revision C. 01 (2016).
69. A. Prjibelski, D. Antipov, D. Meleshko, A. Lapidus, A. Korobeynikov, Using SPAdes de novo assembler. *Current Protocols in Bioinformatics* **70**, e102 (2020).
70. L. T. Nguyen, H. A. Schmidt, A. von Haeseler, B. Q. Minh, IQ-TREE: a fast and effective stochastic algorithm for estimating maximum-likelihood phylogenies. *Mol. Biol. Evol*. **32**, 268-274 (2015).
71. R. Patro, G. Duggal, M. Love, R. Irizarry, C. Kingsford, Salmon provides fast and bias-aware quantification of transcript expression. *Nat. Methods* 14, 417-419 (2017).
72. J. H. Zar, *Biostatistical Analysis*, 2nd ed, Prentice-Hall, Englewood Cliffs (1984).
73. N. McLain, L. Camargo, C. R. Whitcraft, J. G. Dillon, Metrics for evaluating inundation impacts on the decomposer communities in a southern California coastal salt marsh. *Wetlands*, **40**, 2443-2459 (. 2020)
74. E. J. Wenger, "Decomposer community response to sea level rise in a California salt marsh." M.S. thesis, California State University, Long Beach, CA, 81 pp. (2019).

75. EPA, Ecological Processes: What are the trends in the ecological processes that sustain the nation's ecological systems? *United States Environmental Protection Agency* (2020). https://www.epa.gov/report-environment/ecological-processes
76. P. J. Somerfield, R. M. Warwick, Meiofauna Techniques. Pp. 253-284 in: A. Eleftheriou (ed), *Methods for the Study of Marine Benthos* (4th ed), John Wiley & Sons, Chichester (2013).
77. J. T. Carlton, *The Light and Smith Manual: Intertidal Invertebrates from Central California to Oregon* (4th ed). University of California Press (2007).
78. D. Bates, M. Mächler, B. Bolker, S. Walker, Fitting linear mixed-effects models using lme4. *J. Stat. Softw.* **67**, 1-48 (2015).
79. R Core Team, R: A language and environment for statistical computing. *R Foundation for Statistical Computing*, Vienna, Austria (2023). URL https://www.R-project.org/.

Acknowledgments
The authors gratefully acknowledge assistance from L. Harris, A. Lim, A. McCurdy, B. Pernet, C. Whitcraft and A. Zellmer. For access to field sites, we thank L. Arkinstall, T. Leland, J. Passarelli, and B. Spies.

Funding:
U.S. National Science Foundation grant IOS-2127110 (EW, PJK)
U.S. National Science Foundation grant OCE-0648606 (PJK)
U.S. National Science Foundation grant IOS-2127110 (PJK)
U.S. National Science Foundation grant IOS-2127111 (EWS)
U.S. National Science Foundation grant PRFB-1907177 (SAC)
U.S. National Institutes of Health Intramural Program award NIDDK DK031135 (CAB)

Author contributions:
Conceptualization: PW, EWS, PJK
Funding acquisition: SAC, CAB, EMW, EWS, PJK
Data curation: PS, MG, PJK
Investigation: PS, PW, HN, AR, MG, SIO, EP, PJK
Formal Analysis: PS, PW, HN, AR, MG, SIO, EMW, CAB, EWS, PJK
Resources: SAC
Supervision: EWS, PJK
Visualization: PS, PJK
Writing—original draft: PJK
Writing—review & editing: all authors

Competing interests: Authors declare that they have no competing interests.

Data and materials availability: Sequences for AFPK enzymes are available from the NCBI repository (AmPKS 1, OR565848; AmPKS 2, OR565849). All other data are available in the main text or supplementary materials.

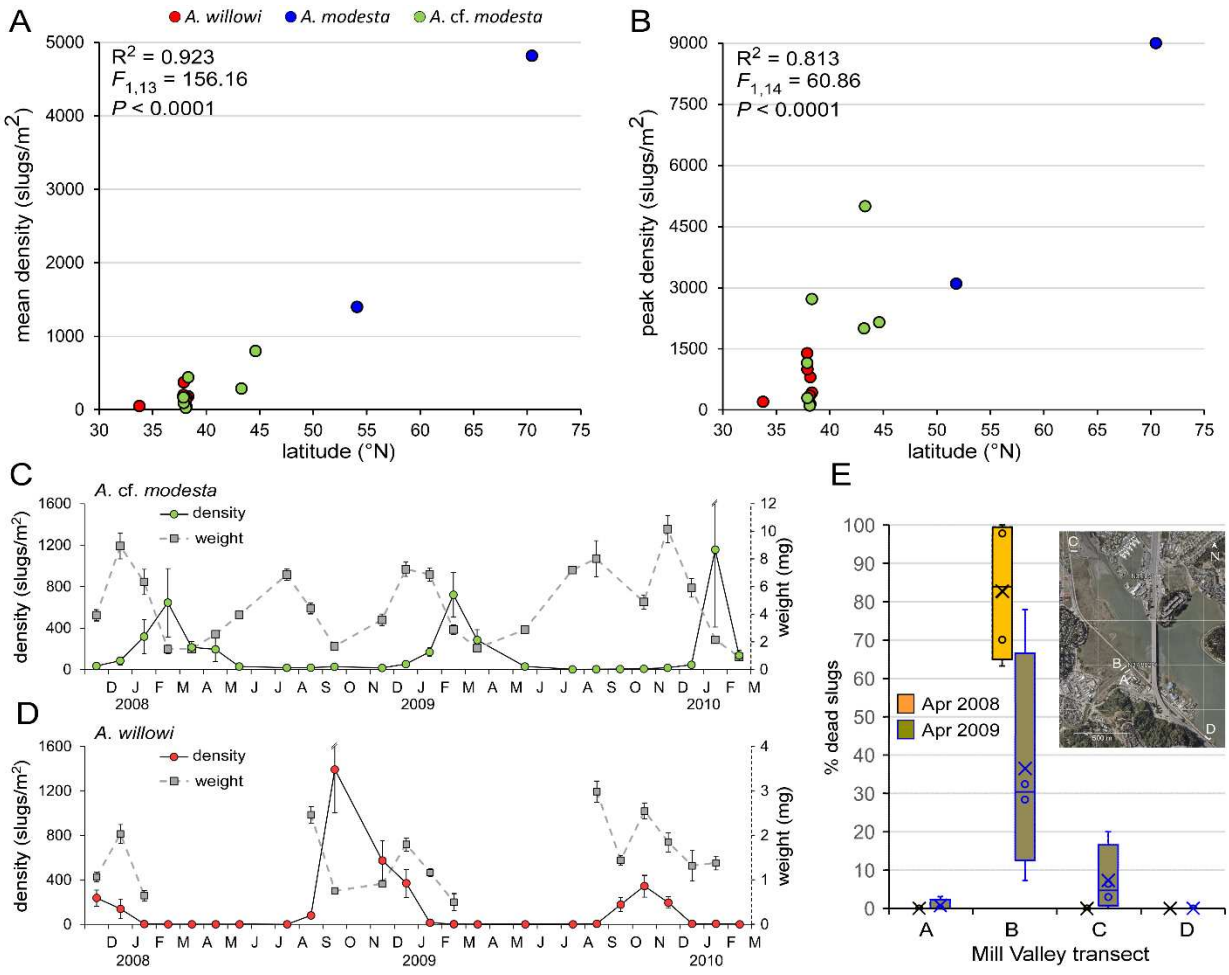

Figure 1. **Density and population dynamics of *Alderia* spp. A-B**, Exceptional mean (A) and peak (B) population densities scale with latitude in *A. modesta* (blue), *A.* cf. *modesta* (green) and *A. willowi* (red). **C-D**, Seasonal abundance and growth of *Alderia* spp. cohorts in San Francisco Bay from 2008-2010. Mean number (± SE) of slugs/m^2 plotted for *A.* cf. *modesta* (green circles) and *A. willowi* (red circles), with wet weight (grey squares, dashed lines); $N = 16$ quadrats per survey. **E**, Mass die-offs in *A.* cf. *modesta* coinciding with peak annual mud temperatures in April of 2008 and 2009. Inset: map of Mill Valley, San Francisco Bay, showing four permanent transects.

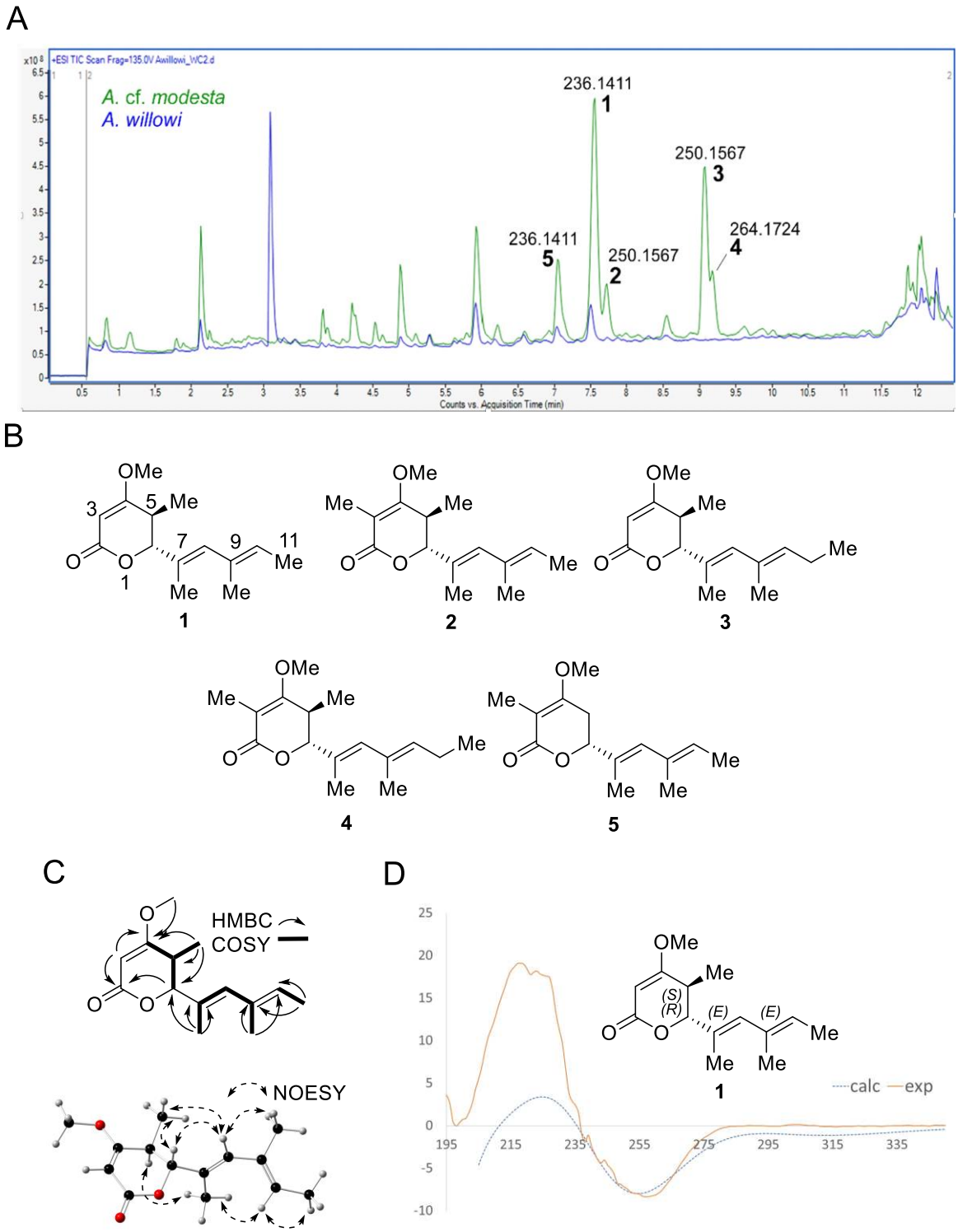

Figure 2. **Alderenes A-E, novel polyketides isolated and characterized from *Alderia*. A**, Overlaid LCMS traces of acetone extracts of an individual *A.* cf. *modesta* (green) and *A. willowi* (blue), showing the molecular masses of five novel polyketides, two from both species (**1** and **5**) and the remainder from *A.* cf. *modesta*. **B**, Structures for alderenes A-E (**1-5**). **C**, Structure elucidation and relative configuration of alderene A (**1**) determined by 2D NMR experiments. **D**, Comparison of experimental vs calculated electronic CD spectra confirmed the structure and absolute configuration of **1** as diagrammed.

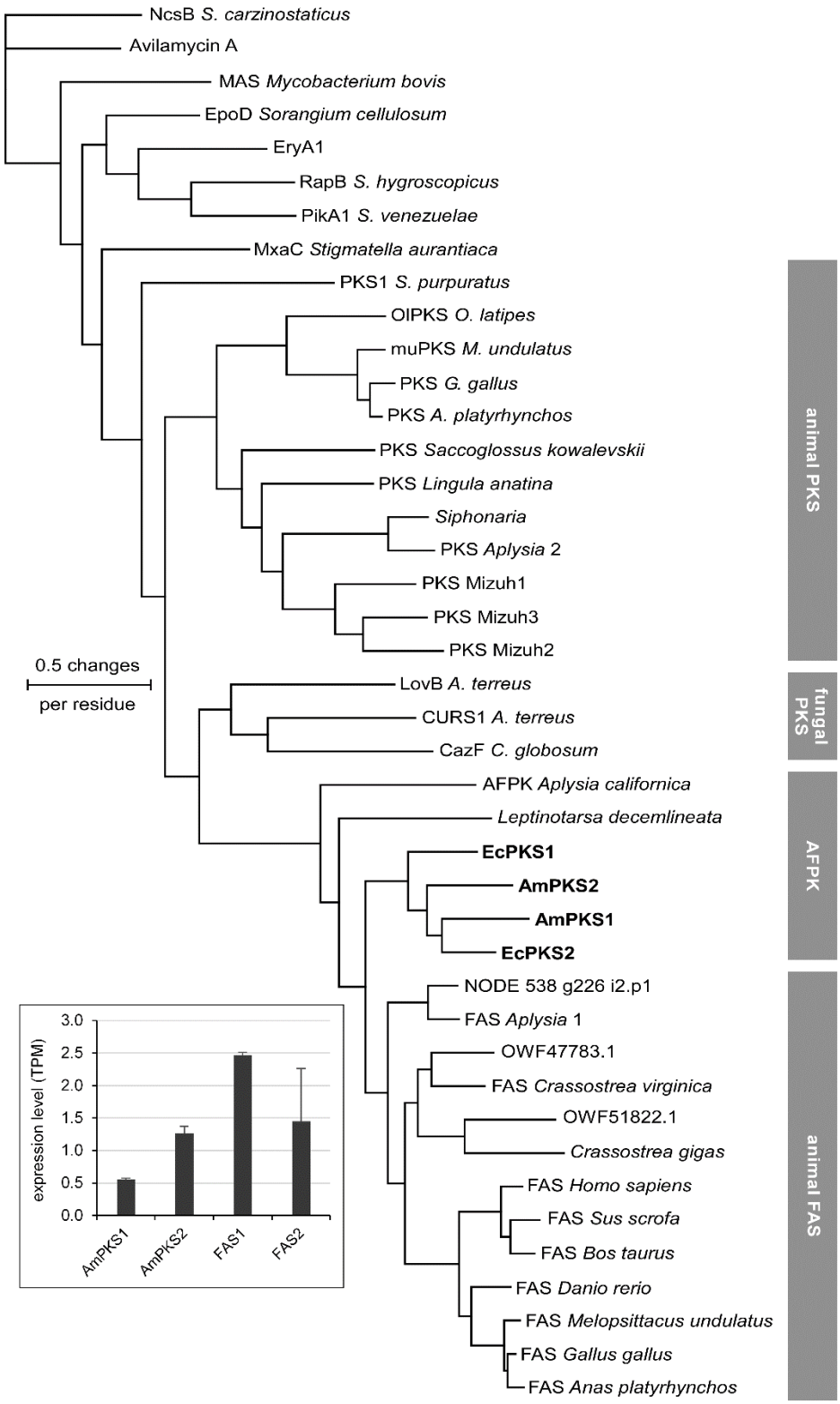

Figure 3. **Evolutionary relationships of animal PKS sequences (blue), AFPKs (purple), and the animal FAS clade (red) based on maximum-likelihood analysis of protein sequences.** Bolded tip labels show a clade comprising AFPK enzymes from photosynthetic sacoglossans (EcPKS1 & EcPKS2) and orthologs from *A*. cf. *modesta* (AmPKS1 & AmPKS2). **Inset**: Expression of FAS and AFPK genes from *A. modesta* relative to GAPDH, estimated as transcripts per million (TPM).

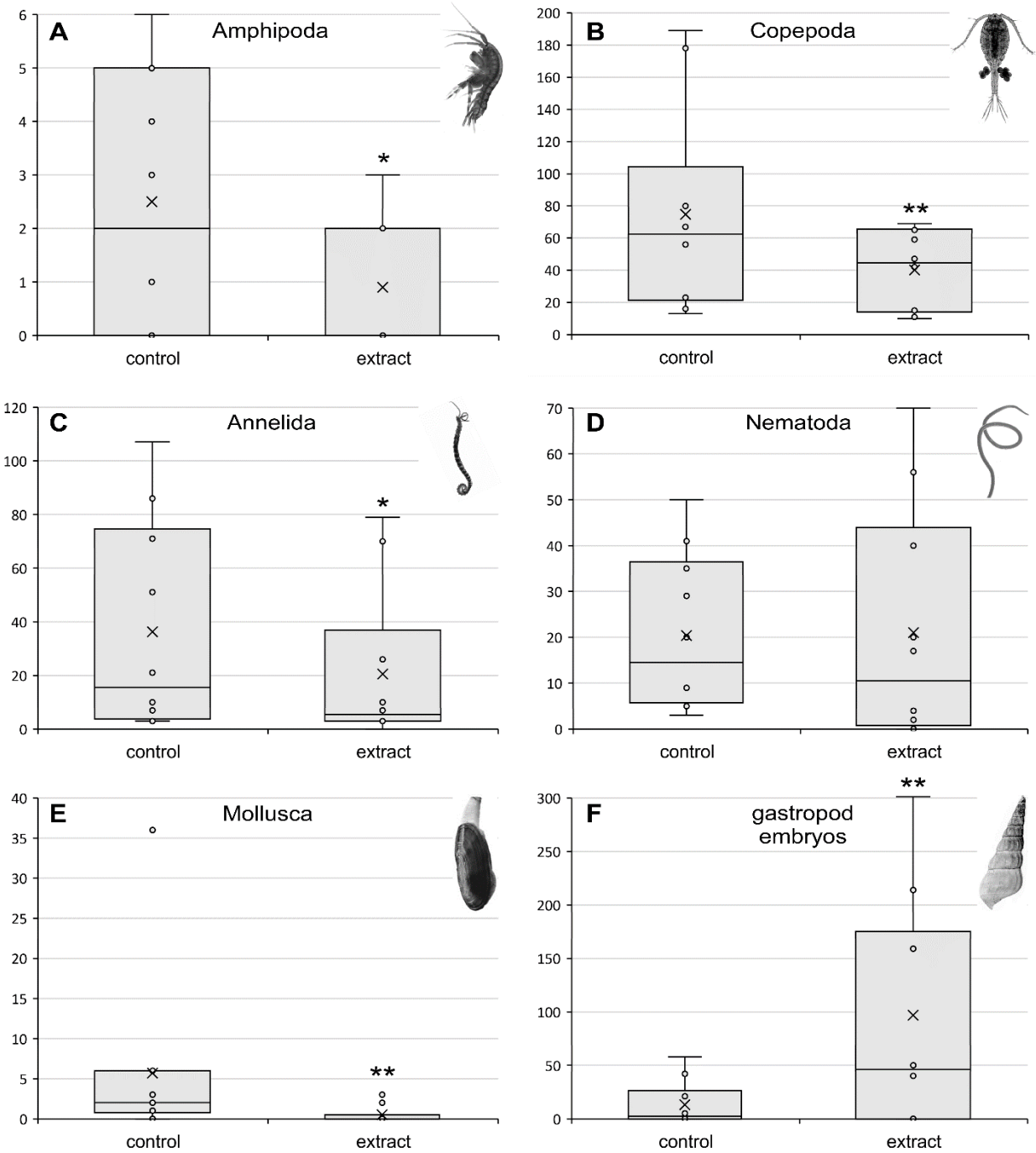

Figure 4. **Changes in infaunal abundance in response to alderenes applied to mud surface.** Box-and-whisker plots show lower and upper quartiles of counts per core for: **A**, amphipods; **B**, copepods; **C**, annelid worms; **D**, nematodes; **E**, adult molluscs; and **F**, embryos of the snail *C. californica*. Horizontal lines are median values; "×" gives the mean ($N = 10$ cores). Data for summer and winter deployments were pooled. Asterisks denote treatments differing from controls; *P<0.01; **P<0.001.

Table 1. Chemical shifts for alderenes A-E (**1-5**) in $CDCl_3$, based on (A) ^{13}C NMR and (B) ^{1}H NMR experiments.

A

position	δ_C				
	1 [a]	**2** [b]	**3** [a]	**4** [a]	**5** [b]
2	167.3 (C)	167.8 (C)	167.2 (C)	168.0 (C)	168.9 (C)
3	89.7 (CH)	105.3 (C)	89.7 (CH)	105.2 (C)	103.3 (C)
4	175.8 (C)	168.6 (C)	175.8 (C)	168.7 (C)	165.4 (C)
5	34.3 (CH)	31.7 (CH)	34.3 (CH)	31.9 (CH)	27.7 (CH_2)
6	88.8 (CH)	85.8 (CH)	88.8 (CH)	85.9 (CH)	80.4 (CH)
7	129.2 (C)	129.9 (C)	131.0 (C)	131.0 (C)	130.6 (C)
8	135.8 (CH)	133.3 (CH)	135.9 (CH)	133.5 (CH)	132.7 (CH)
9	132.5 (C)	132.5 (C)	133.8 (C)	133.4 (C)	132.2 (C)
10	126.1 (CH)	125.7 (CH)	129.4 (CH)	130.2 (CH)	125.8 (CH)
11	13.8 (CH_3)	13.5 (CH_3)	21.6 (CH_2)	21.6 (CH_2)	13.5 (CH_3)
Me-3	-	9.5 (CH_3)	-	9.7 (CH_3)	8.6 (CH_3)
Me-5	12.0 (CH_3)	16.0 (CH_3)	12.0 (CH_3)	16.3 (CH_3)	-
Me-7	13.0 (CH_3)	14.5 (CH_3)	13.0 (CH_3)	14.6 (CH_3)	13.4 (CH_3)
Me-9	16.5 (CH_3)	16.5 (CH_3)	16.6 (CH_3)	16.7 (CH_3)	16.1 (CH_3)
Me-11	-	-	14.1(CH_3)	14.2 (CH_3)	-
Me-O	56.4 (CH_3)	57.0 (CH_3)	56.4 (CH_3)	57.1 (CH_3)	55.2 (CH_3)

[a] Measured at 125 MHz. [b] Measured by inverse detection.

B

position	δ_H				
	1 [a]	**2** [b]	**3** [a]	**4** [b]	**5** [b]
3	5.12 (s)	-	5.12 (s)	-	
5	2.80 (dq, 10.8, 7.0)	2.85 (p, 7.0)	2.79 (dq, 10.8, 7.0)	2.86 (p, 7.0)	2.71 (dq, 17.0, 12.3, 2.3)
	-	-	-	-	2.52 (ddd, 17.0, 4.1, 1.2)
6	4.35 (d, 10.8)	4.44 (d, 5.5)	4.34 (d, 10.8)	4.45 (d, 5.5)	4.69 (dd, 12.3, 3.5)
8	5.91 (s)	5.82 (s)	5.91 (s)	5.82 (s)	5.98 (s)
10	5.43 (br q, 5.9)	5.38 (br q, 5.9)	5.35 (t, 5.9)	5.28 (t, 5.9)	5.45 (br q, 7.0)
11	1.68 (d, 6.4)	1.67 (d, 6.4)	2.10 (p, 7.0)	2.08 (p, 7.0)	1.69 (d, 7.0)
Me-3	-	1.70 (s)	-	1.81 (s)	1.79 (s)
Me-5	1.04 (d, 7.0)	1.22 (d, 7.0)	1.03 (d, 7.0)	1.22 (d, 7.0)	-
Me-7	1.80 (d, 1.2)	1.81 (s)	1.81 (s)	1.76 (s)	1.85 (d, 1.2)
Me-9	1.74 (s)	1.76 (s)	1.73 (s)	1.69 (s)	1.74 (s)
Me-11	-	-	0.99 (t, 7.0)	0.98 (t, 7.0)	-
Me-O	3.74 (s)	3.78 (s)	3.74 (s)	3.79 (s)	3.79 (s)

[a] Measured at 500 MHz. [b] Measured at 600 MHz.

Table 2. Predator response to potential prey items, compared to an identical number of positive control items that were 100% consumed in every trial.

treatment	slug species	predator	# prey items eaten	total # prey offered	*P*-value[1]
live slug	*A. willowi*	worm	0	10	5×10^{-6}
		crab	0	9	2×10^{-5}
		fish	0	10	5×10^{-6}
	A. cf. *modesta*	worm	0	20	7×10^{-12}
		crab	0	9	2×10^{-5}
		fish	0	10	5×10^{-6}
dead slug, intact	*A. willowi*	worm	0	10	5×10^{-6}
		crab	0	10	5×10^{-6}
		fish	0	10	5×10^{-6}
	A. cf. *modesta*	worm	0	10	5×10^{-6}
		crab	0	10	5×10^{-6}
		fish	0	10	5×10^{-6}
dead slug, solvent-extracted	*A. willowi*	worm	10	10	n.s.
		crab	10	10	n.s.
		fish	10	10	n.s.
	A. cf. *modesta*	worm	10	10	n.s.
		crab	10	10	n.s.
		fish	10	10	n.s.
egg mass, intact	*A. willowi*	worm	10	10	n.s.
		crab	10	10	n.s.
		fish	5	10	3×10^{-2}
egg mass, halved	*A. willowi*	fish	10	10	n.s.
pellet: organic layer, slug extract	*A. willowi*	crab	0	10	5×10^{-6}
		fish	0	10	5×10^{-6}
	A. cf. *modesta*	crab	0	10	5×10^{-6}
		fish	0	10	5×10^{-6}
pellet: PK-enriched	*A. willowi*	fish	0	10	5×10^{-6}

[1]*P*-value denotes significant difference based on Fisher's exact test between proportion of prey items vs controls (comparably processed squid mantle) consumed in a trial; n.s. = not significant

Table 3: Results of GLMMs testing effects of *Alderia* extract on (A) abundance of major taxa, and (B) community diversity, in mudflat cores; bolded terms denote a significant change compared to controls.

A

Taxon	**estimate**	**SE**	***Z***	***P***
Amphipoda	-1.022	0.384	-2.660	**0.008**
Copepoda	-0.623	0.062	-10.090	**$<2\times10^{-16}$**
Polychaeta	-0.227	0.086	-2.633	**0.008**
Nematoda	-0.019	0.096	-0.195	0.846
Mollusca (adult)	-2.398	0.467	-5.134	**2.84×10^{-7}**
Gastropoda (embryos)	1.808	0.084	21.500	**$<2\times10^{-16}$**

B

Diversity index	**estimate**	**SE**	***Z***	***P***
Shannon-Wiener	0.136	0.077	1.779	0.075
Simpson's Dominance	0.041	0.039	1.050	0.294

Table S1. Mean and peak abundance data for three species in the gastropod genus *Alderia* with latitude of the sampling site.

Species and site	Latitude	Mean density (slugs/m^2)	Peak density (slugs/m^2)	Reference[1]
A. modesta				
Stellendam, Netherlands	51.8166667		3100	28
Meldorf Bay, Germany, North Sea	54.0964080	1400		29
Klubbukt, Norway	70.4569730	4820	9000	30
A.* cf. *modesta				
Amurskii Bay, Russia	43.1978420		2000	31
USA: Oregon				
Yaquina Bay	44.6144444	800	2152	32
Coos Bay, south slough	43.2897222	290	5000	32
USA: California				
West Bodega Harbor	38.3161111	442	2720	
Hog Island Oyster Co., Tomales Bay	38.1621800	44	144	
south Tomales Bay	38.1147222	28	107	
Bolinas Lagoon	37.9090660	93	293	
Mill Valley A/B, San Francisco Bay	37.8825000	170	1156	
Bolinas Lagoon	37.9090660	93	293	
A. willowi				
USA: California				
West Bodega Harbor	38.3161111	184	428	
Hog Island Oyster Co., Tomales Bay	38.1621800	160	804	
south Tomales Bay	38.1147222	129	350	
Bolinas Lagoon	37.9090660	373	999	
Mill Valley A/B, San Francisco Bay	37.8825000	200	1392	
Golden Shores, Long Beach	33.7640730	50	200	

[1]Data without citations were collected in the present study.

Table S2. Candidate polyketides initially detected by LC/MS analysis of individually extracted *Alderia modesta*.

elution time[1]	rank	mass (Da)	predicted formula	confirmed identity[2]
5.720	19	222.126	$C_{13}H_{18}O_3$	n.d.
6.286	24	236.1409	$C_{14}H_{20}O_3$	n.d.
6.431	2	236.141	$C_{14}H_{20}O_3$	alderene E (**5**)
6.569	30	238.1569	$C_{14}H_{22}O_3$	n.d.
6.885	1	236.141	$C_{14}H_{20}O_3$	alderene A (**1**)
7.030	3	250.157	$C_{15}H_{22}O_3$	alderene B (**2**)
7.768	6	250.157	$C_{15}H_{22}O_3$	n.d.
8.070	25	250.1569	$C_{15}H_{22}O_3$	n.d.
8.253	4	250.157	$C_{15}H_{22}O_3$	alderene C (**3**)
8.364	10	264.172	$C_{16}H_{24}O_3$	alderene D (**4**)

[1]Retention times in minutes (shifted relative to the trace in Fig. 2A).
[2]Compound confirmed as a polyketide by full structure elicidation, or not determined (n.d.)

Table S3. Macrofauna and meiofauna composition of mudflat infauna sampled in cores at the Salinas de San Pedro Salt Marsh, during two field tests of community effects of *Alderia* PKs.

Taxon	Summer abundance (mean ± SE)	Winter abundance (mean ± SE)
Annelida: Oligochaeta	0.8 ± 0.4	3.2 ± 1.5
Annelida: Polychaeta		
Aphelochaeta	n.d.[1]	0.2 ± 0.2
Boccardia	0.1 ± 0.1	1.1 ± 0.5
Dipolydora	2.9 ± 0.8	26.9 ± 8.5
Mediomastus	2.8 ± 1.4	19.8 ± 7.8
Scoletoma	0.1 ± 0.1	N/A
Mollusca: Bivalvia	4.1 ± 3.6	1.5 ± 0.5
Mollusca: Gastropoda		
Acteocina inculta	0.2 ± 0.2	0.2 ± 0.2
Alderia willowi	n.d.	1.7 ± 0.8
Cerithideopsis californica (eggs)	56.0 ± 34.4	60.4 ± 20.1
Nemertea	0.3 ± 0.2	0.4 ± 0.3
Arthropoda: Malacostraca		
Amphipoda	3.2 ± 0.6	0.2 ± 0.1
Arthropoda: Copepoda		
Harpacticoida	48.0 ± 16.2	66.9 ± 15.1
Arthropoda: Insecta	0.6 ± 0.3	1.4 ± 0.4
Nematoda	37.8 ± 55.5	4.8 ± 1.7

[1]n.d. = not detected

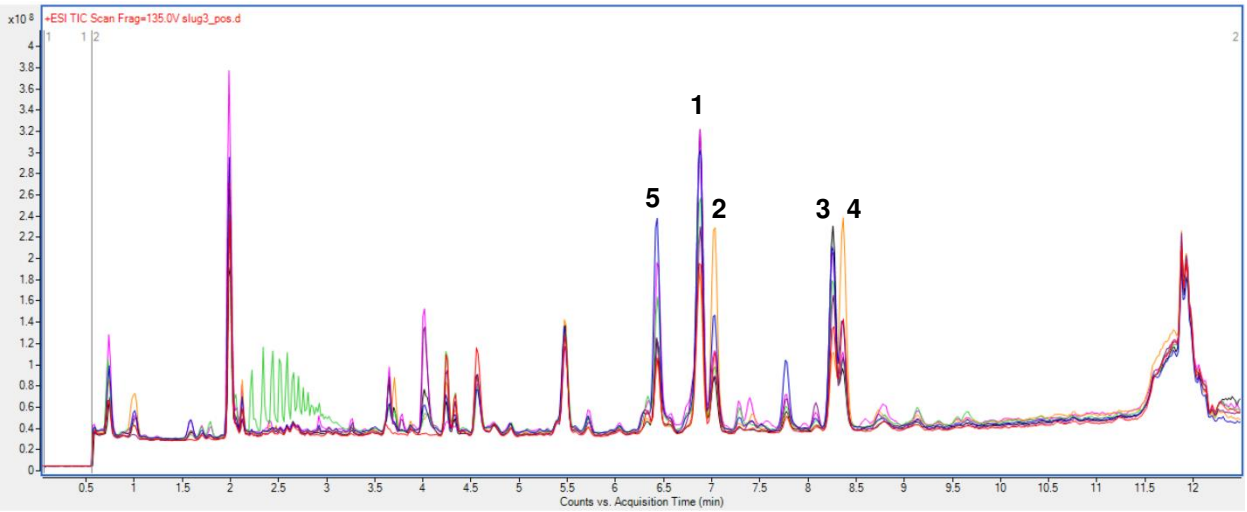

Figure S1. Overlaid LCMS traces of acetone extracts of individual *A*. cf. *modesta* (*N*=7), showing comparable proportions of five major polyketide metabolites among specimens.

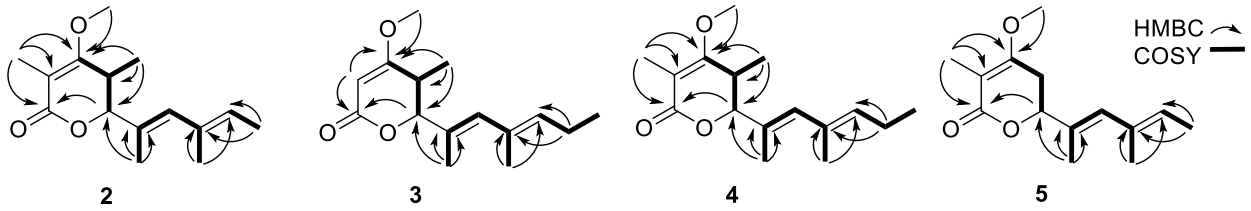

Figure S2. Select 2D NMR correlations for alderenes B-E (**2-5**).

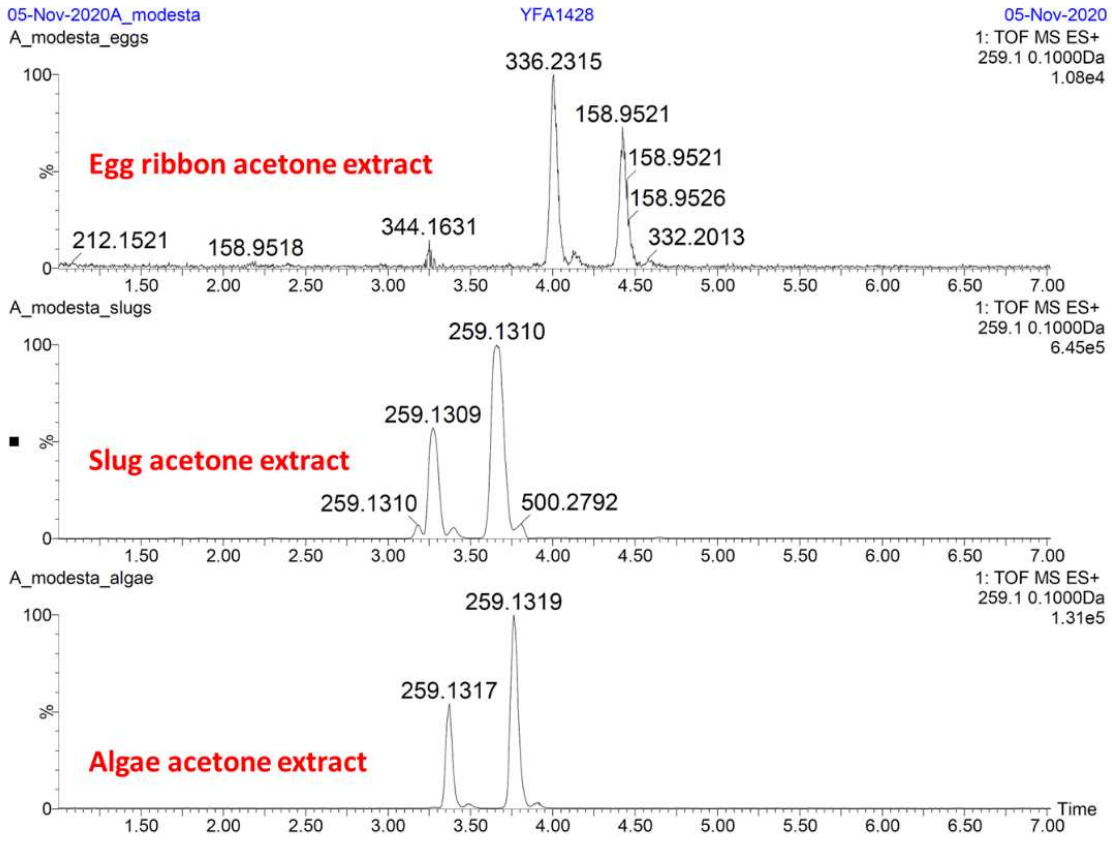

Figure S3. LCMS extracted ion traces for **1** and **5** from crude extracts of egg ribbon, slugs and algae incubated with slugs.

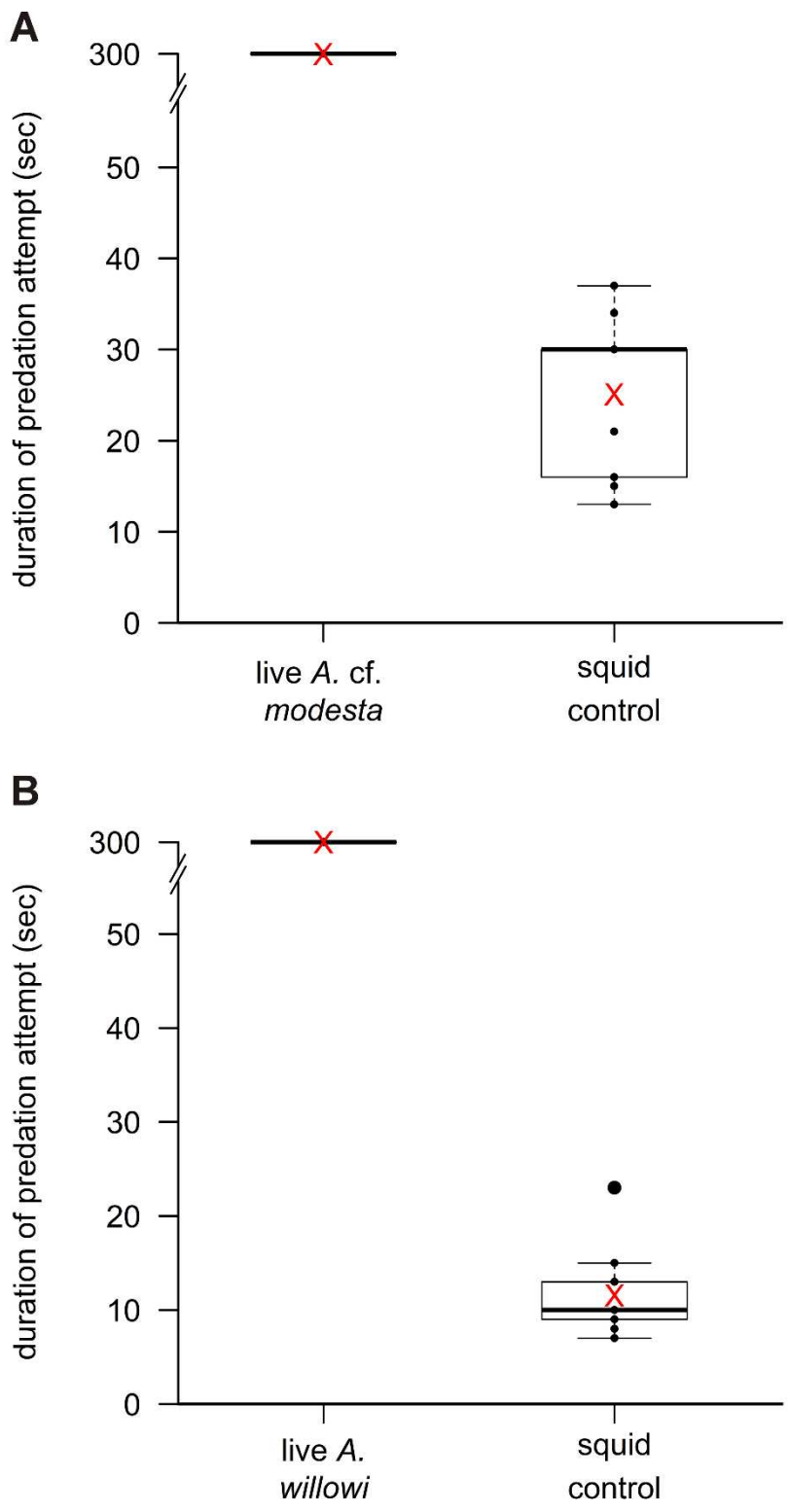

Figure S4. Duration of crab predation attempts on live *Alderia* spp. versus squid controls. Boxplots show times that individual crabs spent attempting to consume live slugs (if not immediately rejected) or to fully consume controls (squid mantle tissue); larger dots are outliers. Horizontal line indicates the median and red X the mean on each box. **A**, Only two crabs attempted to consume *A.* cf. *modesta*, and spent the whole trial. **B**, Four crabs spent the whole trial attempting to consume *A. willowi*. In both trials, all crabs (*N*=9) rapidly consumed squid controls.

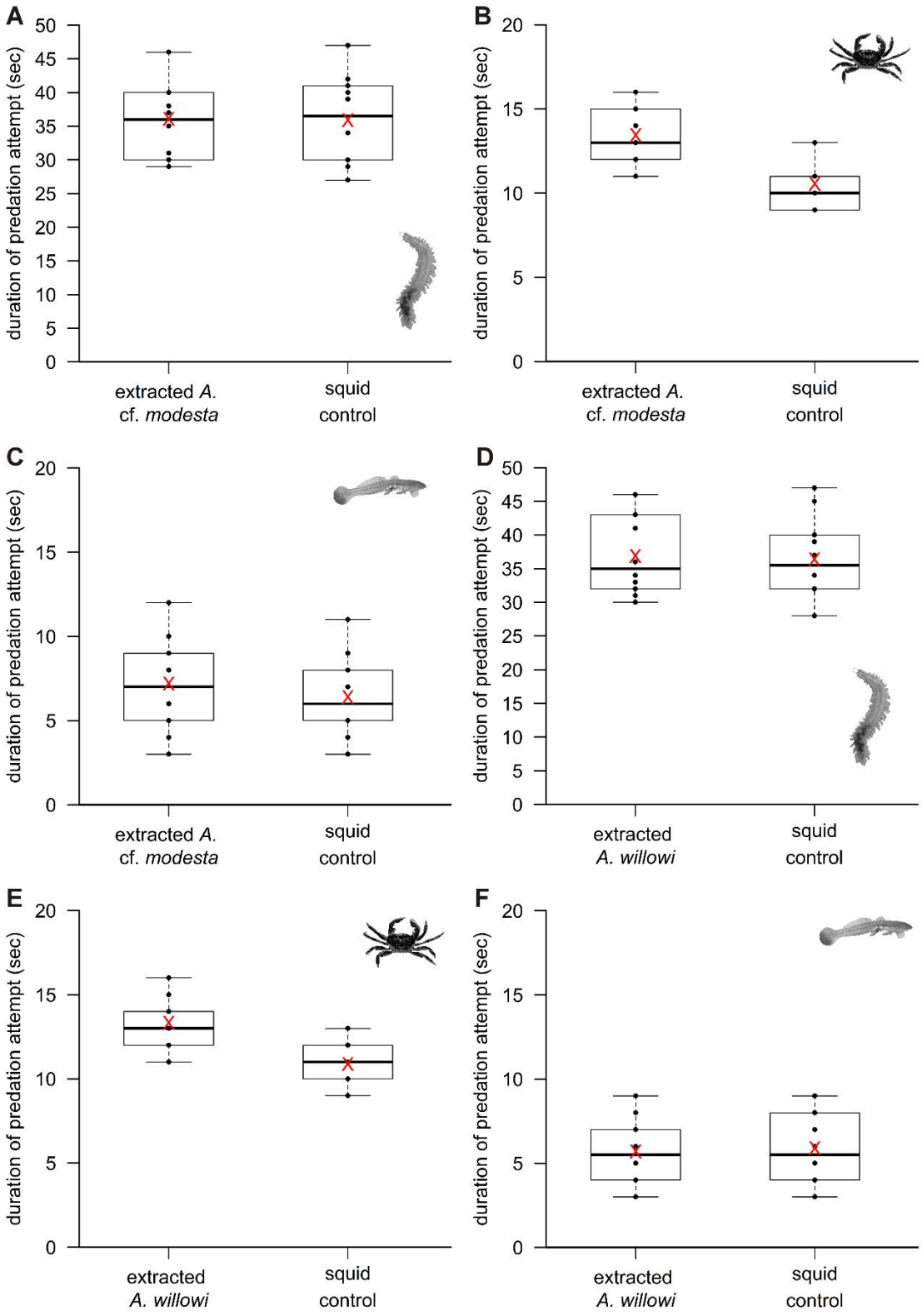

Figure S5. Acetone extraction restores palatability to tissue of *Alderia* spp. for worm (**A**, **D**), crab (**B**, **E**), and fish (**C**, **F**) predators. Boxplots show times for individual predators to consume dead *A.* cf. *modesta* (**A**-**C**) or *A. willowi* (**D**-**F**) extracted with acetone to remove organic metabolites, or similarly extracted squid mantle. Horizontal line indicates the median and red X the mean on each box.

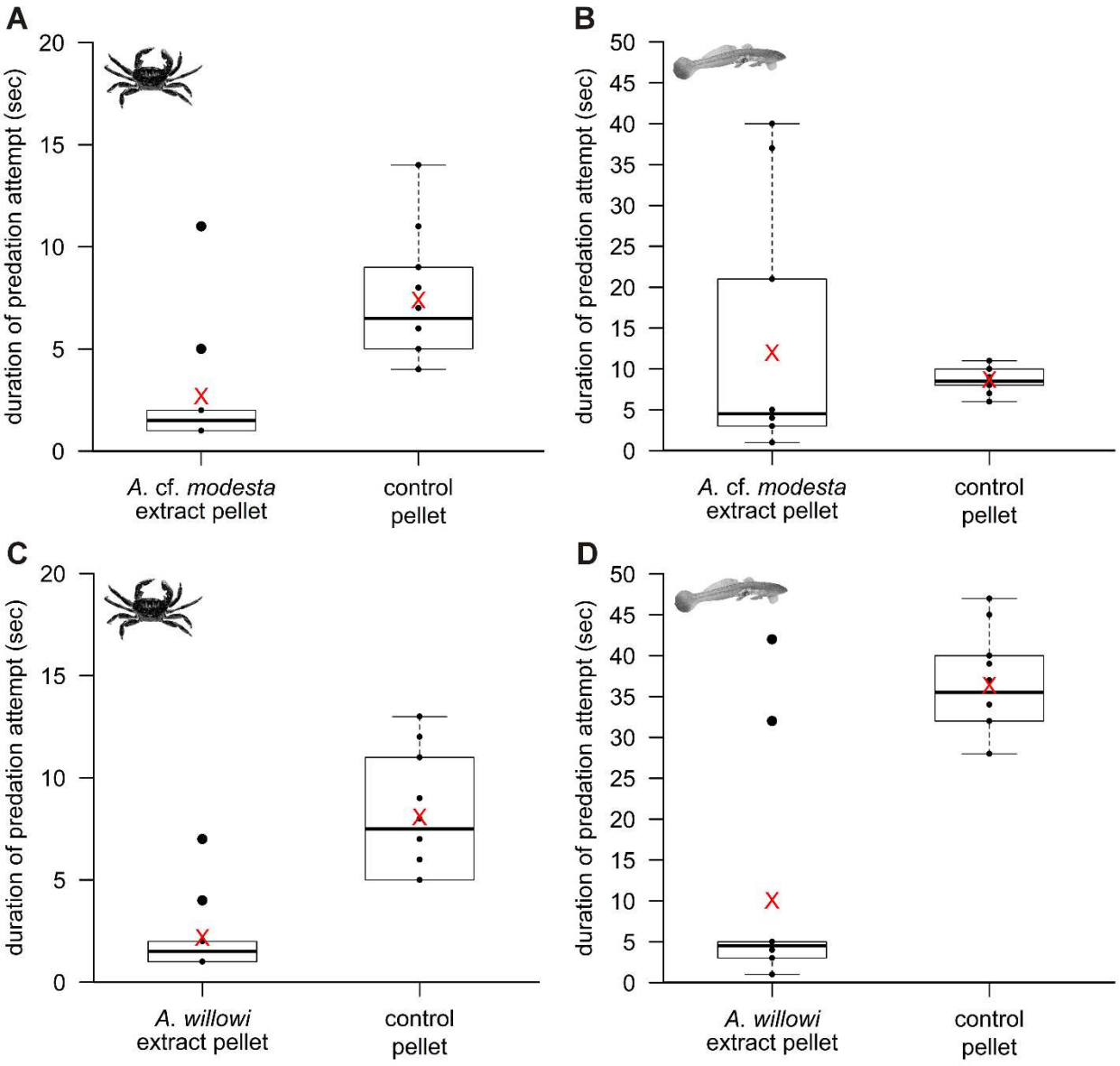

Figure S6. Nonpolar compounds from *Alderia* spp. reduced palatability of squid-based artificial food pellets for individual crab (**A, C**) and fish (**B, D**) predators. Boxplots show times that individual predators spent attempting to feed on pellets incorporating the organic layer of crude extracts from *A.* cf. *modesta* (**A**-**B**) or *A. willowi* (**C**-**D**), or to fully consume squid controls. Horizontal line indicates the median and red X the mean on each box; larger dots indicate outliers.

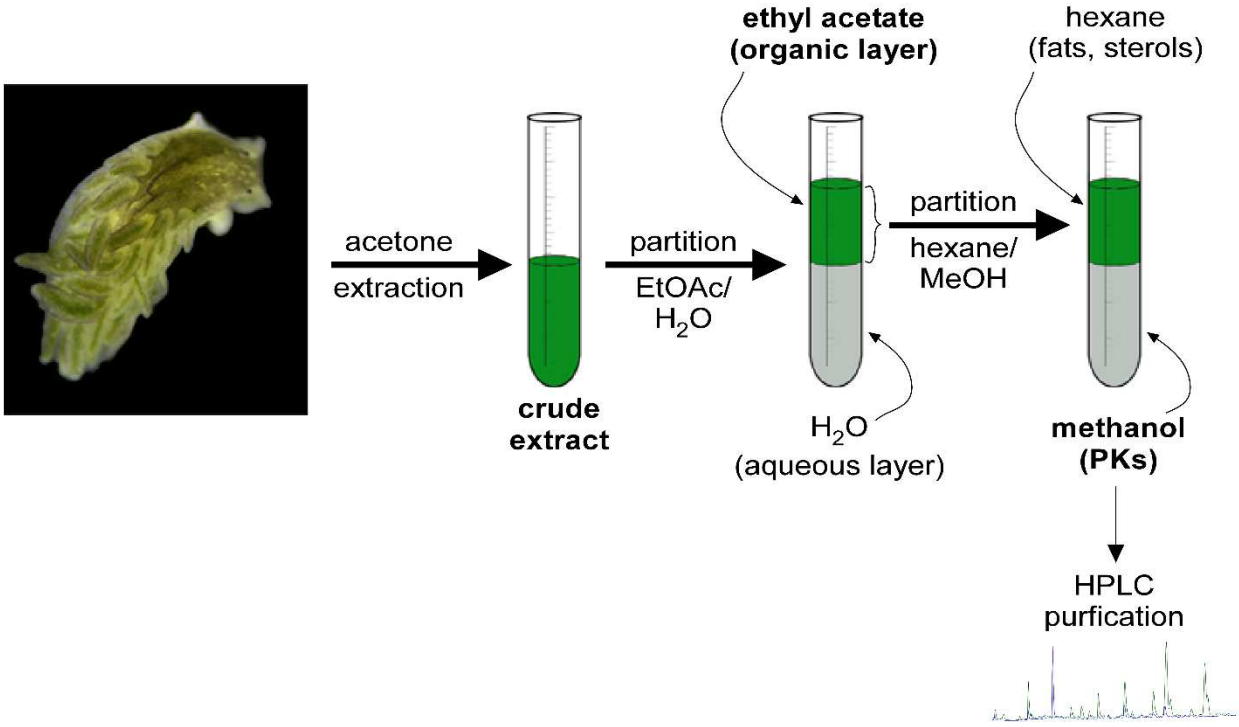

Figure S7. Schematic diagram illustrating extraction scheme to isolate compounds responsible for antipredator bioactivity in *Alderia* spp. Components of concentrated crude extract and each layer from subsequent partitions were tested at native per-weight concentrations or dilutions to determine which layers reduced palatability of squid-based artificial food pellets for predators. Green color denotes layers containing chlorophyl from algal diet of extracted slugs. Bolded layers contained alderene polyketides based on chemical analyses.

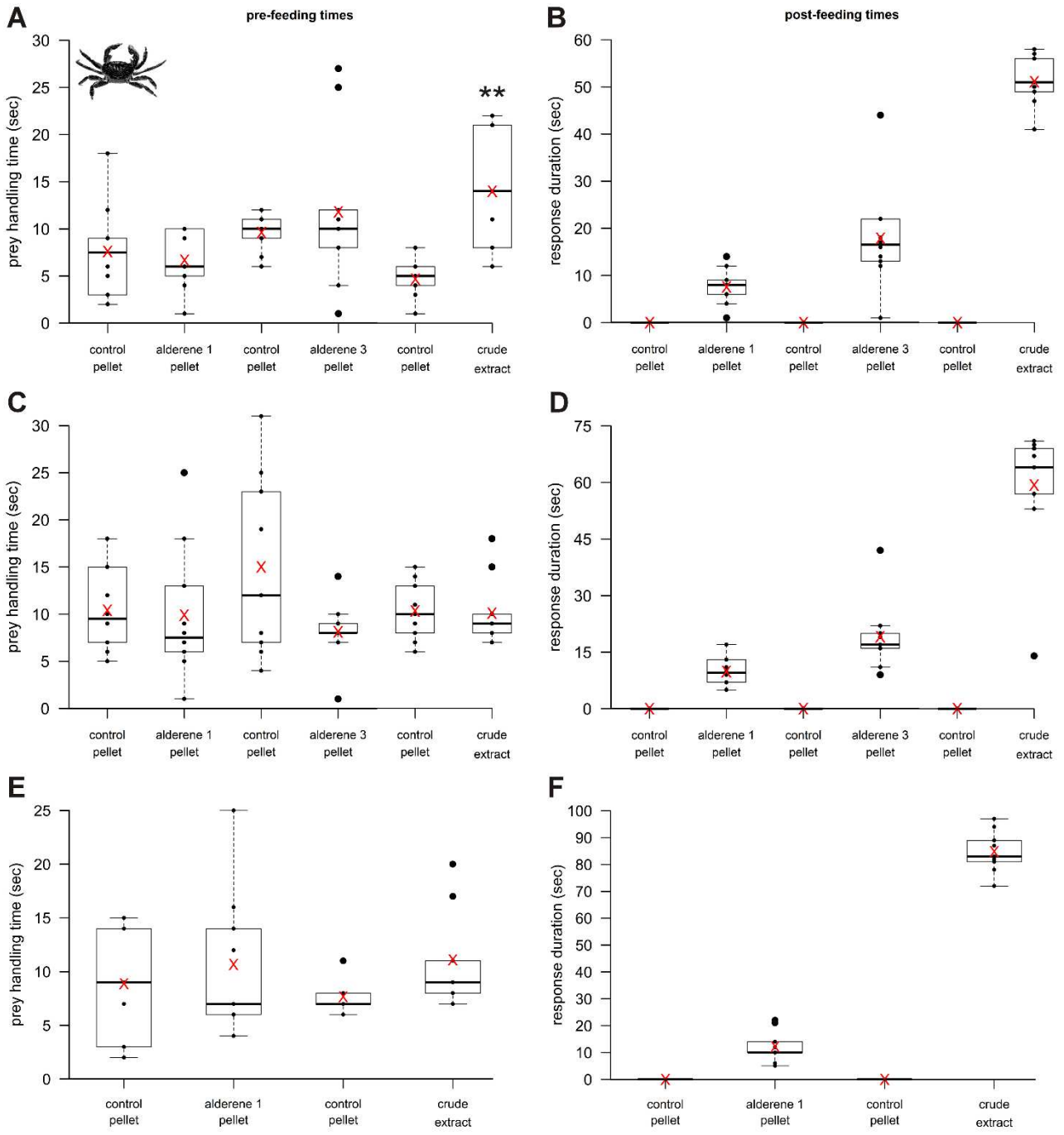

Figure S8. Effects of pure alderenes on crab prey handling and post-ingestion response times, compared to negative and positive controls. Artificial food pellets were prepared incorporating pure alderene **1** or **3**, or with crude extract of *A. willowi* as a positive control for deterrent behavior; feeding response to each was compared to pellets incorporating solvent only as a negative control in paired trials. Compounds and extract were tested at 25% (**A-B**), 50% (**C-D**) or 100% (**E-F**) of natural concentration. Boxplots show times that crabs spent handling pellets prior to consumption (**A, C, E**), or time spent exhibiting adverse reactions after ingesting treated pellets, such as pulling material out of the mouth or rubbing mouthparts on the substrate (**B, D, F**). Horizontal line indicates the median and red X the mean on each box; larger dots indicate outliers. $^{**}P < 0.005$, paired Sign test; all comparison with controls significant for post-feeding times.

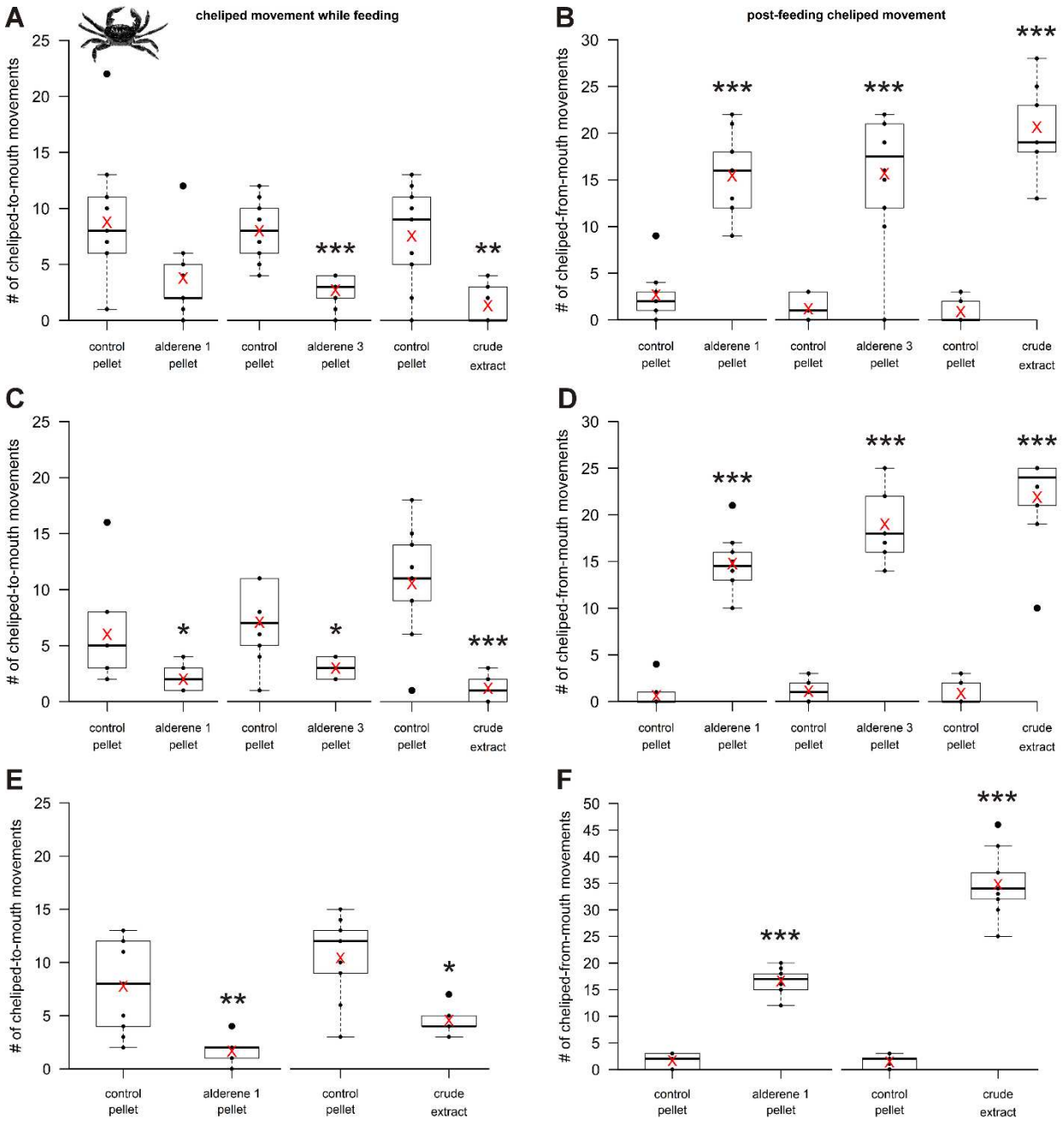

Figure S9. Effects of pure alderenes on cheliped use during crab feeding, compared to negative and positive controls. Artificial food pellets were prepared incorporating alderene **1** or **3**, or crude extract of *A. willowi* (positive control for deterrent behavior), and compared to solvent-only pellets (negative controls) in paired trials. Compounds and extract were tested at 25% (**A-B**), 50% (**C-D**) or 100% (**E-F**) of natural concentration. Boxplots show number of times that crabs moved chelipeds from pellets to mouth during feeding (**A, C, E**), or pulled material out of their mouth after feeding (**B, D, F**). Horizontal line indicates the median and red X the mean on each box; larger dots indicate outliers. **P*<0.05; ***P*<0.01; ****P*<0.005, paired Sign test.

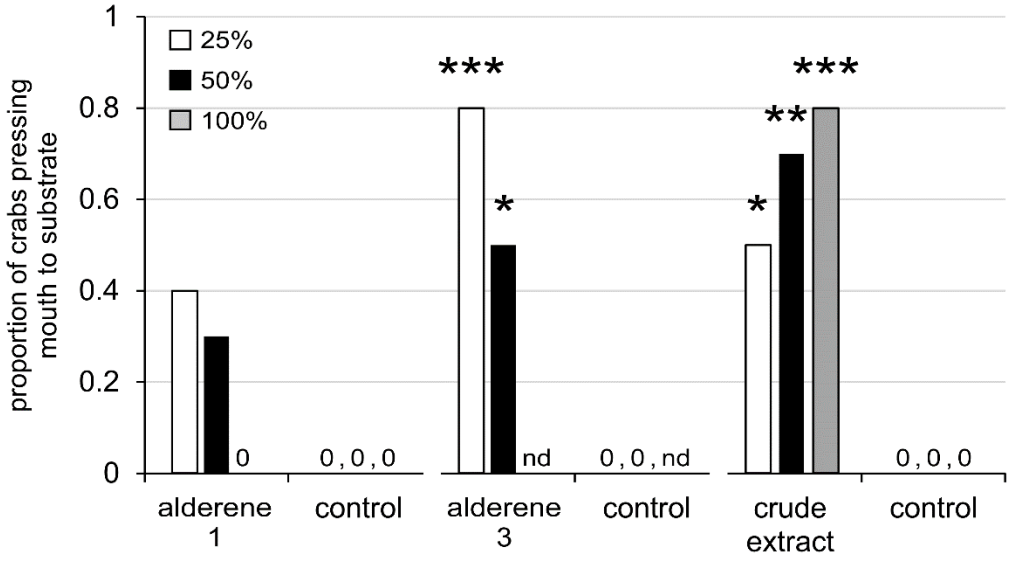

Figure S10. Effects of pure alderenes on crab behavioral response post-ingestion, compared to negative and positive controls. Artificial food pellets were prepared incorporating pure alderene **1** or **3**, or with crude extract of *A. willowi* as a positive control for deterrent behavior; feeding response to each was compared to pellets incorporating solvent only as a negative control in paired trials. Compounds and extract were tested at 25% (white bars), 50% (solid bars) or 100% (grey bars) of natural concentration. Bars show the proportion of crabs that rubbed or pressed mouthparts against substrate after ingesting treated pellets. No crabs exhibited this behavior after feeding on control pellets. ***P<0.001; **P<0.005; *P<0.05, Fisher's exact test; nd = not determined.

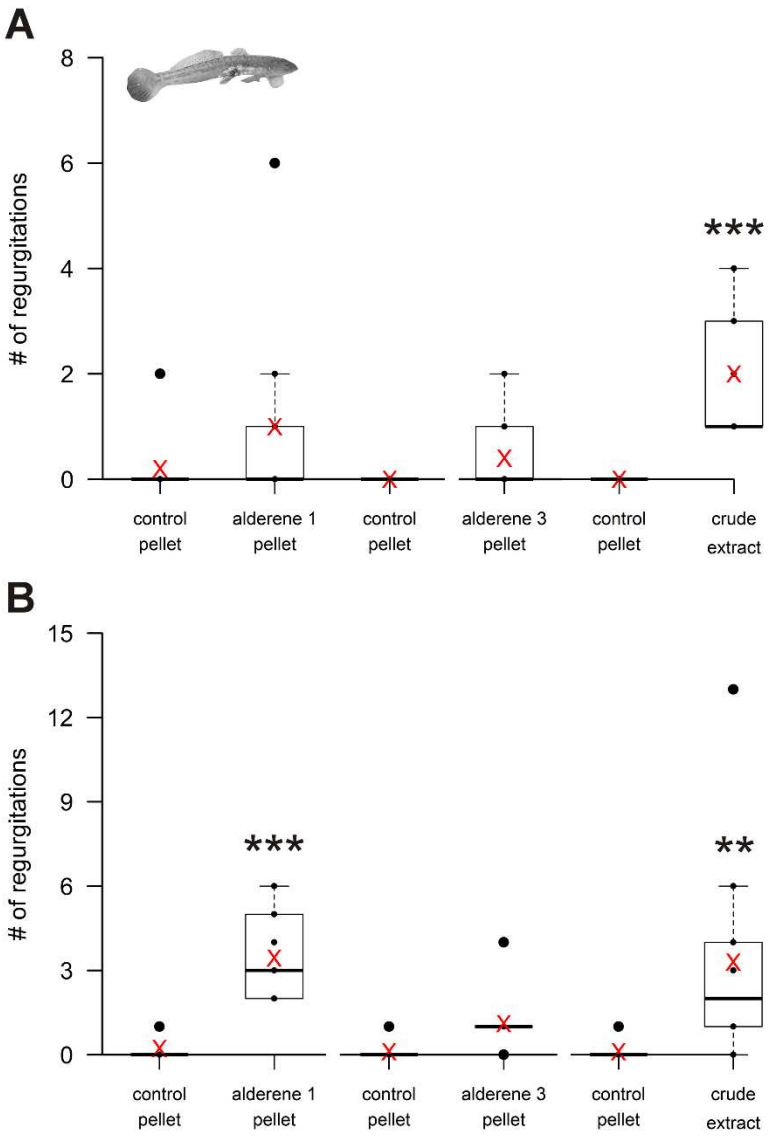

Figure S11. Effects of pure alderenes on fish feeding, compared to negative and positive controls. Artificial food pellets were prepared incorporating alderene **1** or **3**, or crude extract of *A. willowi* (positive control for deterrent behavior), and compared to solvent-only pellets (negative controls) in paired trials. Compounds and extract were tested at 25% (**A**) or 50% (**B**) of natural concentration. Boxplots show number of times that fish regurgitate pellets during feeding attempts. Horizontal line indicates the median and red X the mean on each box; larger dots indicate outliers. $^{**}P < 0.01$; $^{***}P<0.005$, paired Sign test.

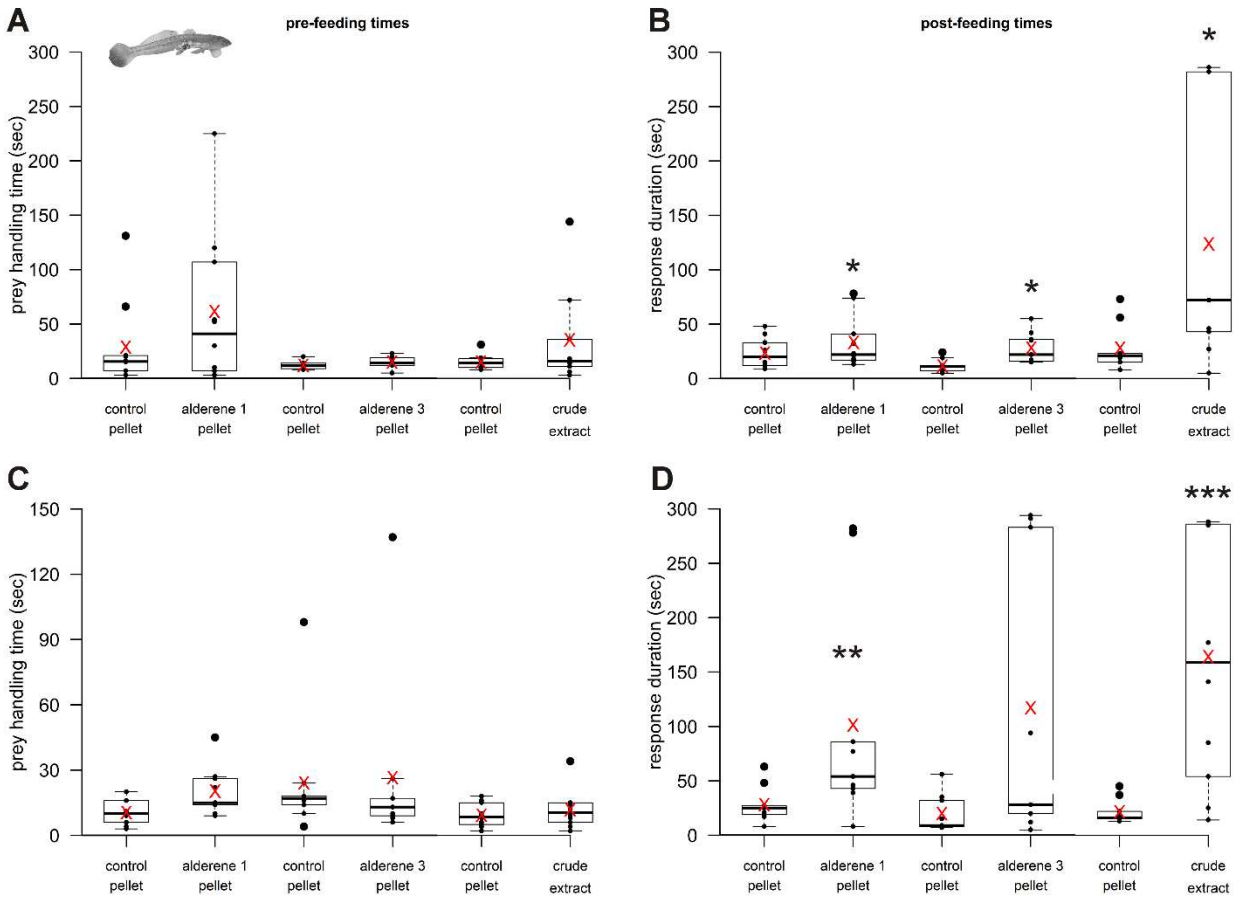

Figure S12. Effects of pure alderenes on fish prey-handing and response times, compared to negative and positive controls. Artificial food pellets were prepared incorporating alderene **1** or **3** at 25% (**A-B**) or 50% (**C-D**) of natural concentration, or crude extract of *A. willowi* (positive control for deterrent behavior, tested at 50% concentration), and compared to solvent-only pellets (negative controls) in paired trials. Boxplots show time that fish delayed the onset of a feeding attempt (**A, C**) or the time spent in prey handling after the onset of feeding (B, D) . Horizontal line indicates the median and red X the mean on each box; larger dots indicate outliers. **P* < 0.05; ***P* < 0.01; ****P*<0.005, paired Sign test.

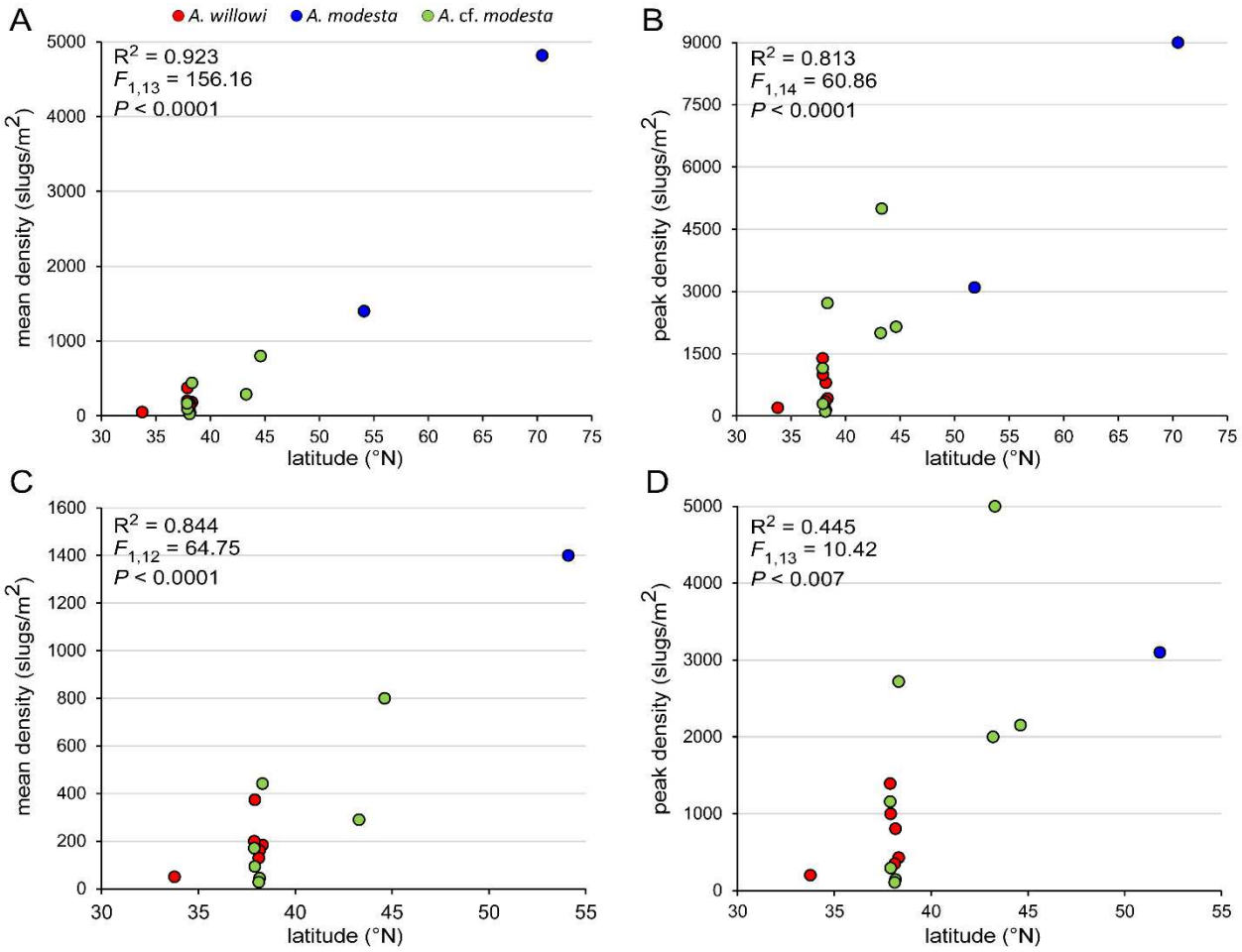

Figure S13. Density-latitude relationships for *Alderia* populations are independent of Norway, the highest density population recorded. Mean (A, C) and peak (B, D) population densities scale positively with latitude in *A. modesta* (blue), *A.* cf. *modesta* (green) and *A. willowi* (red), as described in Fig. 1, but the highest latitude site (Norway) was also the site of highest mean and peak densities. Linear regressions were therefore performed after removing Norway, with little effect on the underlying relationship or goodness-of-fit as measured by R^2. Log-transforming both axes similarly resulted in comparable levels of significance and R^2 values with versus without Norway.

Supplementary NMR data

^{13}C NMR data for **1-5** in $CDCl_3$.

position	δ_C				
	1 [a]	**2** [b]	**3** [a]	**4** [a]	**5** [b]
2	167.3 (C)	167.8 (C)	167.2 (C)	168.0 (C)	168.9 (C)
3	89.7 (CH)	105.3 (C)	89.7 (CH)	105.2 (C)	103.3 (C)
4	175.8 (C)	168.6 (C)	175.8 (C)	168.7 (C)	165.4 (C)
5	34.3 (CH)	31.7 (CH)	34.3 (CH)	31.9 (CH)	27.7 (CH_2)
6	88.8 (CH)	85.8 (CH)	88.8 (CH)	85.9 (CH)	80.4 (CH)
7	129.2 (C)	129.9 (C)	131.0 (C)	131.0 (C)	130.6 (C)
8	135.8 (CH)	133.3 (CH)	135.9 (CH)	133.5 (CH)	132.7 (CH)
9	132.5 (C)	132.5 (C)	133.8 (C)	133.4 (C)	132.2 (C)
10	126.1 (CH)	125.7 (CH)	129.4 (CH)	130.2 (CH)	125.8 (CH)
11	13.8 (CH_3)	13.5 (CH_3)	21.6 (CH_2)	21.6 (CH_2)	13.5 (CH_3)
Me-3	-	9.5 (CH_3)	-	9.7 (CH_3)	8.6 (CH_3)
Me-5	12.0 (CH_3)	16.0 (CH_3)	12.0 (CH_3)	16.3 (CH_3)	-
Me-7	13.0 (CH_3)	14.5 (CH_3)	13.0 (CH_3)	14.6 (CH_3)	13.4 (CH_3)
Me-9	16.5 (CH_3)	16.5 (CH_3)	16.6 (CH_3)	16.7 (CH_3)	16.1 (CH_3)
Me-11	-	-	14.1(CH_3)	14.2 (CH_3)	-
Me-O	56.4 (CH_3)	57.0 (CH_3)	56.4 (CH_3)	57.1 (CH_3)	55.2 (CH_3)

[a] Measured at 125 MHz. [b] Measured by inverse detection.

^{1}H NMR data for **1-5** $CDCl_3$

position	δ_H				
	1 [a]	**2** [b]	**3** [a]	**4** [b]	**5** [b]
3	5.12 (s)	-	5.12 (s)	-	
5	2.80 (dq, 10.8, 7.0)	2.85 (p, 7.0)	2.79 (dq, 10.8, 7.0)	2.86 (p, 7.0)	2.71 (dq, 17.0, 12.3, 2.3)
	-	-	-	-	2.52 (ddd, 17.0, 4.1, 1.2)
6	4.35 (d, 10.8)	4.44 (d, 5.5)	4.34 (d, 10.8)	4.45 (d, 5.5)	4.69 (dd, 12.3, 3.5)
8	5.91 (s)	5.82 (s)	5.91 (s)	5.82 (s)	5.98 (s)
10	5.43 (br q, 5.9)	5.38 (br q, 5.9)	5.35 (t, 5.9)	5.28 (t, 5.9)	5.45 (br q, 7.0)
11	1.68 (d, 6.4)	1.67 (d, 6.4)	2.10 (p, 7.0)	2.08 (p, 7.0)	1.69 (d, 7.0)
Me-3	-	1.70 (s)	-	1.81 (s)	1.79 (s)
Me-5	1.04 (d, 7.0)	1.22 (d, 7.0)	1.03 (d, 7.0)	1.22 (d, 7.0)	-
Me-7	1.80 (d, 1.2)	1.81 (s)	1.81 (s)	1.76 (s)	1.85 (d, 1.2)
Me-9	1.74 (s)	1.76 (s)	1.73 (s)	1.69 (s)	1.74 (s)
Me-11	-	-	0.99 (t, 7.0)	0.98 (t, 7.0)	-
Me-O	3.74 (s)	3.78 (s)	3.74 (s)	3.79 (s)	3.79 (s)

[a] Measured at 500 MHz. [b] Measured at 600 MHz.

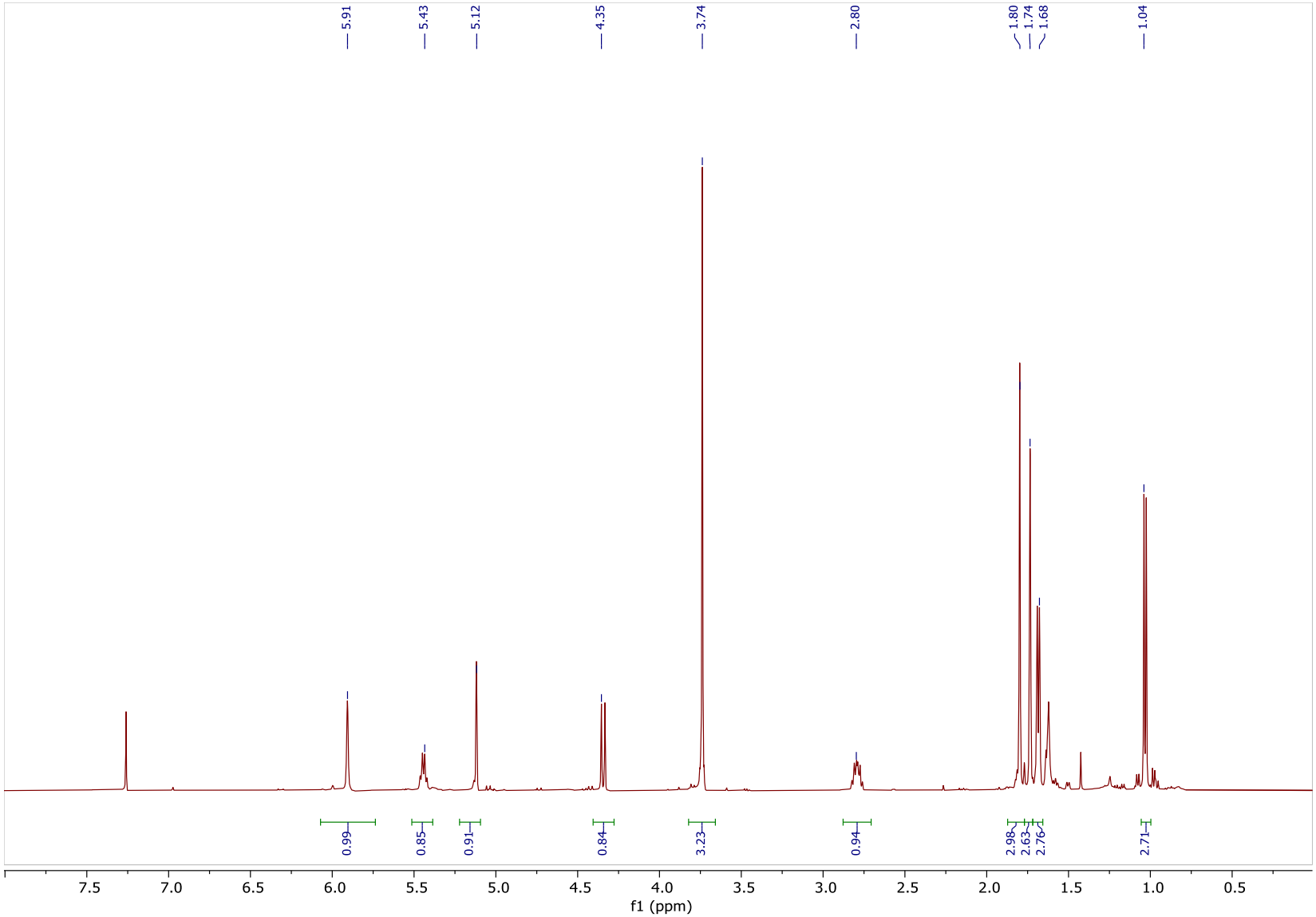

^{1}H NMR spectrum of **1** measured in $CDCl_3$ at 500 MHz

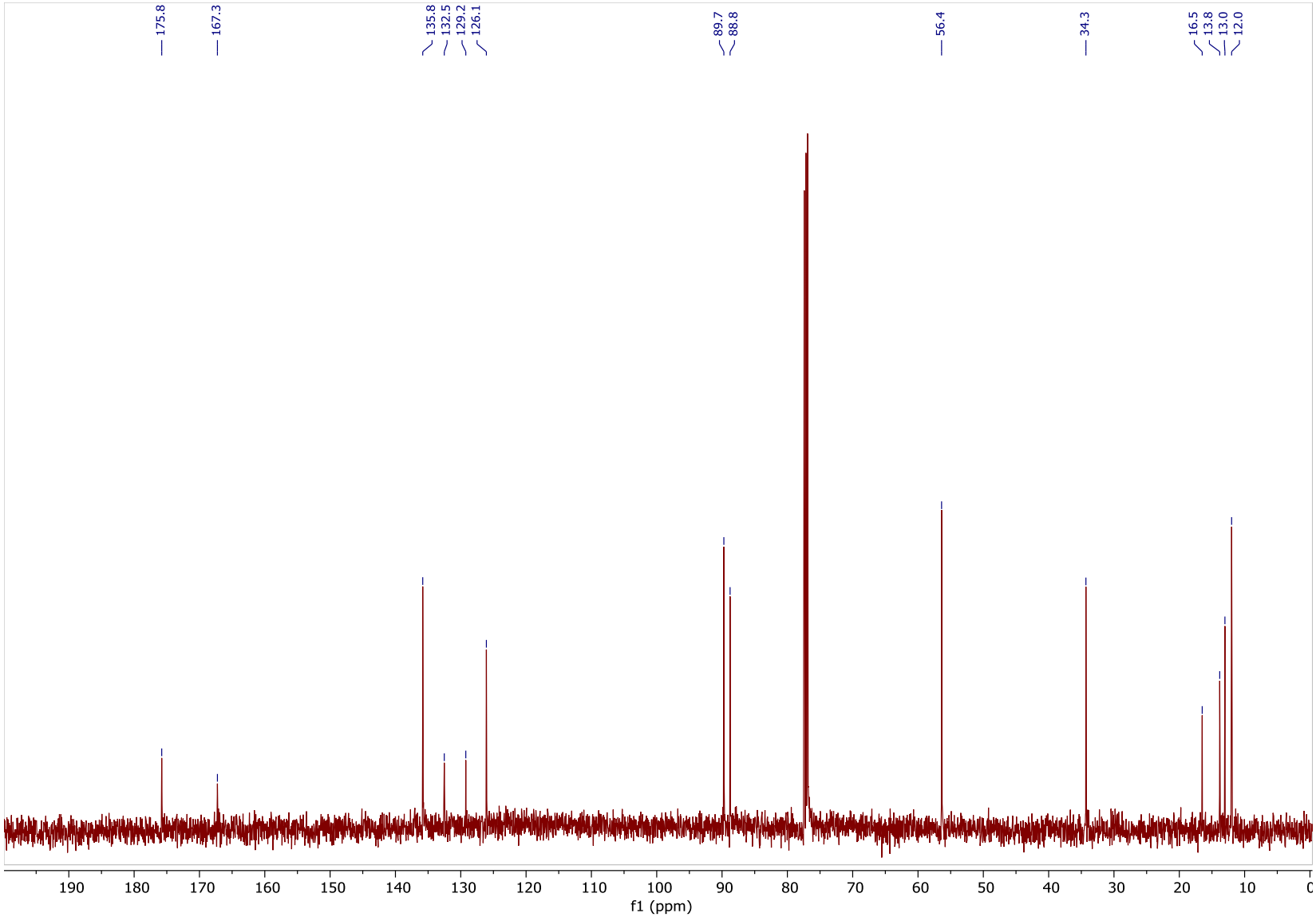

^{13}C NMR spectrum of **1** measured in $CDCl_3$ at 125 MHz

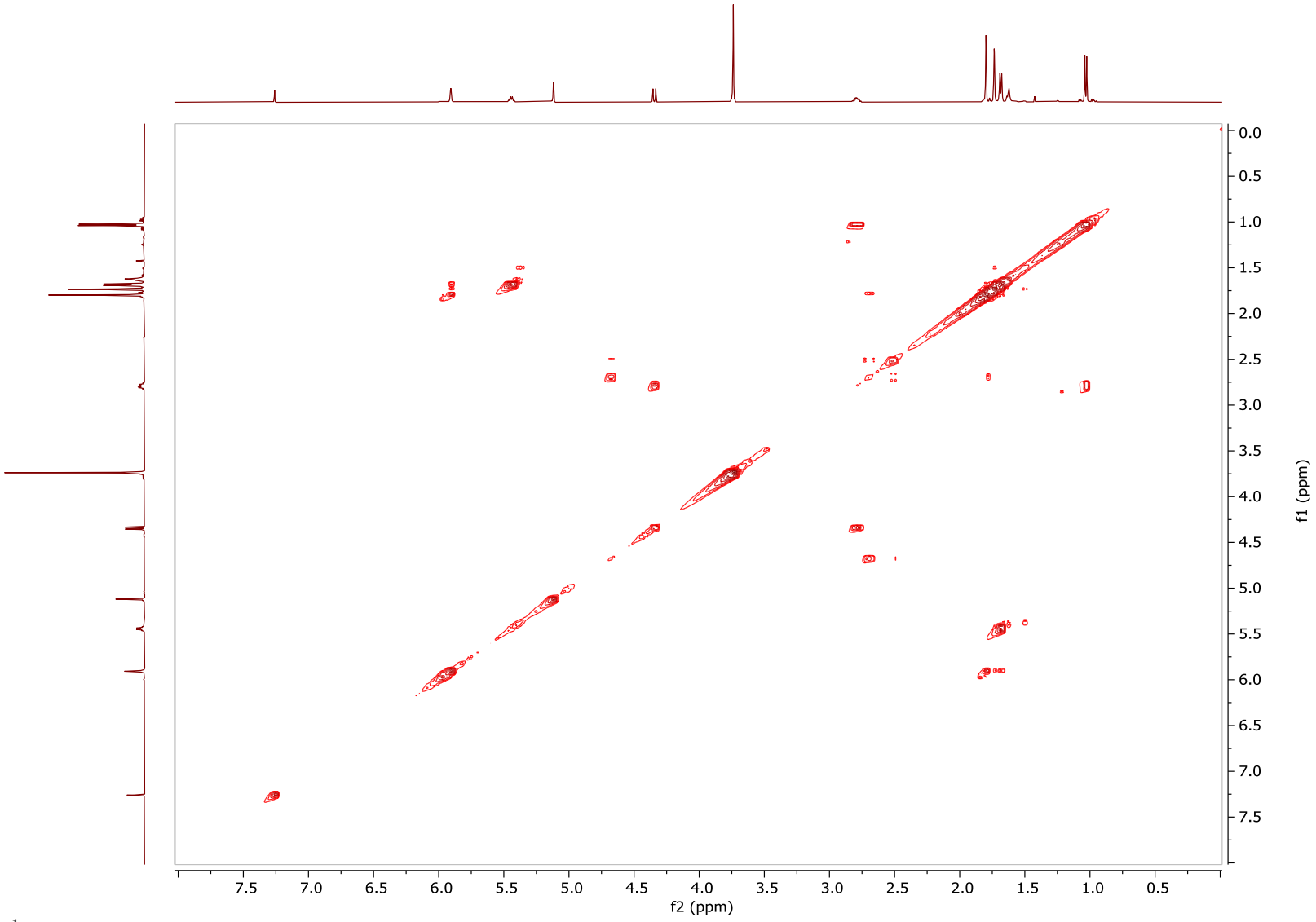

^{1}H-^{1}H COSY NMR spectrum of **1** measured in $CDCl_3$ at 500 MHz

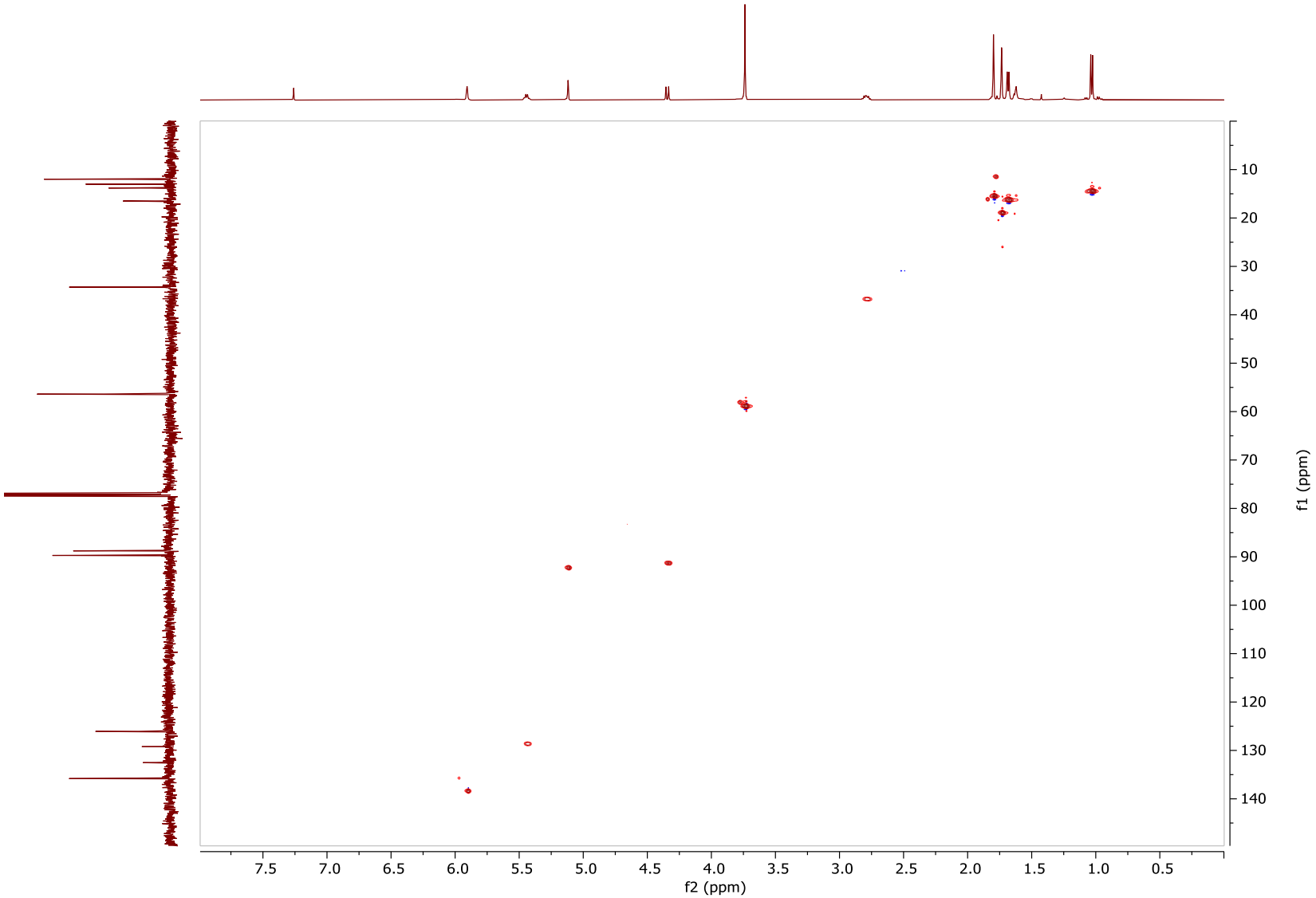

^{1}H-^{13}C HSQC NMR spectrum of **1** measured in $CDCl_3$ at 500 MHz

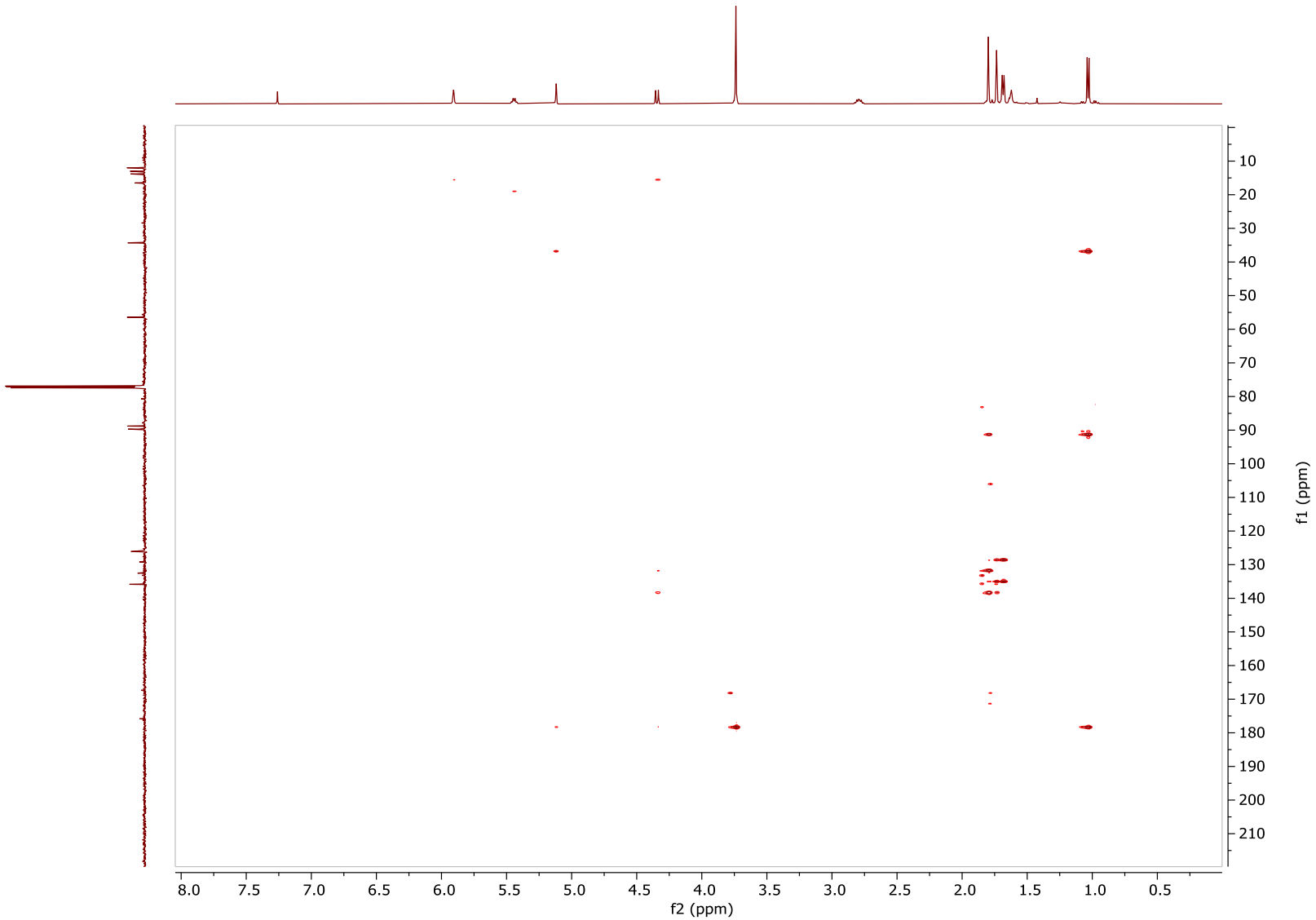

^{1}H-^{13}C HMBC NMR spectrum of **1** measured in $CDCl_3$ at 500 MHz

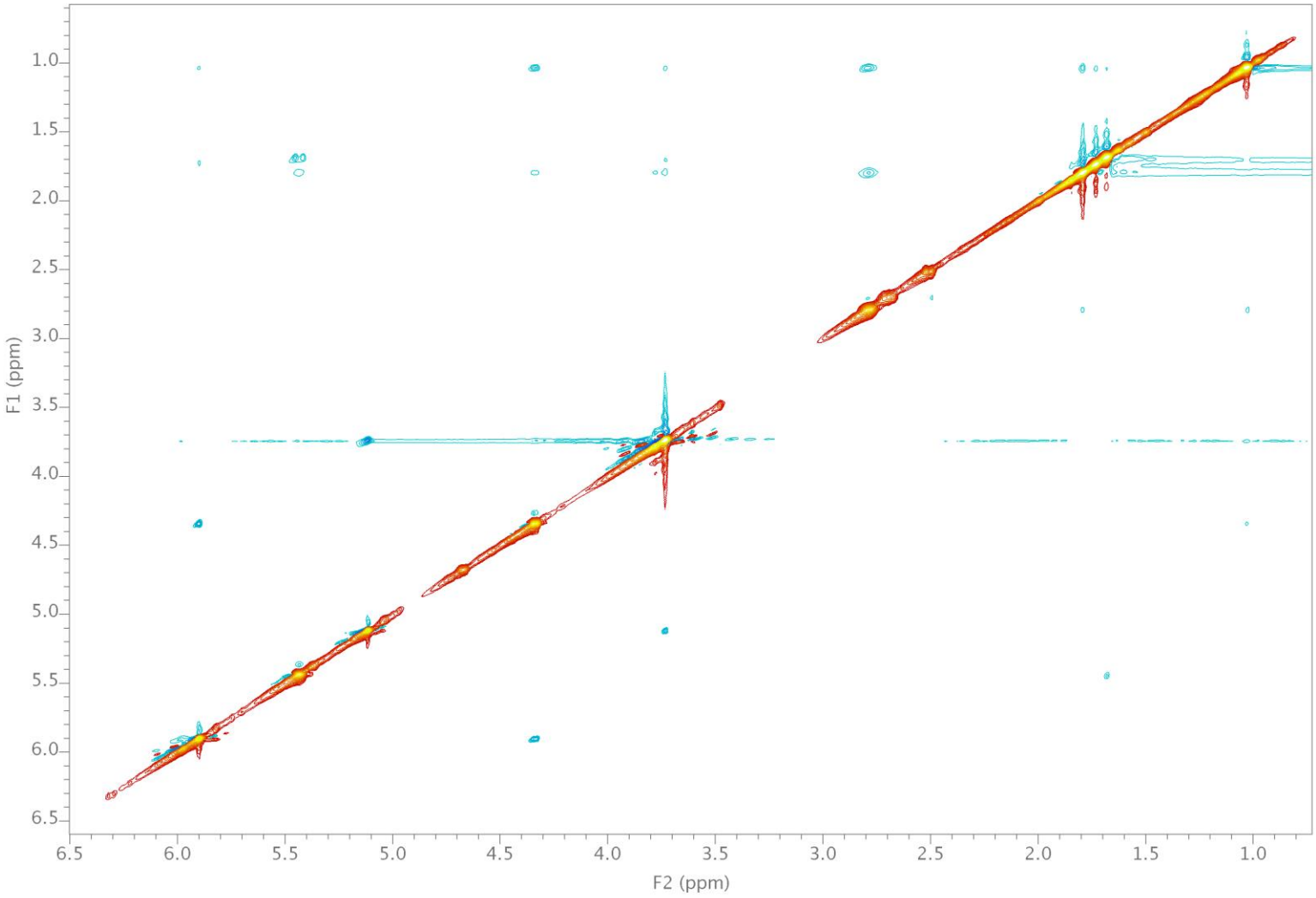

^{1}H-^{1}H NOESY NMR spectrum of **1** measured in $CDCl_3$ at 500 MHz

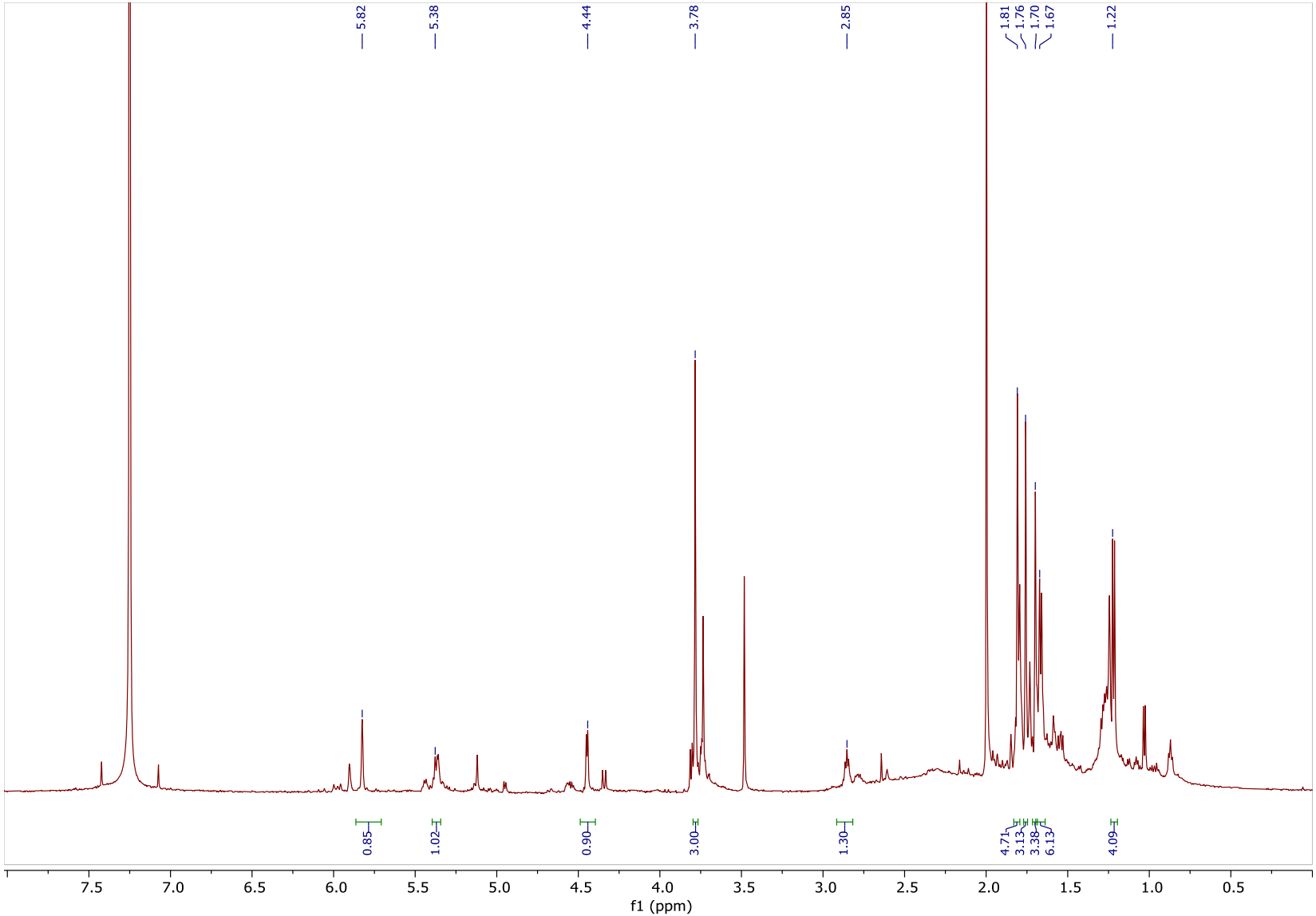

^{1}H NMR spectrum of **2** measured in $CDCl_3$ at 500 MHz

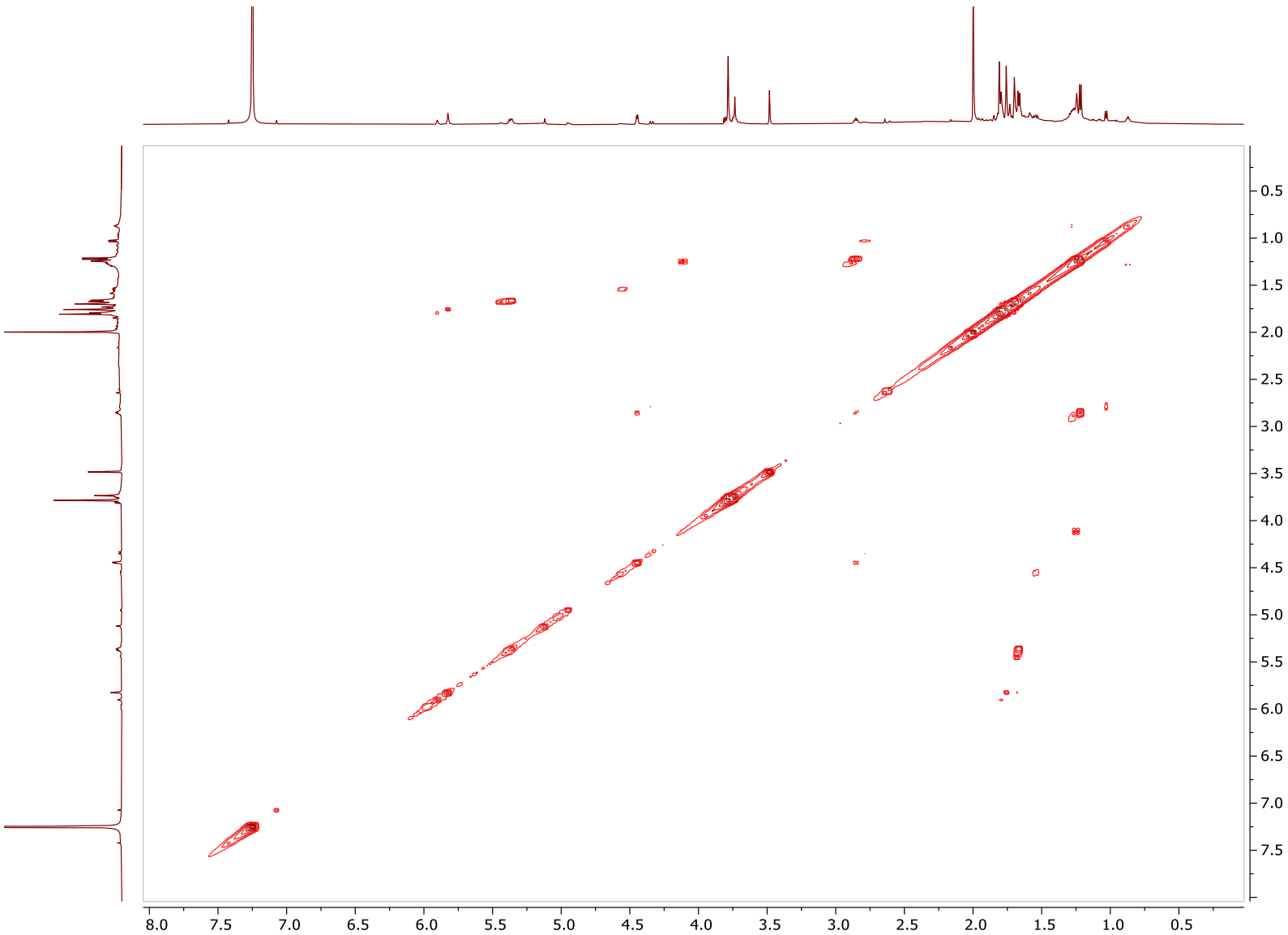

^{1}H-^{1}H COSY NMR spectrum of **2** measured in $CDCl_3$ at 500 MHz

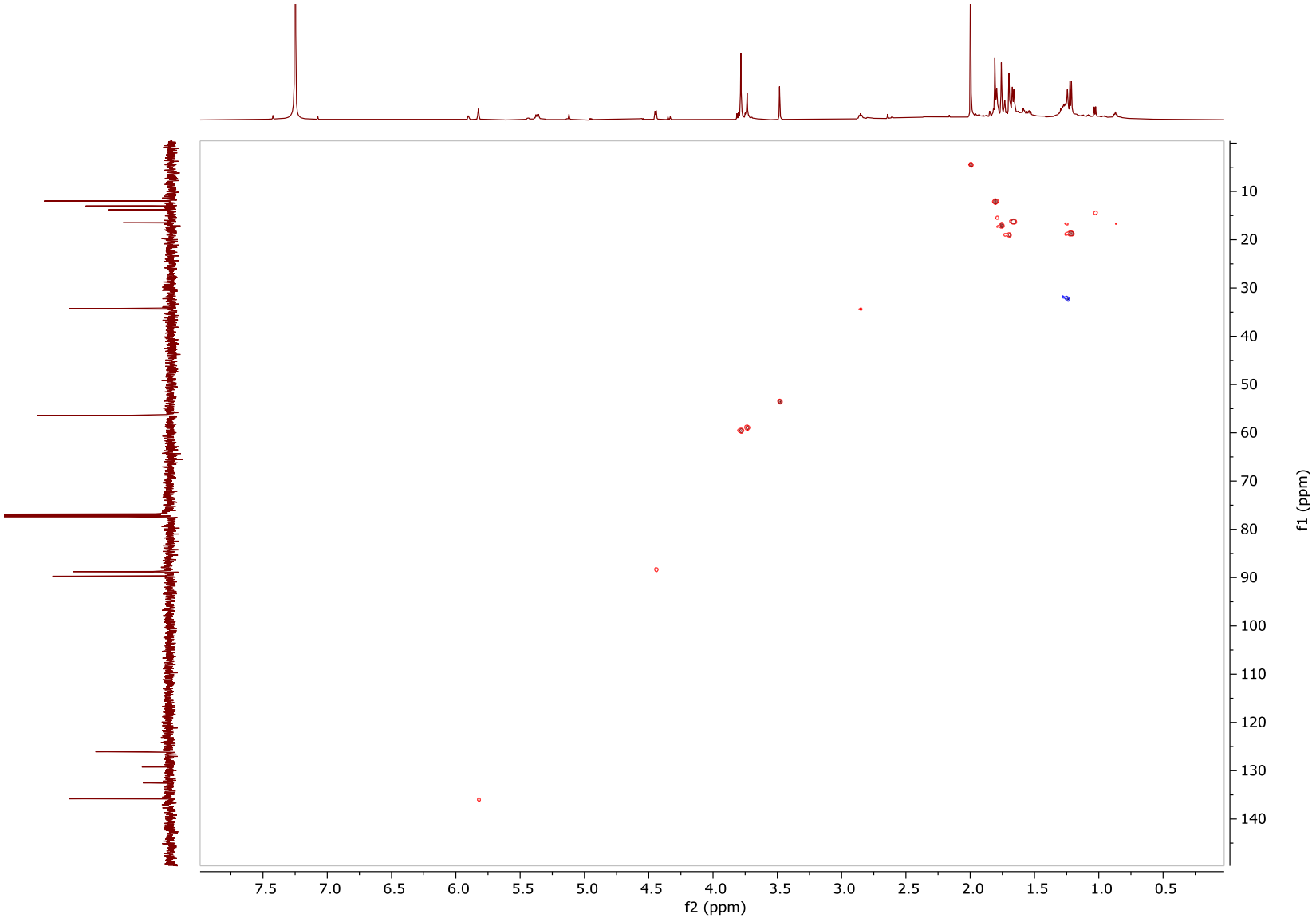

^{1}H-^{13}C HSQC NMR spectrum of **2** measured in $CDCl_3$ at 500 MHz

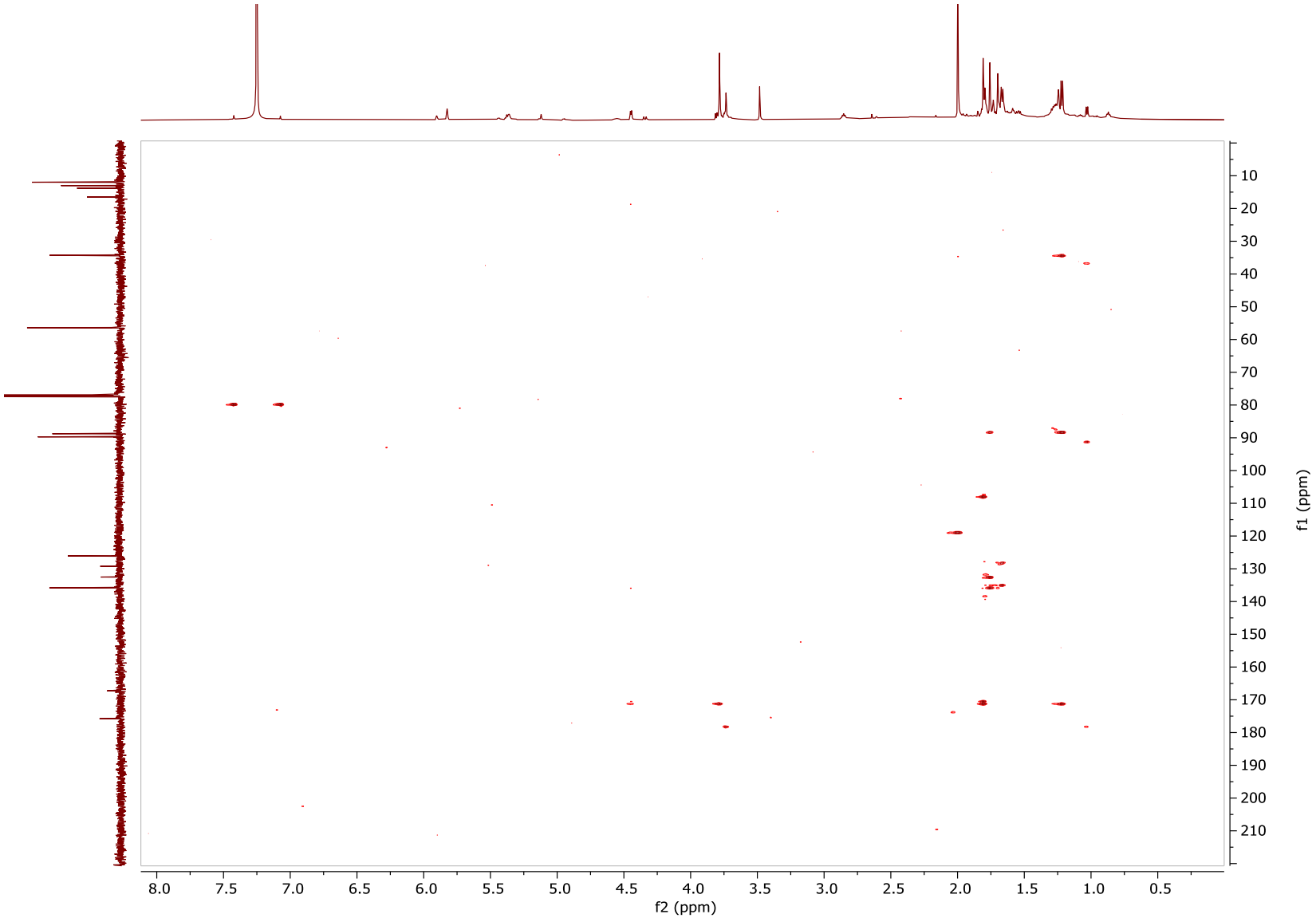

^{1}H-^{13}C HMBC NMR spectrum of **2** measured in $CDCl_3$ at 500 MHz

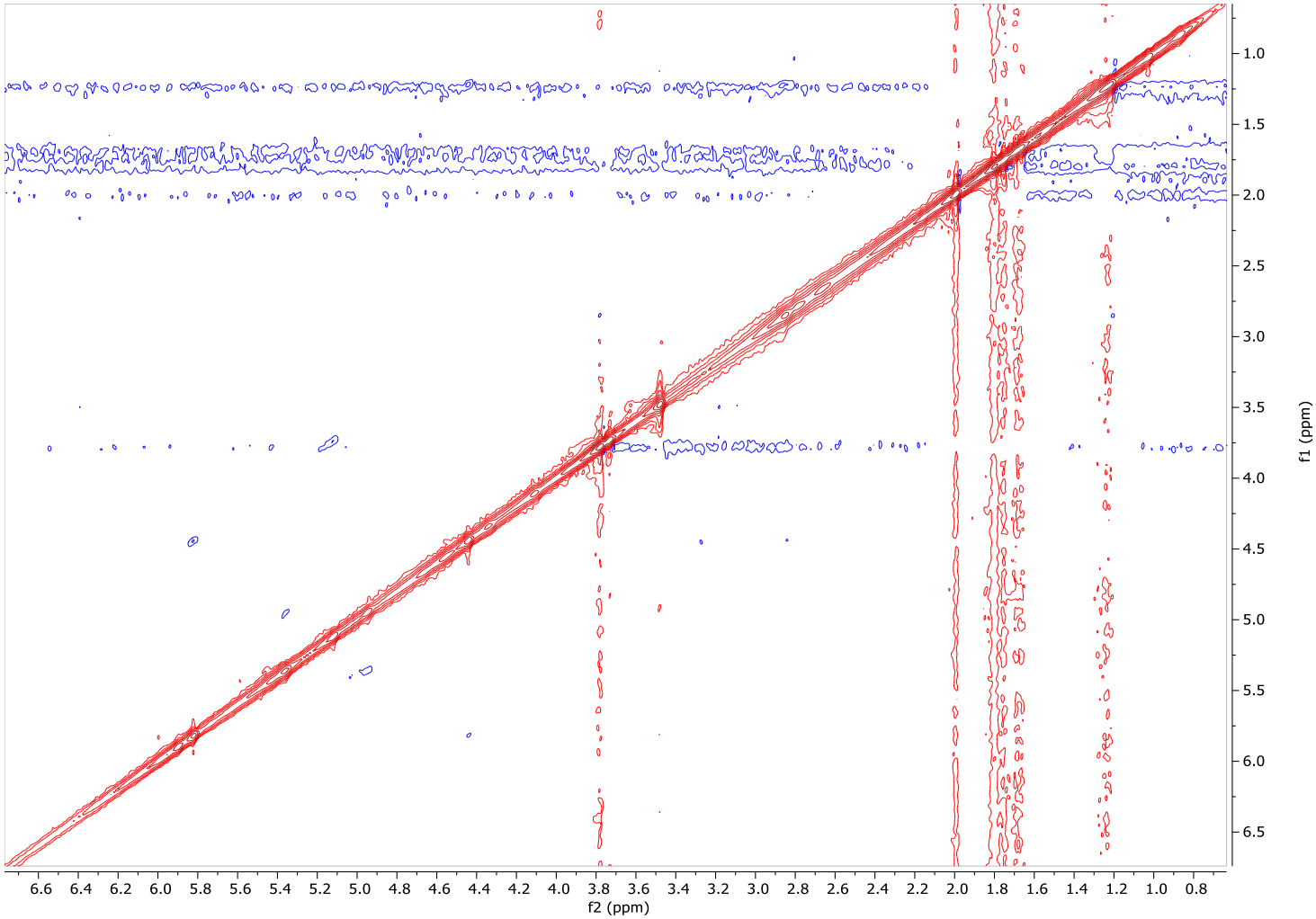

^{1}H-^{1}H NOESY NMR spectrum of **2** measured in $CDCl_3$ at 500 MHz

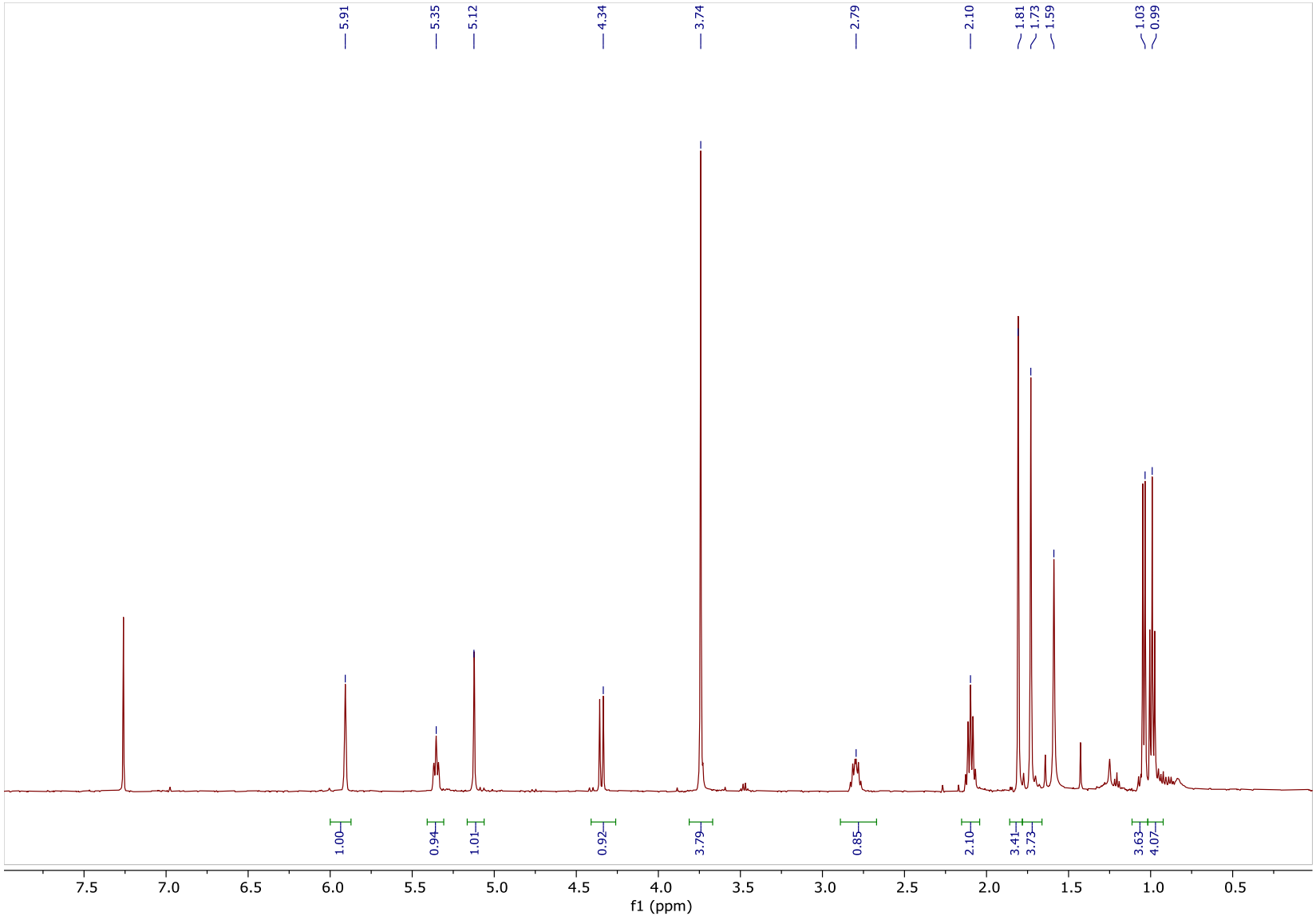

^{1}H NMR spectrum of **3** measured in $CDCl_3$ at 500 MHz

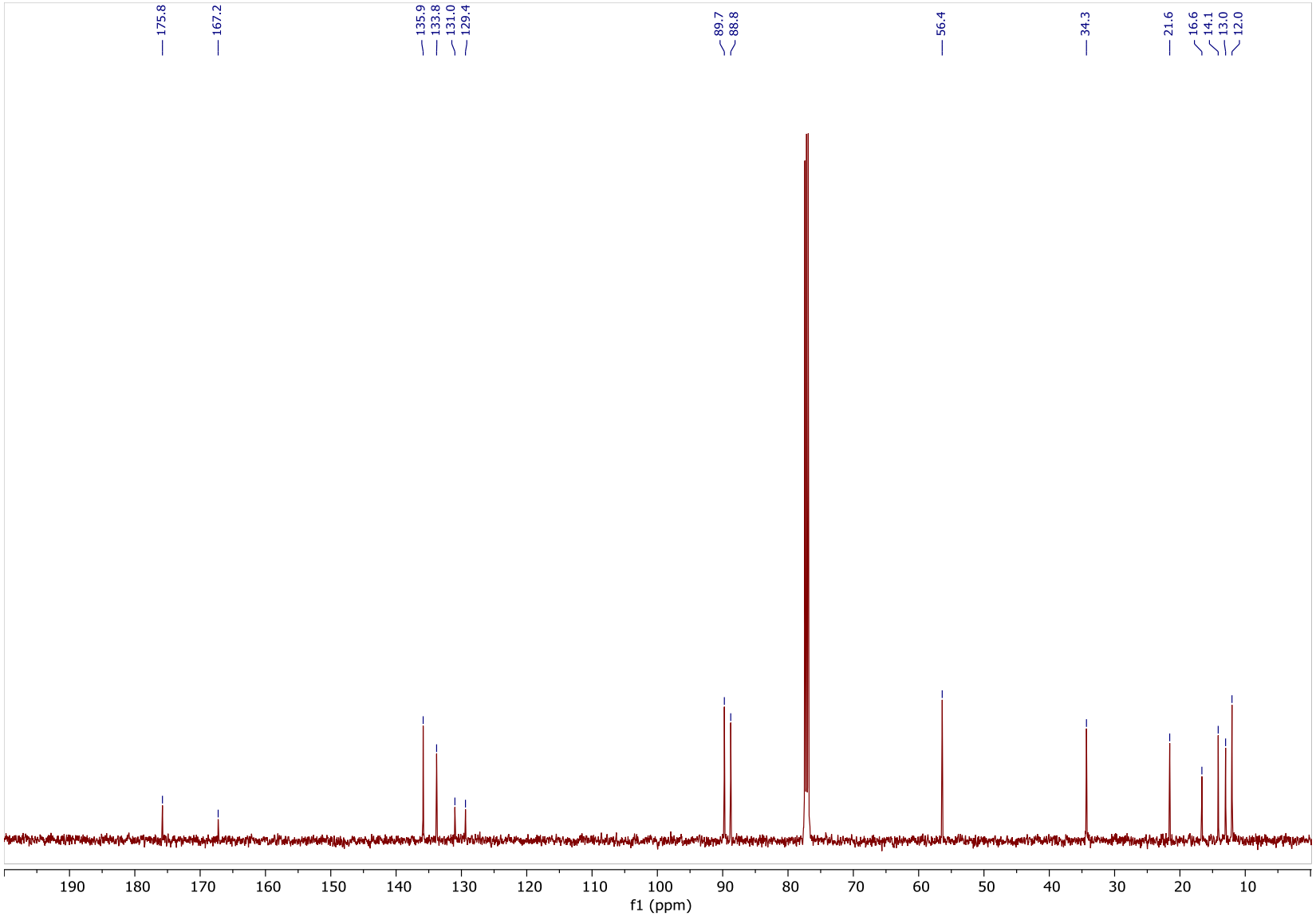

^{13}C NMR spectrum of **3** measured in $CDCl_3$ at 125 MHz

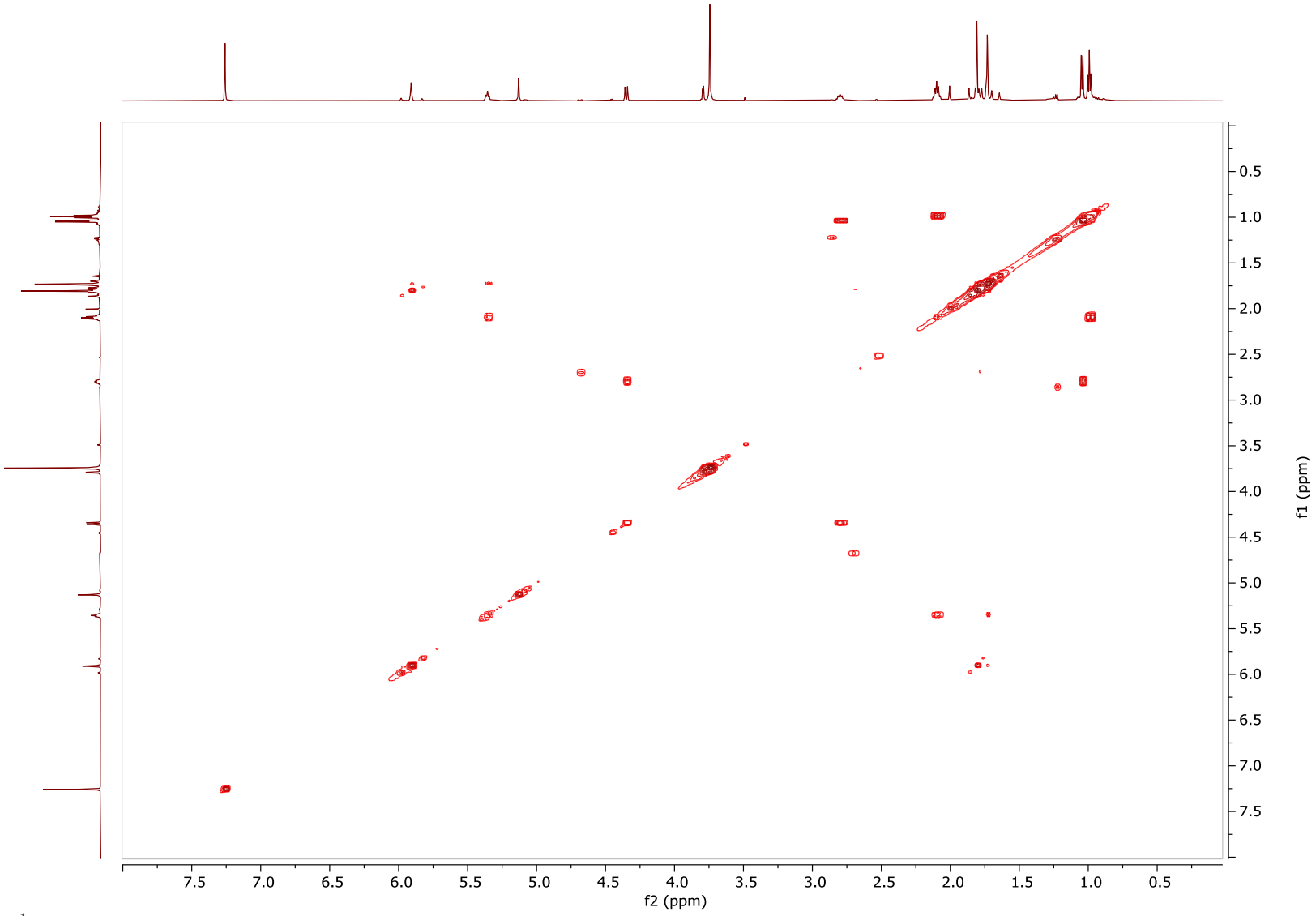

^{1}H-^{1}H COSY NMR spectrum of **3** measured in $CDCl_3$ at 500 MHz

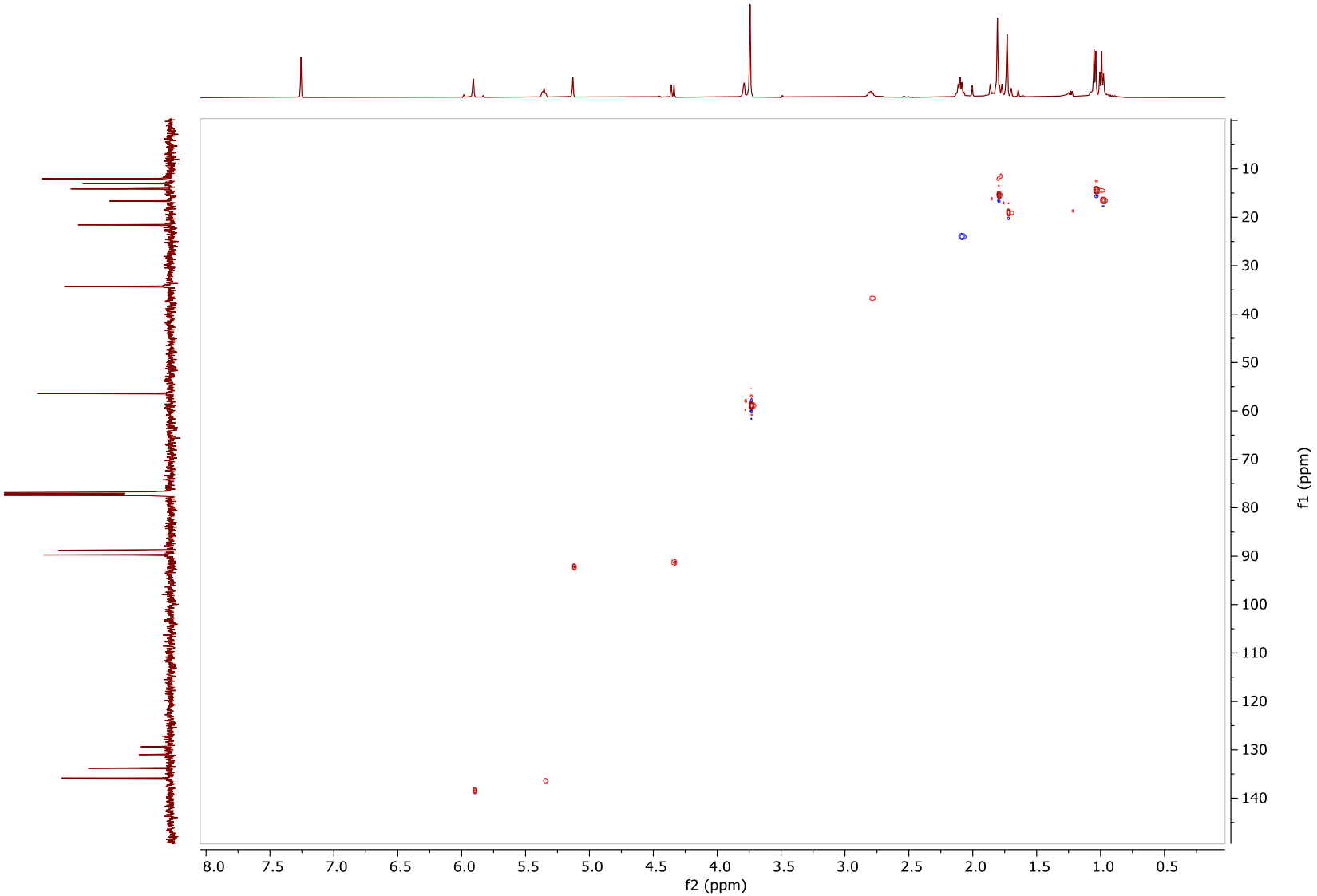

^{1}H-^{13}C HSQC NMR spectrum of **3** measured in $CDCl_3$ at 500 MHz

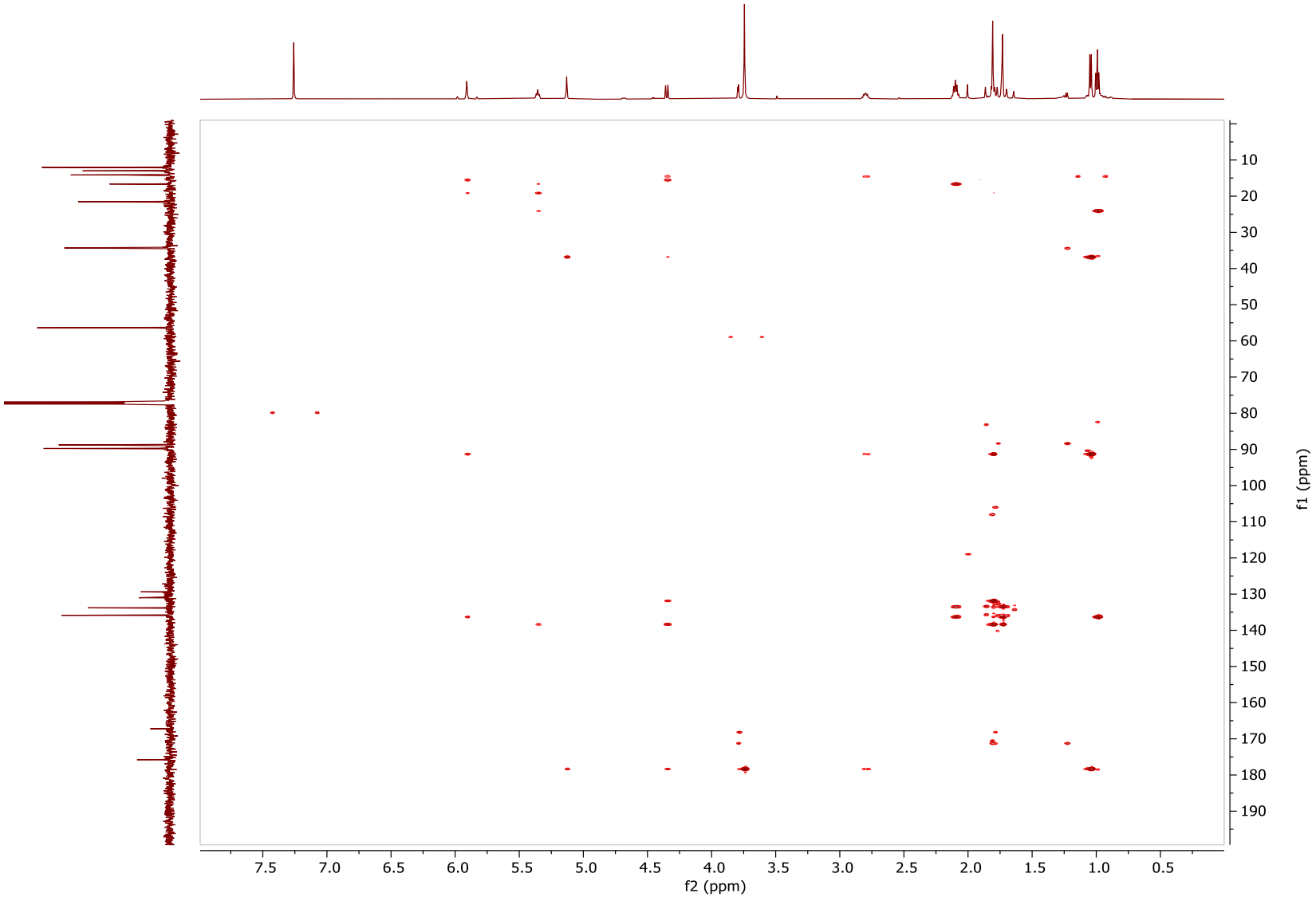

^{1}H-^{13}C HMBC NMR spectrum of **3** measured in $CDCl_3$ at 500 MHz

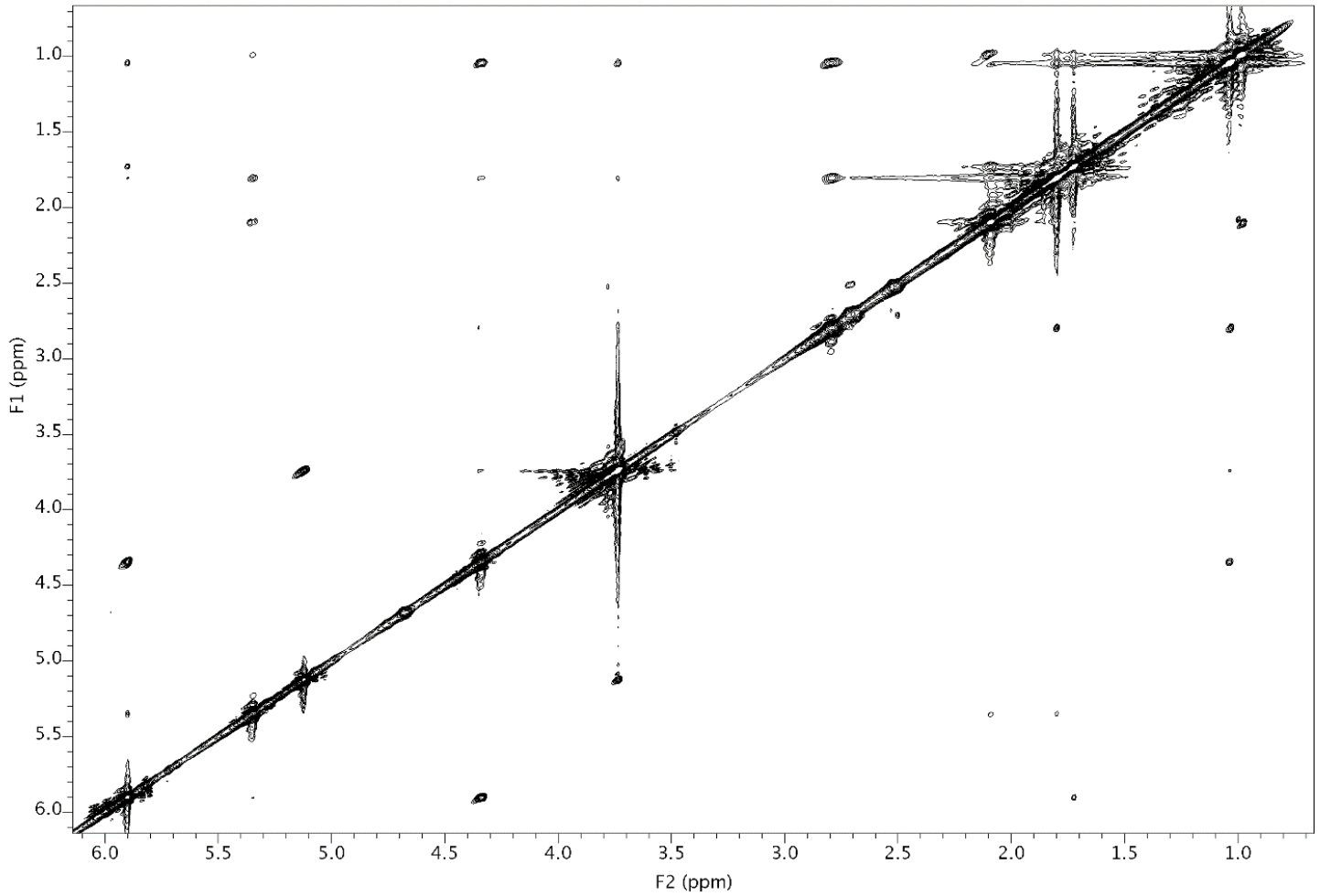

^{1}H-^{1}H NOESY NMR spectrum of **3** measured in $CDCl_3$ at 500 MHz

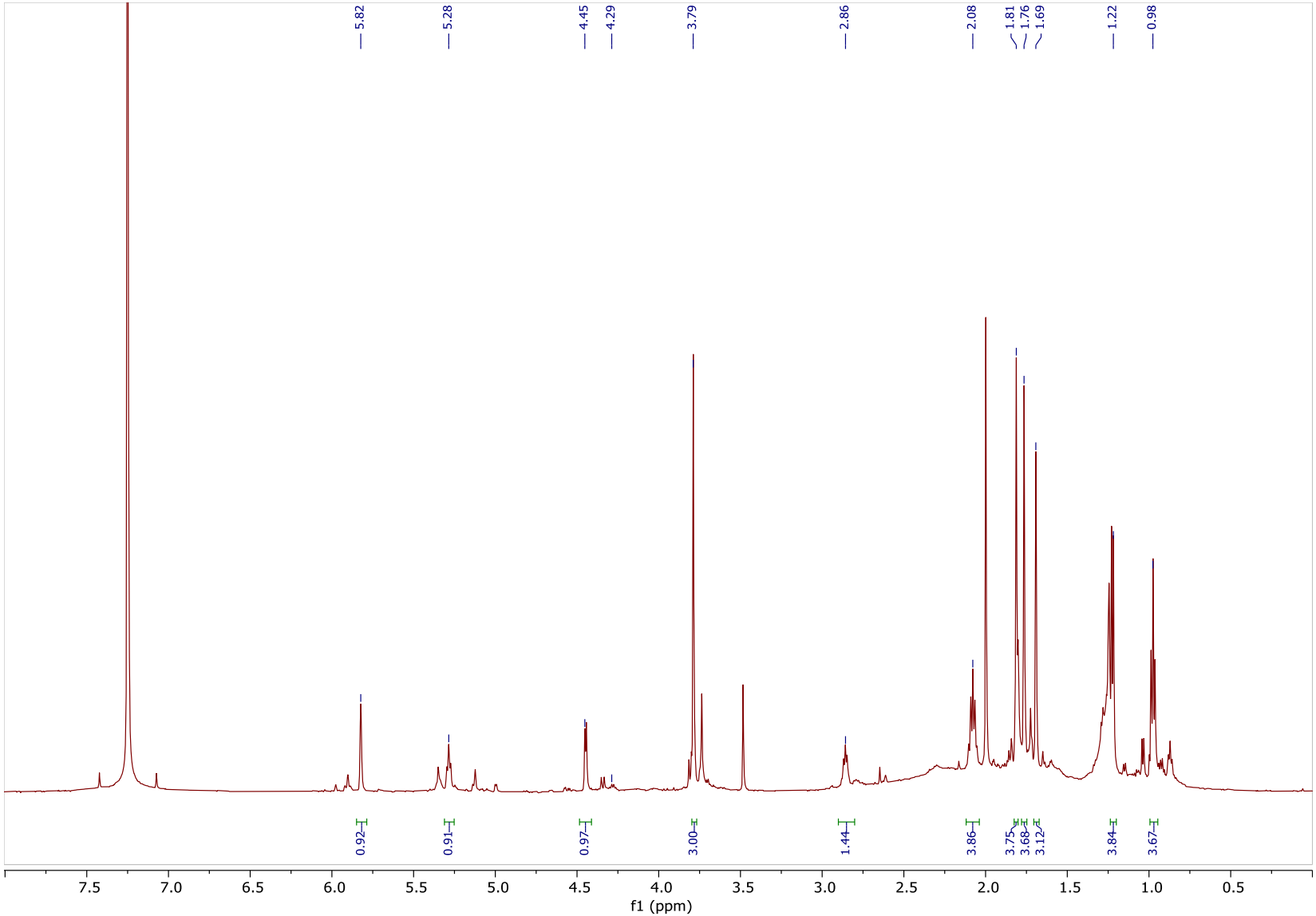

^{1}H NMR spectrum of **4** measured in $CDCl_3$ at 500 MHz

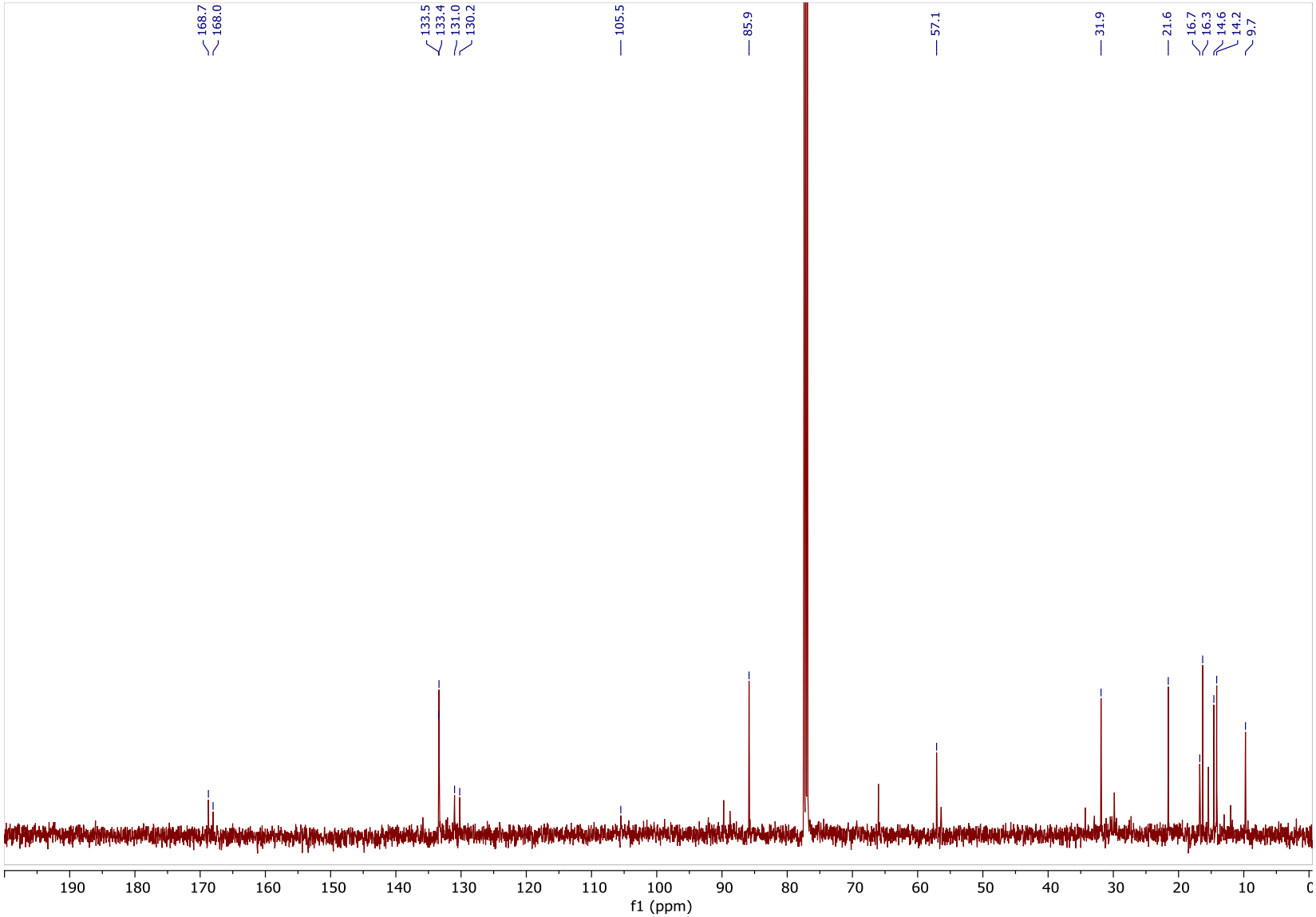

^{13}C NMR spectrum of **4** measured in $CDCl_3$ at 125 MHz

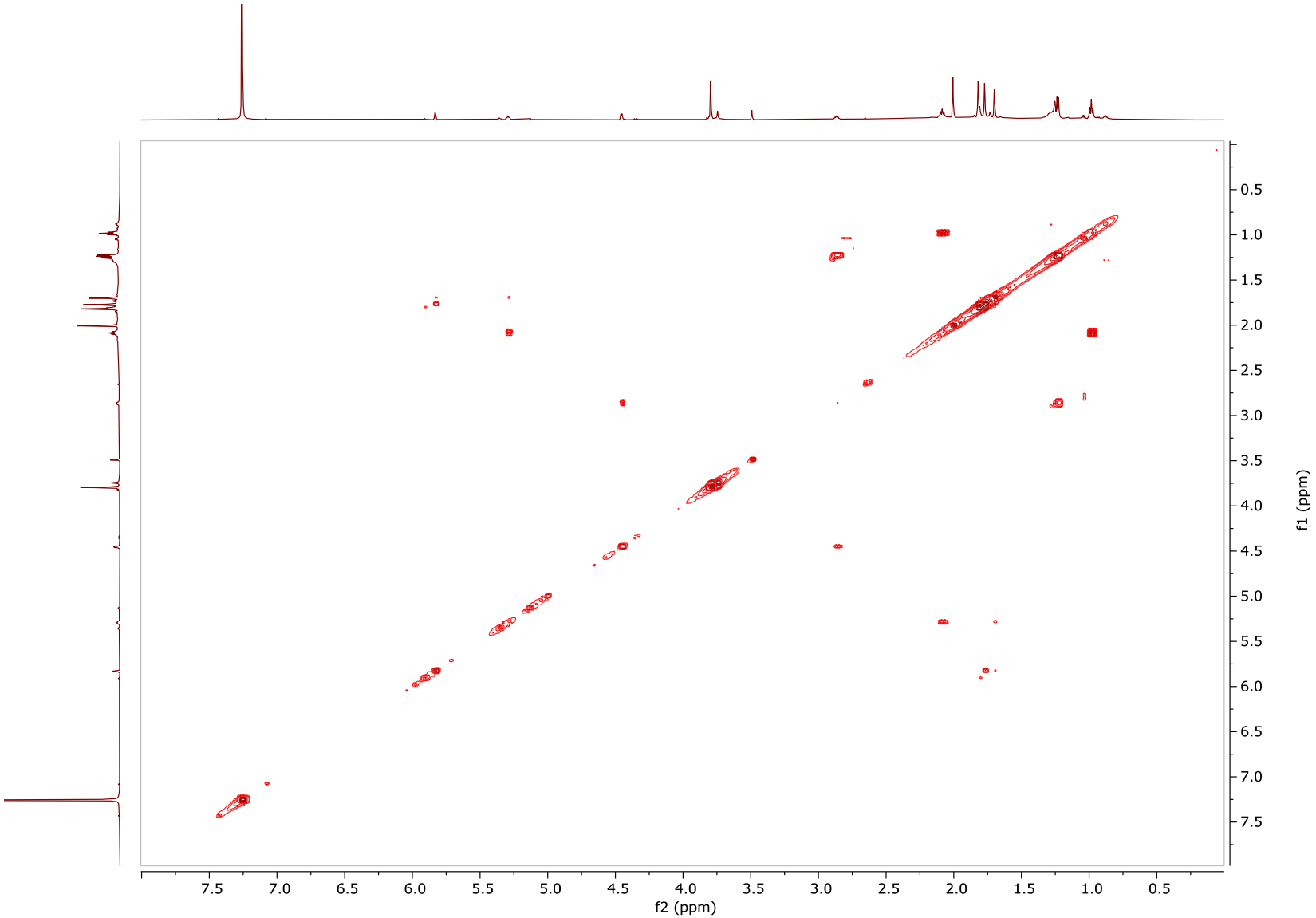

^{1}H-^{1}H COSY NMR spectrum of **4** measured in $CDCl_3$ at 500 MHz

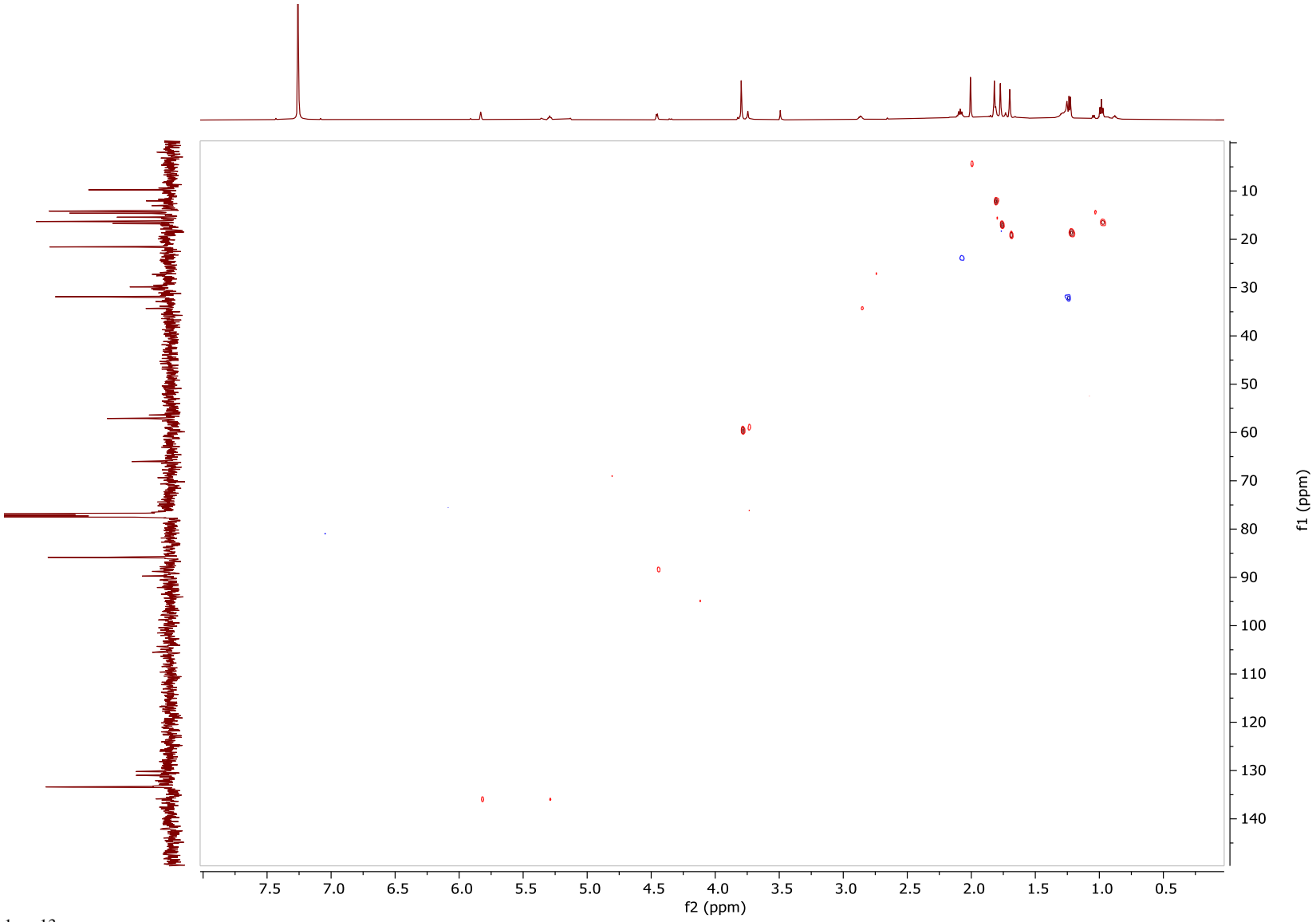

^{1}H-^{13}C HSQC NMR spectrum of **4** measured in $CDCl_3$ at 500 MHz

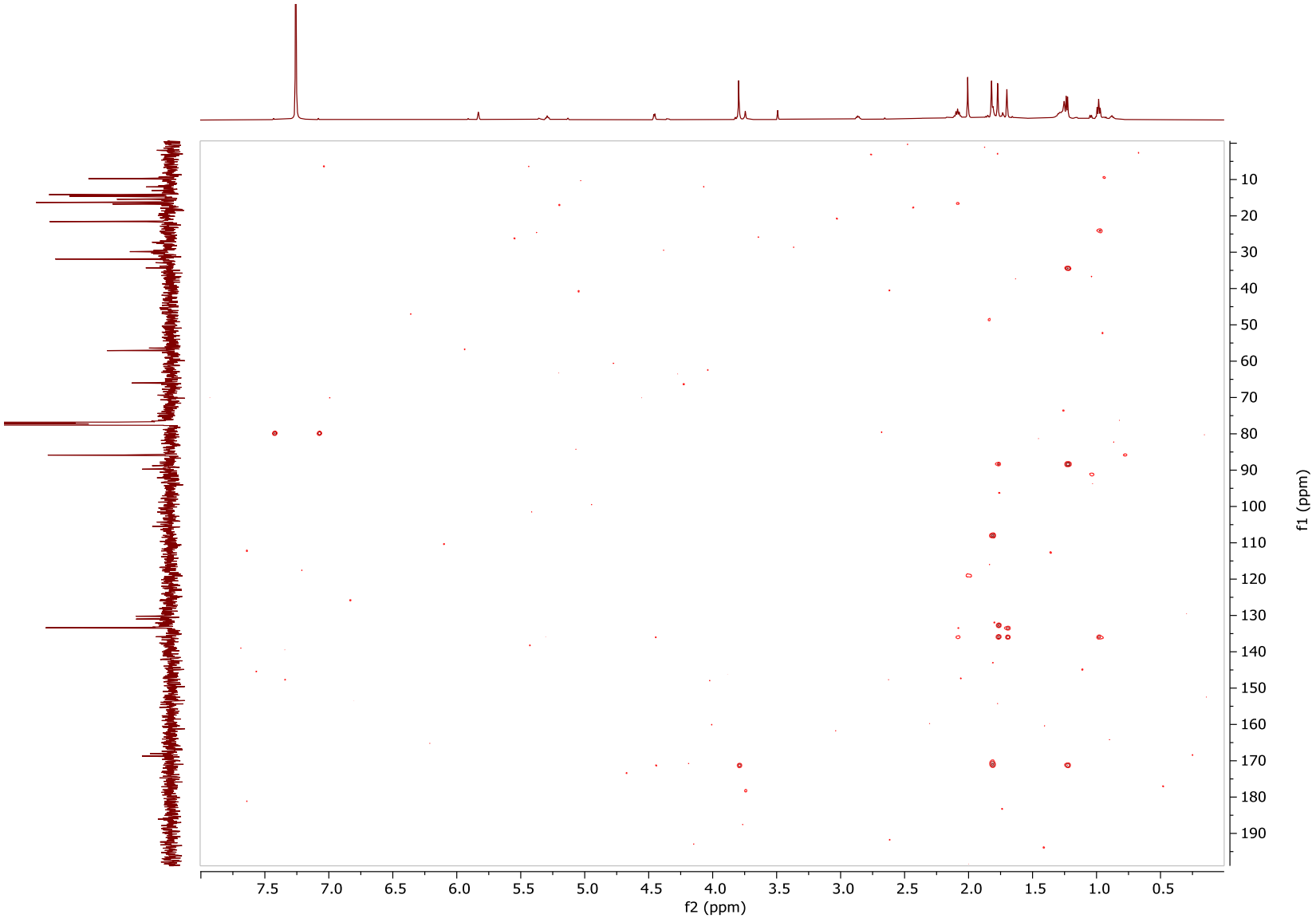

^{1}H-^{13}C HMBC NMR spectrum of **4** measured in $CDCl_3$ at 500 MHz

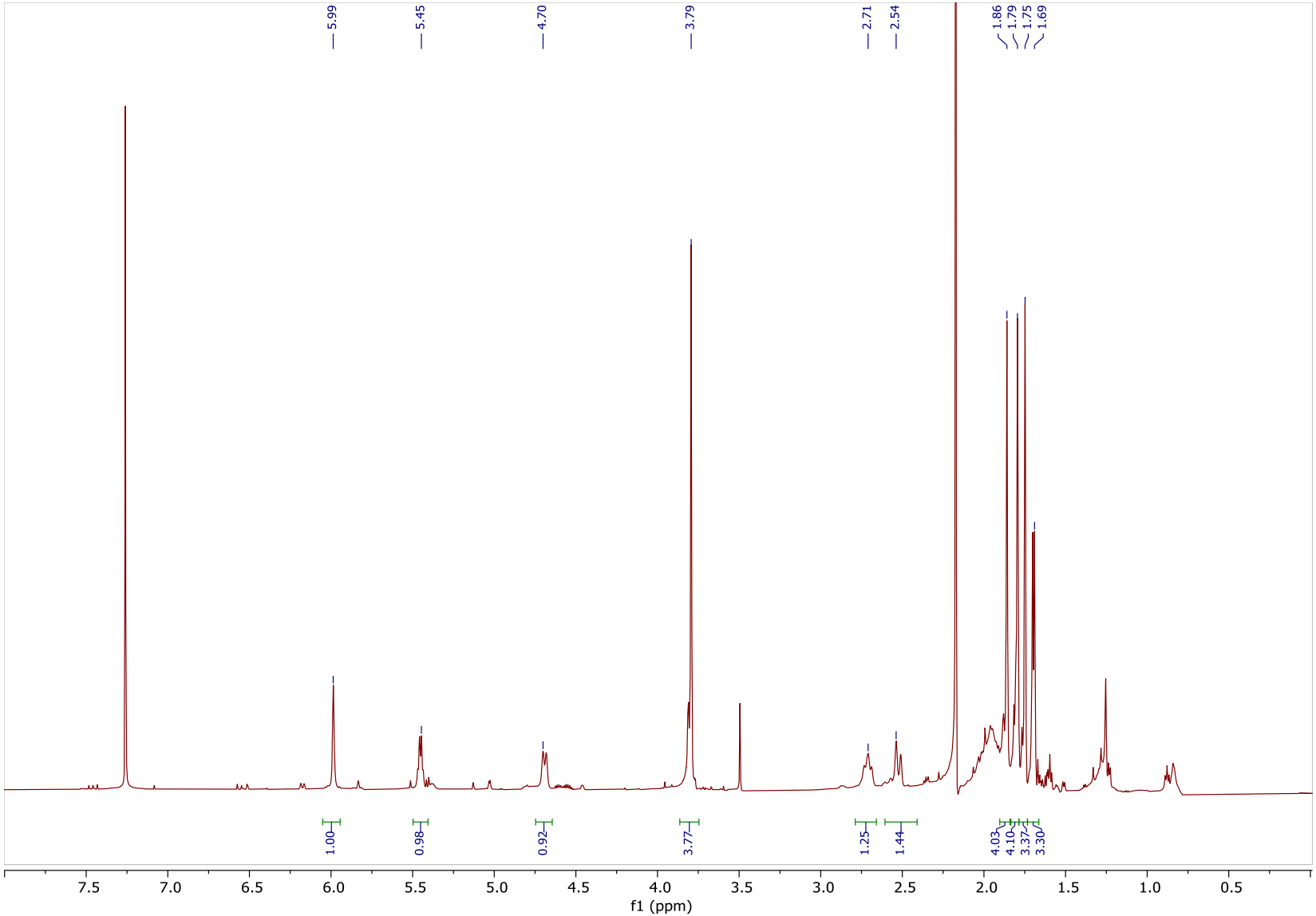

^{1}H NMR spectrum of **5** measured in $CDCl_3$ at 500 MHz

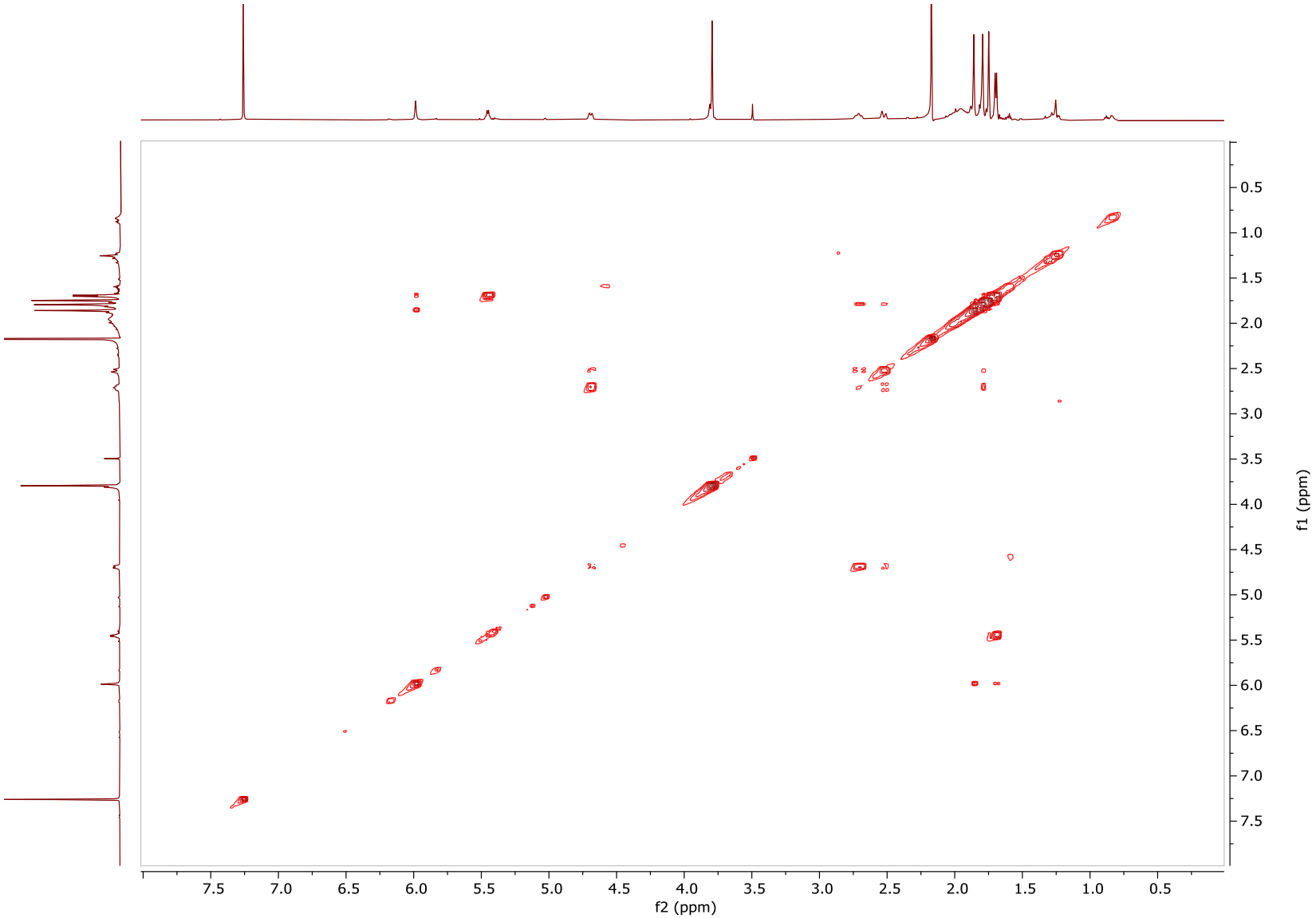

^{1}H-^{1}H COSY NMR spectrum of **5** measured in $CDCl_3$ at 500 MHz

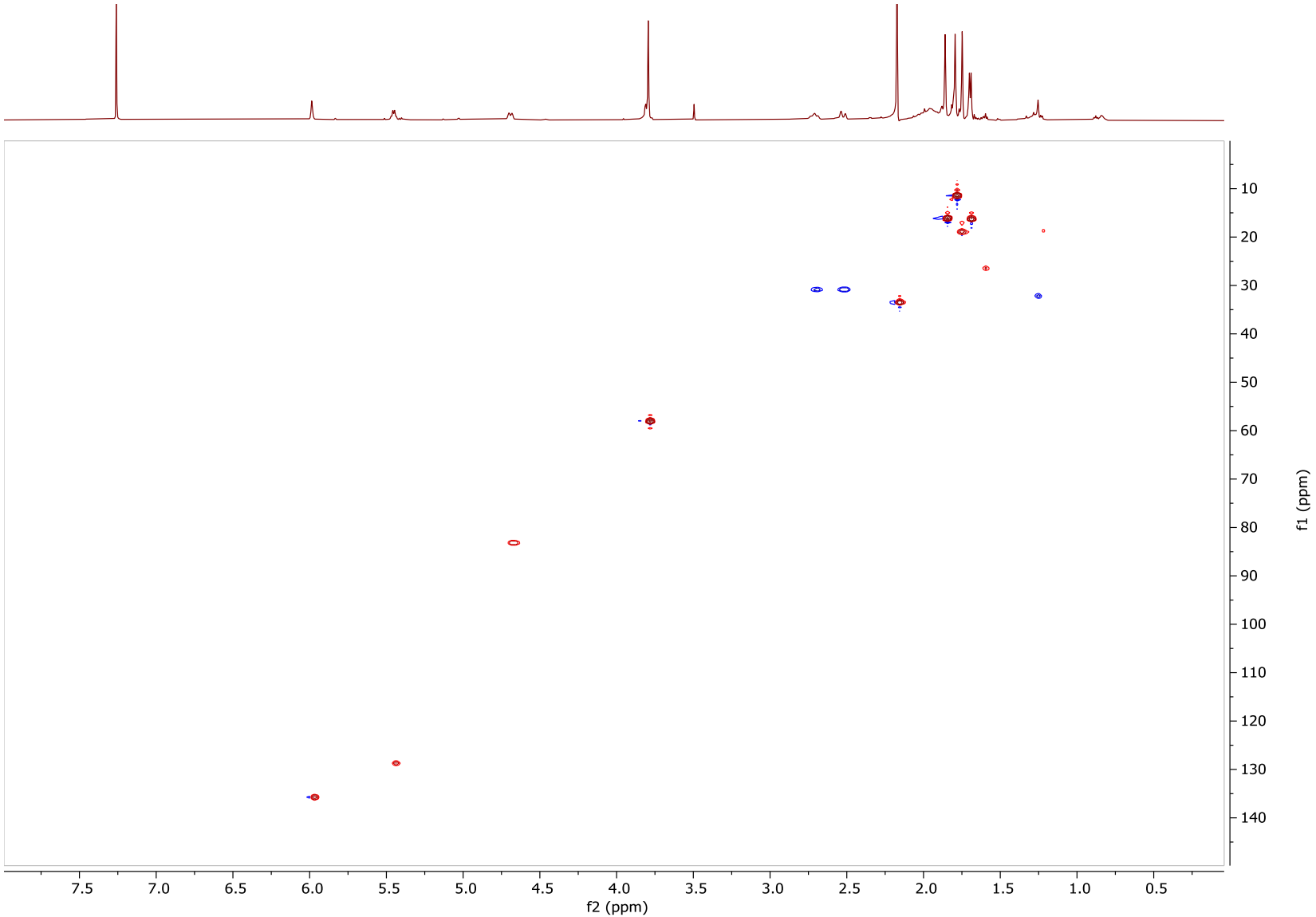

^{1}H-^{13}C HSQC NMR spectrum of **5** measured in $CDCl_3$ at 500 MHz

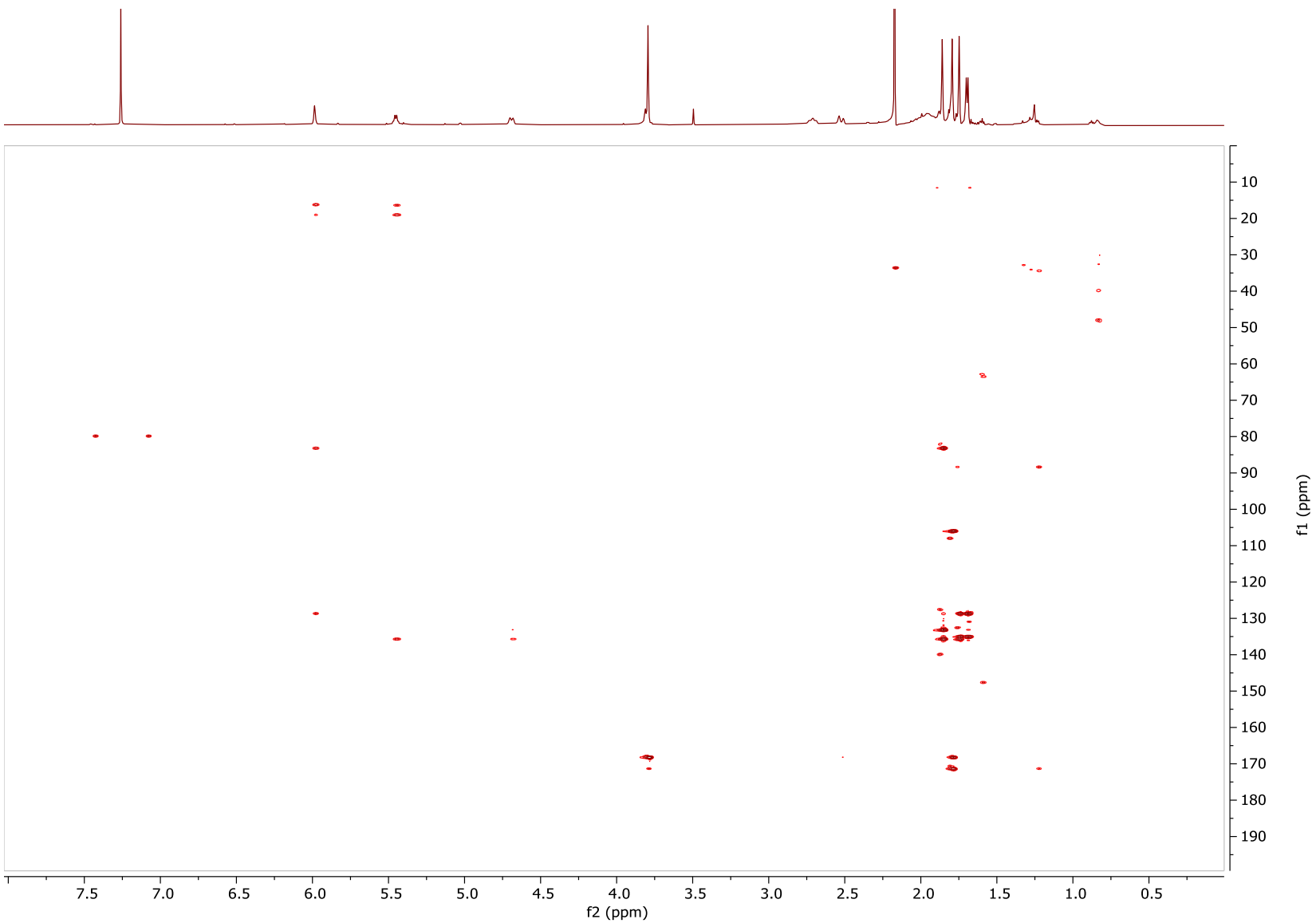

^{1}H-^{13}C HMBC NMR spectrum of **5** measured in $CDCl_3$ at 500 MHz

Computational Data

Conformer A

Calculation Type = FREQ
Calculation Method = RB3LYP
Basis Set = 6-31G(d)
Charge = 0
Spin = Singlet
Solvation = None
E(RB3LYP) = -771.16654 Hartree
RMS Gradient Norm = 4.021e-06 Hartree/Bohr
Imaginary Freq = 0
Dipole Moment = 5.0672525 Debye
Polarizability (?) = 161.106 a.u.
Point Group = C1
Job cpu time: 0 days 1 hours 17 minutes 9.0 seconds.

Thermo Tab Data Section:
Imaginary Freq = 0
Temperature = 298.15 Kelvin
Pressure = 1 atm
Frequencies scaled by = 1
Electronic Energy (EE) = -771.16654 Hartree
Zero-point Energy Correction = 0.316863 Hartree
Thermal Correction to Energy = 0.335693 Hartree
Thermal Correction to Enthalpy = 0.336637 Hartree
Thermal Correction to Free Energy = 0.269465 Hartree
EE + Zero-point Energy = -770.84967 Hartree
EE + Thermal Energy Correction = -770.83084 Hartree
EE + Thermal Enthalpy Correction = -770.8299 Hartree
EE + Thermal Free Energy Correction = -770.89707 Hartree
E (Thermal) = 210.65 kcal/mol
Heat Capacity (Cv) = 68.988 cal/mol-kelvin
Entropy (S) = 141.376 cal/mol-kelvin

Opt Tab Data Section:
Step number = 1
Maximum force = 1.1e-05 Converged
RMS force = 3e-06 Converged
Maximum displacement = 0.003567 Not converged
RMS displacement = 0.000564 Converged
Predicted energy change = -1.986134e-08 Hartree

C	3.11991300	0.72417800	0.16360200
C	2.23504900	1.86543000	-0.09256000
O	0.90197100	1.59860300	-0.26012600
C	0.37842500	0.32890700	0.20006200
C	1.23805700	-0.84765600	-0.31033800
C	2.68558600	-0.54635900	0.01452600
O	2.62489200	3.00779800	-0.20367400
C	-1.07085100	0.27259900	-0.23705700
C	-2.02254300	0.15530000	0.70953400
C	-3.48917100	0.06128100	0.55097200
C	-4.04944900	-0.75550300	-0.36265900
O	3.45063800	-1.65305100	0.09700500
C	4.84554600	-1.49052300	0.35083800
C	0.75977600	-2.18540900	0.27432900
C	-1.32309300	0.39873900	-1.71881800
C	-4.26741100	0.91288600	1.53115400
C	-5.50705500	-0.97531000	-0.65017500
H	4.15183100	0.98195000	0.36237800
H	0.42878600	0.32594500	1.29770400
H	1.15266000	-0.89439500	-1.40623900
H	-1.68721600	0.17749200	1.74915600
H	-3.37485100	-1.35692000	-0.97075800
H	5.31990500	-0.89861800	-0.44039500
H	5.01193400	-1.00497200	1.31928900
H	5.26483900	-2.49726800	0.36459400
H	1.37095300	-3.01135700	-0.09540500
H	-0.28232200	-2.36722200	-0.00182800
H	0.82319900	-2.18228300	1.36871800
H	-2.36240400	0.66669500	-1.92175800
H	-0.66868400	1.16790900	-2.14227500
H	-1.11445100	-0.53693300	-2.25687700
H	-4.07884400	1.98010100	1.35662300
H	-3.94525300	0.70374600	2.56021400
H	-5.34588100	0.74838100	1.48101400
H	-6.16878500	-0.36409200	-0.03169200
H	-5.78029600	-2.02853300	-0.49711300
H	-5.73179600	-0.74778200	-1.70146200

Conformer B

Calculation Type = FREQ
Calculation Method = RB3LYP
Basis Set = 6-31G(d)
Charge = 0
Spin = Singlet
Solvation = None
E(RB3LYP) = -771.1661 Hartree
RMS Gradient Norm = 6.41e-06 Hartree/Bohr
Imaginary Freq = 0
Dipole Moment = 5.033974 Debye
Polarizability (?) = 160.91567 a.u.
Point Group = C1
Job cpu time: 0 days 1 hours 17 minutes 27.5 seconds.

Thermo Tab Data Section:
Imaginary Freq = 0
Temperature = 298.15 Kelvin
Pressure = 1 atm
Frequencies scaled by = 1
Electronic Energy (EE) = -771.1661 Hartree
Zero-point Energy Correction = 0.316869 Hartree
Thermal Correction to Energy = 0.335663 Hartree
Thermal Correction to Enthalpy = 0.336607 Hartree
Thermal Correction to Free Energy = 0.269686 Hartree
EE + Zero-point Energy = -770.84923 Hartree
EE + Thermal Energy Correction = -770.83044 Hartree
EE + Thermal Enthalpy Correction = -770.8295 Hartree
EE + Thermal Free Energy Correction = -770.89642 Hartree
E (Thermal) = 210.632 kcal/mol
Heat Capacity (Cv) = 68.997 cal/mol-kelvin
Entropy (S) = 140.846 cal/mol-kelvin

Opt Tab Data Section:
Step number = 1
Maximum force = 2.4e-05 Converged
RMS force = 4e-06 Converged
Maximum displacement = 0.003055 Not converged
RMS displacement = 0.000636 Converged
Predicted energy change = -1.916905e-08 Hartree

C	3.07565200	0.78858500	0.35809100
C	2.11649100	1.89793800	0.36308300
O	0.80524100	1.59227800	0.11144400
C	0.36777900	0.21830500	0.24358500
C	1.30733400	-0.74529500	-0.51483000
C	2.72919700	-0.43525300	-0.09724300
O	2.42805900	3.05689100	0.53357400
C	-1.07716900	0.18967500	-0.21313500
C	-2.00653600	-0.31193700	0.62356300
C	-3.46613800	-0.44929600	0.42572900
C	-4.21267700	0.57621800	-0.02809000
O	3.56776300	-1.47744700	-0.26386900
C	4.94716500	-1.28927700	0.04983500
C	0.92031900	-2.21226700	-0.27349800
C	-1.35256100	0.73943000	-1.58976000
C	-4.01979600	-1.79614800	0.83982200
C	-5.69490300	0.61753200	-0.26731700
H	4.08690200	1.05777100	0.63324800
H	0.41713700	-0.04713400	1.30865300
H	1.23379200	-0.53895600	-1.59261400
H	-1.64762500	-0.71312000	1.57463600
H	-3.69619300	1.51300500	-0.23226000
H	5.38348500	-0.49642200	-0.56856000
H	5.07575300	-1.03837300	1.10901700
H	5.43415100	-2.24078300	-0.16699400
H	1.58719000	-2.88392800	-0.81804800
H	-0.10600400	-2.38928100	-0.60542300
H	0.98179600	-2.46673600	0.79116100
H	-2.35090300	0.46465700	-1.93681500
H	-1.27277000	1.83303400	-1.59491300
H	-0.61898300	0.37414800	-2.31911300
H	-3.70820100	-2.03983400	1.86463300
H	-3.62902300	-2.59609900	0.19691300
H	-5.11048800	-1.84070100	0.80572200
H	-6.19610900	-0.33121700	-0.06002200
H	-5.91001600	0.88579100	-1.31093000
H	-6.16733400	1.39114800	0.35350100

Conformer C

Calculation Type = FREQ
Calculation Method = RB3LYP
Basis Set = 6-31G(d)
Charge = 0
Spin = Singlet
Solvation = None
E(RB3LYP) = -771.16201 Hartree
RMS Gradient Norm = 8.406e-06 Hartree/Bohr
Imaginary Freq = 0
Dipole Moment = 5.4258612 Debye
Polarizability (?) = 160.04267 a.u.
Point Group = C1
Job cpu time: 0 days 1 hours 21 minutes 17.6 seconds.

Thermo Tab Data Section:
Imaginary Freq = 0
Temperature = 298.15 Kelvin
Pressure = 1 atm
Frequencies scaled by = 1
Electronic Energy (EE) = -771.16201 Hartree
Zero-point Energy Correction = 0.317046 Hartree
Thermal Correction to Energy = 0.335788 Hartree
Thermal Correction to Enthalpy = 0.336732 Hartree
Thermal Correction to Free Energy = 0.269747 Hartree
EE + Zero-point Energy = -770.84496 Hartree
EE + Thermal Energy Correction = -770.82622 Hartree
EE + Thermal Enthalpy Correction = -770.82528 Hartree
EE + Thermal Free Energy Correction = -770.89226 Hartree
E (Thermal) = 210.71 kcal/mol
Heat Capacity (Cv) = 68.963 cal/mol-kelvin
Entropy (S) = 140.981 cal/mol-kelvin

Opt Tab Data Section:
Step number = 1
Maximum force = 3.3e-05 Converged
RMS force = 5e-06 Converged
Maximum displacement = 0.003047 Not converged
RMS displacement = 0.000846 Converged
Predicted energy change = -3.16651e-08 Hartree

C	-2.55984800	0.91511800	0.34711600
C	-1.82790500	1.75999000	-0.60352900
O	-0.85144600	1.17741000	-1.36395200
C	-0.33844300	-0.15067800	-1.07091900
C	-1.44423700	-1.11202600	-0.57489100
C	-2.37840500	-0.42018100	0.38037000
O	-2.06432500	2.93895500	-0.76349400
C	0.89716900	-0.05970900	-0.18823000
C	2.07626900	-0.41439600	-0.73723400
C	3.42881800	-0.41446000	-0.13656200
C	3.91432000	0.67289200	0.49298000
O	-3.01501800	-1.29510000	1.18774500
C	-3.99343000	-0.78194100	2.09159400
C	-2.24287600	-1.71529100	-1.75000200
C	0.72709200	0.39833500	1.23845300
C	4.20488700	-1.69405500	-0.36448300
C	5.26068300	0.85803800	1.13250200
H	-3.26422500	1.44181200	0.97754800
H	-0.01302700	-0.50684300	-2.05197700
H	-0.95794000	-1.93169600	-0.03174100
H	2.04977300	-0.79191200	-1.76284500
H	3.26934900	1.54974600	0.53425200
H	-3.54190900	-0.07259500	2.79482200
H	-4.80683000	-0.28793100	1.54761900
H	-4.38024200	-1.64533400	2.63423000
H	-3.05116100	-2.35443700	-1.38195900
H	-1.58748200	-2.32234300	-2.38437100
H	-2.67996400	-0.92214800	-2.36563600
H	1.65685100	0.28667200	1.79952100
H	0.42566500	1.45226900	1.29019200
H	-0.05501400	-0.17565300	1.74966400
H	4.21641600	-1.95020000	-1.43268000
H	3.73048000	-2.53832700	0.15312700
H	5.24186300	-1.63275000	-0.02712400
H	5.89273300	-0.03207600	1.08184200
H	5.15105400	1.12794600	2.19199200
H	5.80534400	1.68587500	0.65815000

Conformer D

Calculation Type = FREQ
Calculation Method = RB3LYP
Basis Set = 6-31G(d)
Charge = 0

Spin = Singlet
Solvation = None
E(RB3LYP) = -771.16246 Hartree
RMS Gradient Norm = 1.1331e-05 Hartree/Bohr
Imaginary Freq = 0
Dipole Moment = 5.4690219 Debye
Polarizability (?) = 159.573 a.u.
Point Group = C1
Job cpu time: 0 days 1 hours 21 minutes 50.9 seconds.

Thermo Tab Data Section:
Imaginary Freq = 0
Temperature = 298.15 Kelvin
Pressure = 1 atm
Frequencies scaled by = 1
Electronic Energy (EE) = -771.16246 Hartree
Zero-point Energy Correction = 0.317063 Hartree
Thermal Correction to Energy = 0.335769 Hartree
Thermal Correction to Enthalpy = 0.336713 Hartree
Thermal Correction to Free Energy = 0.269862 Hartree
EE + Zero-point Energy = -770.84539 Hartree
EE + Thermal Energy Correction = -770.82669 Hartree
EE + Thermal Enthalpy Correction = -770.82574 Hartree
EE + Thermal Free Energy Correction = -770.89259 Hartree
E (Thermal) = 210.698 kcal/mol
Heat Capacity (Cv) = 68.926 cal/mol-kelvin
Entropy (S) = 140.7 cal/mol-kelvin

Opt Tab Data Section:
Step number = 1
Maximum force = 4.6e-05 Converged
RMS force = 6e-06 Converged
Maximum displacement = 0.001989 Not converged
RMS displacement = 0.000397 Converged
Predicted energy change = -2.440839e-08 Hartree

C	2.61833200	-0.17239100	0.82632900
C	2.07945600	-1.53592000	0.89181200
O	1.06202600	-1.86900300	0.03828600
C	0.35503000	-0.86934500	-0.73710400
C	1.29159700	0.26041500	-1.23293900
C	2.24541700	0.68076200	-0.14867800
O	2.50249300	-2.38292800	1.64978300
C	-0.89448000	-0.38690400	-0.01320800
C	-2.07246000	-0.54062600	-0.65130600
C	-3.42702800	-0.12069900	-0.23187500
C	-3.66787500	1.12380400	0.22454900
O	2.69642000	1.94020500	-0.32760100
C	3.67388000	2.43672200	0.58650600
C	2.07557000	-0.15966900	-2.49430800
C	-0.74236500	0.20819900	1.36372000
C	-4.48643100	-1.18483400	-0.42353000
C	-4.97125700	1.71685700	0.67768500
H	3.35013000	0.06595000	1.58705900
H	0.02682500	-1.42547200	-1.61968500
H	0.66685700	1.12532900	-1.48558300
H	-2.05318500	-1.08556000	-1.59872300
H	-2.82247600	1.81005600	0.26129900
H	3.28091900	2.44956600	1.60974800
H	4.58461400	1.82754500	0.55362200
H	3.89590400	3.45419700	0.26252300
H	2.76795900	0.63014800	-2.80134400
H	1.38649600	-0.35298500	-3.32396600
H	2.65111800	-1.07166500	-2.30451100
H	-1.71457100	0.32509300	1.84687700
H	-0.11889300	-0.43441700	1.99496100
H	-0.25860100	1.19369100	1.33981400
H	-4.29814300	-2.04529200	0.23154100
H	-4.46398600	-1.56676000	-1.45319800
H	-5.49818000	-0.82454400	-0.22499100
H	-5.80706500	1.01444400	0.63186900
H	-5.23361300	2.59303100	0.06875000
H	-4.89395100	2.07322400	1.71427200